République Algérienne Démocratique et Populaire

Ministère de l'enseignement supérieur et de la recherche scienti...que

Université colonel Hadj Lakhder-BATNA

Faculté des sciences

Département de physique

Laboratoire PRIMALAB

Mémoire

Présenté pour obtenir le diplôme de

Magister

Physique des rayonnements

Option : Physique Subatomique

Thème

Atomes légers dans les champs magnétique et électrique des objets astrophysiques compacts

Par :

FAIROUZ AMEZIANE

Devant le jury :

A.Belgacem-Bouzida	Pr. Univ. Batna. Président
A.Bouldjedr	Pr. Univ. Batna. Rapporteur
D. Boudjaadar	M.C Univ. Skikda Examinateur
D.Bahloul	M.C Univ. Batna. Examinateur

General introduction

The end-products of the stellar evolution, when the nuclear fuel is exhausted, are one of three di¤erent possibilities: a black hole, which means the ultimate victory of gravitation, a neutron star, where the pressure of degenerate neutrons supplies the pressure independent of temperature, and, …nally, white dwarfs, where the pressure is supplied by the degenerate electron gas.

A small number of white dwarf stars show extremely high magnetic …elds, of the order of 10^8G. These are the only known physical system in which the behaviour of spectral lines, especially of hydrogen, in the presence of very strong magnetic …elds can directly be studied, thus, we can compare observed energy shifts and transition probabilities with the predictions of theory.

In addition, white dwarfs are very interesting objects from an astronomical point of view, since they are the most common end-product of stellar evolution, and since they o¤er the opportunity to study important astrophysical processes as convection, pulsation, accretion. But they are also fascinating for a physicist, because they o¤er conditions that cannot, or not easily be achieved in terrestrial laboratories.

These strange objects deserve to be the topic of this work, where we will attempt, as an introduction, to describe what are white dwarfs and neutron stars, where do they come from, and what are the physical conditions we …nd in them. Our contribution concerns the calculations of the atomic energies and the transition probabilities, in the atmosphere of these compact objects.

The designation "strong …elds" applies to external static magnetic, and/or electric …elds that are su¢ciently intense to induce drastic changes in the atomic or molecular structure and dynamics. Therefore, atomic properties like energy- levels and wavelengths need to be reconsidered for matter under these conditions. These strong-…eld strengths cannot be reached in laboratory, while they are a feature of astrophysical objects like white dwarf (B » 10^2 ¡ 10^5T) or neutron stars (B » 10^7 ¡ 10^9T). Astrophysicists possess, therefore, a vivid interest in the behavior and properties of matter in strong magnetic and electric …elds.

Our work, treating the behavior of light atoms in strong (stellar) magnetic and electric (static) …elds of astrophysical compact objects (white dwarf and neutron stars), is divided into …ve chapters. The …rst chapter is merely an overview of astrophysics. We recall, in a simpli…ed way, the stellar evolution, Chandrasekhar limit, the compact objects structure and …nally, we present the magnetic …elds origin of these degenerate stars.

In the second chapter, we present the hydrogen atom structure in two sections; the …rst one describe its structure non-external …elds, while the second gives details about the e¤ect of external weak magnetic (Zeeman) and electric (Stark) …elds.

In the third chapter, the e¤ect of strong (stellar) magnetic and electric …eld is studied using the standard method to calculate the binding energies of hydrogen atom. We show, …rst, that the Zeeman quadratic term makes a great contribution and cannot be ignored. Our numerical calculations show that a signi…cantly large alteration of the binding energies occurs. In a second step, the joint e¤ect of magnetic and electric …elds (either parallel or with arbitrary mutual orientations) is discussed. We will show that a more dramatic impact is obtained in this case, either for the ground state or the excited ones.

The electromagnetic transition probabilities are studied in the fourth chapter, where we focus on the transitions occurring between the …rst low-lying states. The values of the dipole strength, oscillator strength and transition probabilities are calculated, since they give rich information about the structure and the spectrum of light atoms existing in these strange compact objects.

Finally, in chapter …ve, we try to treat the helium atom in such …elds where it plays an important role in the atmospheres of magnetic white dwarfs and neutron stars.

Chapter 1

Elements of astrophysics

To understand compact objects we need to understand stars.So before we go there, it is important to understand at least the basics of what makes stars shine, where they get their energy from? Why they last so long and why they don't last forever ? also fundamental to our work is why it is that not all stars produce white dwarfs or neutron stars?

We now know that stars are huge sphere of gas, mainly hydrogen and helium. Gravity not only holds the gas of a star together in a sphere, but is forever trying to collapse it into an ever small volume. This compresses the material in the centre of the star. So great is the resulting heat and pressure that atoms of lighter elements are fused together to produce heavier elements, releasing energy in the process. As that energy is released it prevents the star from collapsing in on itself entirely. As long as there is su¢cient fuel, the energy released within the star will keep the star in‡ated against the pull of energy. But when the fuel runs out, the star will collapse on itself and perish. This is the ultimate fate of all stars.

1.1 *Extremely simpli…ed overview of stellar evolution*

Our knowledge of celestial objects such as the sun, the comets, the stars and the galaxies is mainly based on the analysis of the electromagnetic radiation which arrives to us from these projects (the cosmic ray particles, meteorites, etc. entering the earth's atmosphere also provide astronomical information).

Thus, most of what we know about the universe comes from information brought to us by photons. To read their messages, we must understand how the photons came into existence and the histories of their journeys through intergalactic and interstellar space.

So interpreting the abundant data of astrophysics demands a deep understanding atomic, molecular and optical processes. In addition, it demands a broad data base of atomic and molecular parameters such as binding energies, transition energies, oscillator strengths, photon polarization...

We recall that the stars classi…ed, previously, into groups called "*The Harvard classi…cation system*" in which the stars were grouped according to the strength of the hydrogen lines in their spectra. Letters of the alphabet were used to identify the classes, with class A corresponding to the stars having the strongest hydrogen lines, class B the next strongest, and so on. At that time it was thought that the amount of hydrogen in the star decreased from class A to B, and so on.

Today we know that the stars are nearly uniform in composition, being composed mainly of hydrogen and helium, and the di¤erences in their absorption spectra are due primarily to their surface temperature so that the spectral classes correspond in fact to di¤erent surface temperatures. However, the *Harvard* identi…cation has been kept, and when the classes are arranged in order of decreasing temperature, the letters that designate each group from the sequence O B A F G K M.

1.1.1 *Stellar evolution*

Stellar evolution is the history of the changes wrought in the interior structure of a self-gravitating mass by the competition between energy loss and energy generation while attempting to maintain mechanical equilibrium in the face of its self-gravitation.

The Hertzspuring-Russell diagram (HRD)

We already know that early spectral classi…cation (Harvard system) provides some qualitative information about the temperature sequence alone, but there were already indications by the …rst decade of the twentieth century that another factor governed detailed spectral morphology.

The …rst decisive step occurred when *Ejnar Hertzsprung* and *Henry Norris Russell*, in 1910, introduced a diagram that has since become the standard interperative plane for all stellar

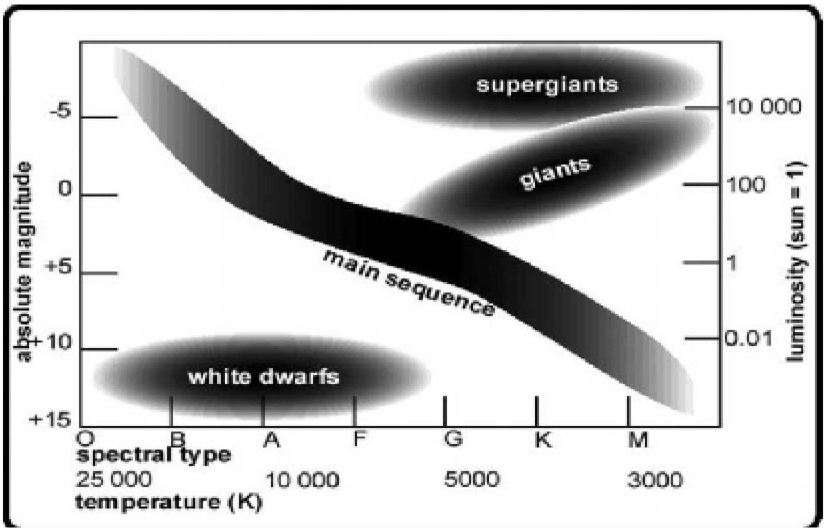

Figure 1-1: ***The Hertzsprung - Russell diagram compares the brightness and temperature of stars*****[Geo08]:**

models, now known as the *Hertzsprung-Russell diagram*.

The Hertzsprung-Russell diagram Fig(1-1)(usually referred to by the abbreviation H-R diagram or HRD, also known as a colour-magnitude diagram, or CMD) shows the relationship between absolute magnitude, luminosity, classi...cation, and temperature of stars. This diagram representing a huge leap forward in understanding stellar evolution, or the 'lives of stars', has since become the standard interpretative plane for all stellar models, now known as the Hertzsprung-Russell diagram.

Overview of stellar evolution, by utilising the H-R diagram

Star formation starts with the collapse of an overdense self-gravitating mass within a molecular cloud. That breaks into smaller and smaller pieces. As its temperature and pressure increase, the fragments condense into spheres of gas. Once the gas is hot enough for the internal pressure to support the fragment against further gravitational collapse, the object is known as *a protostar*.

Accretion of material onto the protostar continues partially from the surrounding cloud. When the density and temperature are high enough, the pressure of the resultant radiation

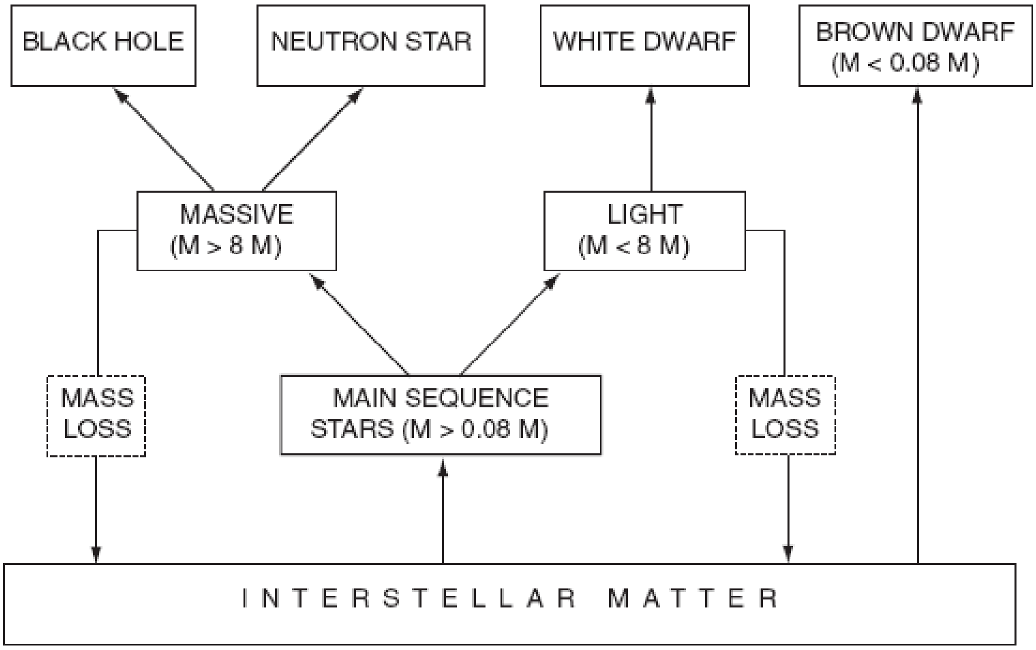

Figure 1-2: End products of stellar evolution[Hoy06].

slows (but does not stop) the collapse, where material comprising the cloud continues to "rain" onto the protostar.

For $M < 0.08$ solar masses, nuclear reactions cannot be sustained in the contracting cloud for becoming a star. Such objects end up as planets or brown dwarfs. In Fig. $(1-2)$, we show the end products of stellar evolution for the three levels (low, intermediate and high-mass) of stars.

Similarly, systems with masses higher than approximately $(60-100)$ solar masses are unstable and cannot last for a significant period of time.

It should also be noted that stars with $M \leq 1.3$ solar masses are structurally different from those with $M \geq 1.3$ solar masses. We recall that the hydrogen fusion leading to helium can occur through $p-p$ reactions or through a carbon-nitrogen - oxygen (CNO) cycle, depending on the temperature.

Stars with $M \geq 1.3\ M_{\odot}$ have the CNO cycle as the dominant reaction channel whereas stars with $M \leq 1.3\, M_{\odot}$ have $p-p$ reactions as the dominant channel.

We return now to the case of $M > 0.08 M_{\odot}$ in which hydrogen begins to fuse in the core of the star, this is the begins of the star's main sequence phase on the H-R diagram, which is the first- and longest- phase of stellar evolution. When the nuclear reactions, fusing hydrogen into helium, are taking place in the center, then such stars are called zero-age main- sequence ZAMS (The diagonal line where stars of various masses first reach the main sequence).

Thus, the vast majority of stars lie along a band that runs from the upper left corner (bright and hot) to the lower right (dim and cool), a collection known as the main sequence (see Fig.1-1).There were other collections of stars, such as bright yet cool stars in the upper right, and dim, hot stars scattered along the bottom.

From the diagram, we see that the hotter main sequence stars are bluer, when the dimmer, cooler main sequence stars are redder.

The next region of interest in Fig.$(1-1)$ is the group of stars labelled Giants; this giant phase of stellar evolution follows the main sequence phase. When the hydrogen is nearly exhausted in the central core of a star, the star begins to undergo a lot of convulsions. During this process, pressure and density increases within the star. Energy released during this process causes the outer parts of the star to swell to enormous proportions, then the star becomes less dense where the central core and the outer regions are expanding. This expansion of the outer regions results in surface cooling and in their red appearance.

The red giants stars move to the upper right side of the H-R diagram (low temperature, high luminosity), therefore, these stars characterized by very large diameters and relatively low surface temperatures. Their large diameters, and consequently their large surface areas, make them relatively bright.

Eventually, after the hydrogen burning and the expanding outer regions, the core becomes sufficiently hot to trigger helium burning, this helium ignition will occur after electron degeneracy pressure has a chance to become prevalent(helium flash in a time scale of a few days). this part of the evolution is called the asymptotic giant branch (AGB) or Hot Onions. After the He shell burning is exhausted, this leads to the contraction and the increasing of its surface effective temperature until degeneracy is reached.

Thereafter, the star evolves at roughly constant radius to become an equilibrium white dwarf supported by the degeneracy pressure of electrons. The most dramatic evidence for mass loss leading to the white dwarf stage is provided by planetary nebula. These objects display a star merging back into the interstellar gas from whence it came. They can only be described as breathtakingly beautiful objects[Sho03].

Figure $(1-3)$ represents the Hubble Space Telescope image of the planetary nebula NGC 6543, also known as the Cat's Eye nebula, at a distance of about 1 kpc. The nebula is ejected from the central bright star as it develops into a white dwarf.

Figure 1-3: The Cat's Eye nebula[Hoy06].

There is also a group of stars labelled supergiants, if stars have high mass ($M > 8M_\odot$), the onset hydrogen shell burning and helium ignition will occur before electron degeneracy pressure has a chance to become prevalent.

Eventually, its core will become sufficiently hot to fuse carbon to neon, and then to fuse neon to iron. Thus, when these stars expand and cool, they will be brighter than the red giants formed from less massive stars. These stars are known as red supergiants in which, they will explode in a core-collapse supernova resulting a neutron star or a black hole.

The final group of stars in Fig.$(1-1)$ is white dwarfs. Near the end of a star's life, as it begins to exhaust its supply of energy, it begins to shrink. During this process, the star may ultimately attain an enormous density.

There are also two other possible end states in stellar evolution: neutron stars and black holes, but neither of these are luminous enough to appear in the H-R diagram. The cores of these stars do not become degenerate and nuclear fusion continues until elements of the iron-group are formed, where the massive star continues to make heavier elements, piling one upon the other in the core: the heavier elements sink to the center while the successive layers of lighter elements surround it like the layers of an onion. See($Fig.1-4$):

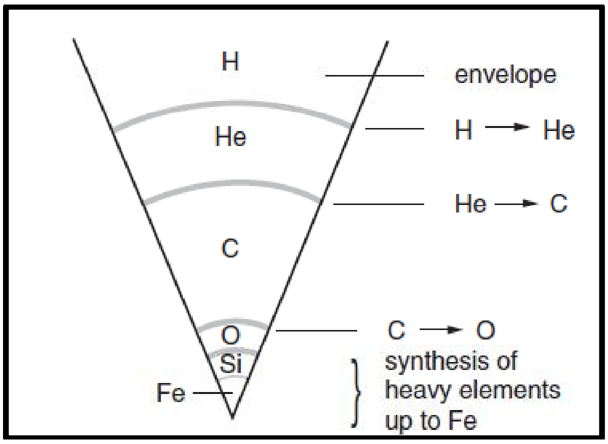

Figure 1-4: Several shells of star[Geo08]:

The compression of the core continues until $T_C = 5 \times 10^9 K$. At that point much energy is lost through photo-disintegration of ^{56}Fe, an endothermic reaction and by the emission of neutrinos[Ant04].

The situation is now as follows; The electron density decreases and so does the associated electron pressure that sustained the core. At the same time free neutrons are formed in progressively larger quantities, this runaway process seals the fate of the star in which the core contracts rapidly and collapses in about $0.1s$ until nuclear densities are attained $10^{14} - 10^{15} g/cm^3$, the core now consists of a degenerate neutron gas, with a small amount of protons and electron; thus,a neutron star is formed.

we recall that a black hole may form when the mass of the collapsed core exceeds the maximum mass of a neutron star (about 2 solar masses).

As a summary, there are three main classes of stars on the H-R diagram. A star begins its evolution at a point on the main sequence determined by its mass, matures into a red giant or supergiant stage, and can end its life as a white dwarf, but heavy stars explode as a supernova leaving an expanding remnant and a neutron star or a black hole.

Stellar evolution, thus, recycles and enriches the interstellar medium, and the four types of stellar remnant are showed in the top of the Fig.(1 ¡ 2).

1.1.2 *Chandrasekhar limit*

Chandrasekhar realized that there is a limit to how massive white dwarf can be. Note that we say massive, not big. It's a peculiar thing about white dwarfs that have the more mass but they shrink in the tinier star.

Chandrasekhar's brilliance was to develop the theory of white dwarf stars, presenting that quantum mechanical degeneracy pressure cannot stabilize a massive star. He showed that a star of a mass greater than 1:44 times that of the Sun (now known as the Chandrasekhar limit) had to end his life by collapsing into an object of enormous density.

Chandrasekhar considered the structure of white dwarf stars as a compact stellar remnants in which gravitational forces are balanced by electron degeneracy pressure, which depends only on density, not on temperature, and if a white dwarf were to exceed the Chandrasekhar limit, and nuclear reactions did not take place, the pressure exerted by electrons would no longer be able to balance the force of gravity, and it would collapse into a denser object such as a neutron star or black hole.Thus, Chandrasekhar's theory becomes the basic to much modern astrophysics[Geo08].

1.2 *Overview on compact objects (white dwarfs and neutron stars)*

As a class of astronomical objects, compact objects include white dwarfs, neutron stars and black holes. As the endpoint states of stellar evolution, they form today fundamental constituents of galaxies.

The supermassive black holes are the most extreme objects found in the Universe, these objects also live in practically every centre of a galaxy.We should denote that this subject needs a deep study but we restricted to the white dwarf stars and neutron stars's structure.

Compact objects are quite numerous: about $(5-6)\%$ of all objects of stellar-size mass in our galaxy is estimated to be a white dwarf, 0.5% a neutron star and $(1-5)\times 10^{-4}$ are black holes.

A study of compact objects - white dwarfs, neutron stars, and black holes -begins when normal stellar evolution ends. All these objects differ from normal stars in at least two aspects:

- They are not burning nuclear fuel, and they cannot support themselves against gravitational collapse by means of thermal pressure. Instead white dwarfs are supported by the pressure of the degenerate electrons, and neutron stars are largely supported by the pressure of the degenerate neutrons and quarks. Only black holes represent completely collapsed stars, assembled by mere self-gravitating forces.

- The second characteristic property of compact stars is their compact size. They are much smaller than normal stars and therefore have much stronger surface gravitational fields. Often compact objects carry strong magnetic fields, much stronger than found in normal stars.

1.2.1 *White dwarf stars*

White dwarf, also called a degenerate dwarf, is a small star composed mostly of electron degenerate matter. Because a white dwarf's mass is comparable to that of the sun and its volume is comparable to that of the earth, it is very dense.

Discovery, Composition and structure

The first white dwarf ever to be discovered was found because it is a companion star to Sirius, a bright star near the constellation Canis Major. In 1844, astronomer *Friedrich Bessel* noticed that Sirius had a slight back and forth motion, as if it were being orbited by an unseen object. In 1863, this mysterious object was finally resolved by optician *Alvan Clarkand*, it was found to be a white dwarf. This pair is now referred to as Sirius A and B, B being the white dwarf.

With strong surface gravity, the atmosphere of white dwarf is a very thin layer, that, if were it on Earth, would be lower than the tops of our skyscrapers. Underneath the atmosphere, there is a 50 km thick crust, and the bottom which is a crystalline lattice of carbon and oxygen atoms. One might make the comparison between a cool carbon/oxygen white dwarf and a diamond .

Fig.(1 ¡ 5) showed the core of a cool white dwarf consists of a C/O crystallized lattice (a kind of gigantic diamond), surrounded by a thick crust consisting of He and H and a small H atmosphere.

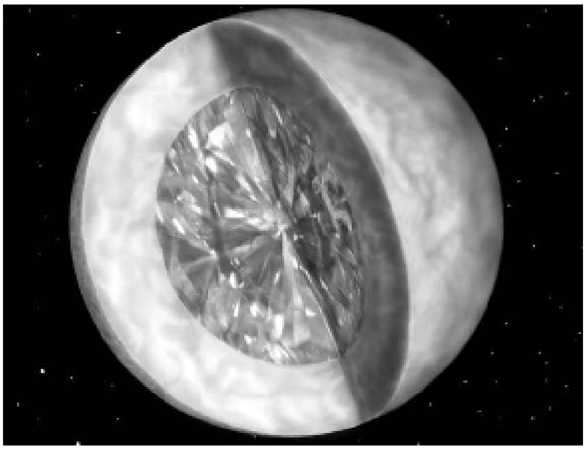

Figure 1-5: Internal structure of old C/O WD's [Max07].

Classi...cation of white dwarf stars

The system currently in use was introduced by *Edward M.Sion* and his coauthors in 1983 and has been subsequently revised several times.

Optical spectra of white dwarfs have been classi...ed according to their dominant element in the atmosphere such as:

DA: strong hydrogen lines.

DB: strong He, He I lines.

DO: strong He I, He II lines.

DC: no strong lines(continuous) spectrum.

DZ: strong metal lines(excluding carbon).

DQ: strong carbon lines.

Surface Compositions(Atmosphere)

The atmospheres of white dwarfs (i.e. the layers in which the observed radiation originates) are often of very simple chemical composition (almost pure hydrogen or helium); the reason is element separation due to the strong gravitational acceleration of about $g = 10^8 cm=s^2$.

With a surface gravity of 100 000 times that of the Earth, the atmosphere of a white dwarf is very strange. The heavier atoms in its atmosphere sink and the lighter ones remain at the surface; the basic explanation for this is gravitational separation which is unknown in any other object in the universe (except the compact objects of course)[Sch02]:

The surface composition is quite well known from spectroscopic observations, where 80% of all WDs are DAs, and most WDs have pure or nearly pure H or He atmospheres.

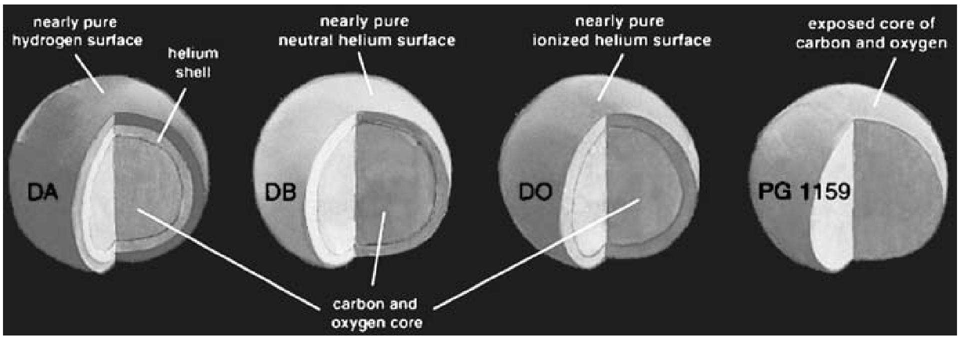

Figure 1-6: Classi...cation of white dwarfs. [Max07]

We must note that the dominant element is usually at least one times more abundant than all other element. Thus, this atmosphere, the only part of the white dwarf visible to us, is thought to be the top of an envelope which may also contain material accreted from the interstellar medium.

1.2.2 *Neutron stars*

The prediction of the existence of neutron stars was independent of observations. Following the discovery of the neutron by *Chadwick*, it was realized by many people that at very high densities electrons would react with protons to form neutrons via inverse beta decay. Neutron stars had been found at the end of the 1960's as radio pulsars and in the beginning of the 1970's as X-ray stars.

The structure of a neutron star

Neutron star is a compact star which contains matter of supernuclear density in the interior (presumably with a large fraction of neutrons).The masses of these stars are close to the solar mass $M_\odot = 1.989 \times 10^{33}$g, but their radii are about 10^5 times smaller than the solar radius $R_\odot = 6.96 \times 10^5$km.

A neutron star can be subdivided into the atmosphere and four main internal regions: the outer crust, the inner crust, the outer core, and the inner core as showing in Fig.(1 − 8).These regions can be described briefly as following:

- ***The atmosphere:*** The atmosphere which is only a few cm thick, is a thin plasma layer, in which their radiation contains valuable information on the parameters of the surface layer (on the effective surface temperature, surface gravity, chemical composition, strength of the surface magnetic field,...)[Med07].

  Therefore, to interpret the observations of NS surface emission and to provide accurate constraints to the physical properties of NSs, it is important to understand in detail the structure and the radiative properties of NS atmospheres in the presence of strong magnetic and electric fields.[Wyn04]

- ***The outer crust:*** This crust consists of a lattice of atomic nuclei and electrons. In deeper layers, the electrons are strongly degenerate, this is essentially white dwarf matter ($\rho = 4 \times 10^{11}$g/cm^3).

- ***The inner crust:*** The outer crust envelops this inner crust which may be about one kilometer thick and it extends from

  $\rho = 4 \times 10^{11}$g/cm^3 to a density $\rho = 1.7 \times 10^{14}$g/cm^3.

- ***The outer core:*** It occupies the density range $0.5\rho_0 \leq \rho \leq 2\rho_0$, Here, ρ_0 is the saturation nuclear matter density ($\rho_0 = 2.8 \times 10^{14}$g/cm^3), this layer is several Kilometers thick. Its matter consists of neutrons with several per cent admixture of protons, electrons, and possibly muons [1] (the so-called npe[1] composition)[Ali06]:

² ***The inner core:*** This layer occupies the central regions of massive neutron stars (and does not occur in low-mass stars whose outer core extends to the very center). Its radius can reach several kilometers, and its central density can be as high as (3 ¡ 9)$½_0$:

When enters the core, all atomic nuclei have been dissolved into their constituents, neutrons and protons. Due to the high pressure, the core might also contain hyperons, baryon and strange quarks. Finally, ¼ and k-meson may be found there too:

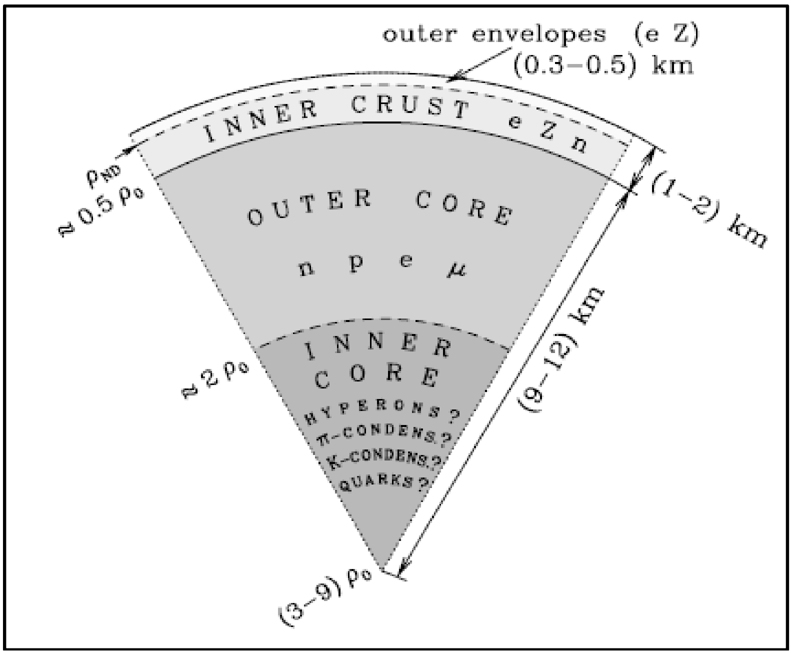

Figure 1-7: The cross-section through the interior of a NS [Hae07]:

Today, neutron stars come in various ‡avours depending on the composition of the core. In this respect, we speak now of traditional neutron stars (or hadronic stars), where the core mainly consists of neutrons, protons and electrons. For given mass, the traditional neutron star has the biggest radius, while neutron stars including quark cores are found to be more compact. Strange stars have the smallest radii.

Pulsars

Pulsars are born in supernova explosions of massive stars; they are highly magnetized, rotating neutron stars which emit a narrow radio beam along the magnetic dipole axis. As the magnetic axis is inclined to the rotation axis, the pulsar acts like a cosmic light-house emitting a radio pulse that can be detected once per rotation period when the beam is directed towards Earth (Fig.1 ¡ 9). For some very fast rotating pulsars, the so-called millisecond pulsars, the stability of the pulse period is similar to that achieved by the best terrestrial atomic clocks:

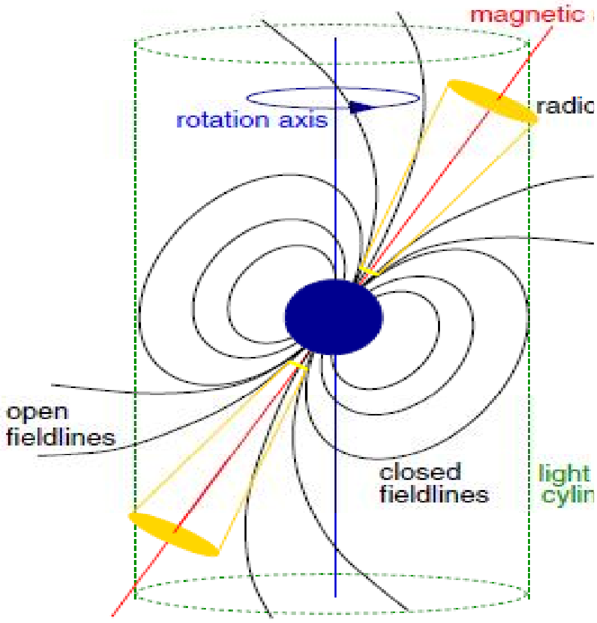

Figure 1-8: The pulsar, a rotating, highly magnetised neutron star[Kar04]:

1.3 *Magnetic and electric …elds of these degenerate stars*

Magnetism is one of the most pervasive features of the universe, it is perhaps the single most important quantity that determines the various observational manifestations of degenerate stars. Thus it is natural that a large amount of work has been devoted to the study of white dwarf and neutron stars magnetic …eld evolution, and also the origin of even magnetic …eld.

Moreover, there are strong electric …elds present caused by free electrons and ions in the stellar atmospheres. In addition to their in‡uence on the binding energies and oscillator strengths, these electric …elds might be responsible for further variations in the transition probabilities.We shall turn to this point later in chaprter 4.

1.3.1 *White dwarf stars magnetic …eld*

Magnetic …elds in white dwarfs, its surface's strength is about 1 million gauss (100T), were predicted by ***P.M.S.Blackett*** in 1947; he had proposed that an uncharged, rotating body (star or planet) should generate a magnetic …eld proportional to its angular momentum ¹ = BR^3, with surface …eld B and radius R. This law (***Blackett e¤ect***) was never generally accepted, and in 1950 even ***Blackett*** refuted it.

Another possibility was proposed by ***Ginzburg*** and ***Woltjer*** (1964). They argued that if the magnetic ‡ux, which is proportional to BR^2, is conserved during evolution and collapse, very strong magnetic …elds can be reached in degenerate stars. Hence a main sequence star with a radius $R = 10^{11}$cm and a surface magnetic …eld of 1 ¡ 10kG can therefore become a white dwarf ($R = 10^9$cm) with a magnetic …eld strength of 10^5 ¡ 10^7G.

In this case of magnetic white dwarfs (with measured …elds in the range 3 £ 10^4 ¡ 10^9G), there is strong evidence that the …elds are the remnants from a main-sequence phase.

But the absence of detectable magnetic …elds in the majority of white dwarfs is puzzling. Hence, the possibility that they are born with strong magnetic …elds which subsequently decay has been explored.

At present, there is no known viable mechanism for the generation of white dwarf magnetic …elds after they are born[Chan92].

Thus, in the absence of a satisfactory theory for the origin of the degenerate star's magnetic …elds, ‡ux conservation remains an attractive hypothesis.

The goal of magnetic white dwarf spectroscopy is to determine the …eld strength, the detailed geometry of the magnetic …eld, and the rotational period of the star (which is very di¢cult to measure in non-magnetic white dwarfs). The results provide important constraints for the theory of the origin of magnetic white dwarfs[Sch02]:

1.3.2 *Neutron stars magnetic field*

Neutron stars are the densest objects known (excluding of course black holes, for which density is not properly defined at all), and also have the strongest magnetic fields, with field strengths of around 10^{8-9}G for millisecond pulsars, 10^{11-13}G for classical radio and X-ray pulsars, and perhaps as much as 10^{14-15}G for the so-called magnetars.

Another interesting feature of these objects is the correlation between field strength and age, with magnetars, classical (radio) pulsars and high-mass X-ray binaries are relatively young, 10^{3-7} year old, but millisecond pulsars and low-mass X-ray binaries are much older, 10^{8-10} year old.

The magnetic fields of neutron stars were most likely already present at birth. The traditional fossil field hypothesis suggests that the magnetic field is inherited from the progenitor, with magnetic flux conserved and field amplified during core collapse.

If magnetic flux is assumed to be conserved during the evolution of the red giant and collapse of the core, then the neutron star or white dwarf produced would have comparable magnetic fluxes.

Other idea of field evolution considered that, the fields are generated in the crust of the neutron stars after they are born. Note, however, that this model does require the star to be born with a weak seed field whose origin is unexplained.

Regarding the origin of these fields, *Blandford, Applegate & Hernquist* 1983, *Wiebicke & Geppert* 1996 consider the possibility that the temperature gradients, which are enormous in the first few thousand years of the neutron stars life, act as a battery, generating substantial fields, this process is called thermoelectric effect.

We note that, even fields as large as 10^{15}G do not require any dynamo or battery effects, but may have been amplified by nothing more exotic than simple compression of the first magnetic field.

Once the field was generated in the crust, it was assumed to decay in a few million years. Despite this proposal provided an explanation as to why few pulsars are found in supernova remnants, since it was shown that it would take typically about $10^4 - 10^5$ yr for the field to be created from a field of about 10^9G, but a difficulty with this model is that the Crab pulsar is only 1000 yr old and has a strong magnetic field of $\sim 4 \times 10^{12}$G [Ali06].

The most plausible explanation for this problem is that all neutron stars start out with relatively strong fields, which then gradually decay away. This in turn raises two questions, namely (i) what is the origin of these very strong initial fields?, and (ii) what is the mechanism responsible for the subsequent decay?

If the neutron star was born with a strong magnetic field because of, for example, flux conservation and the field penetrated the regions interior to the crust where the electrical conductivity is very high, then mechanisms other than simple decay had to explain the field decay. It was therefore proposed that convective instabilities could take place in the degenerate interior of a neutron star. Thus, the external field would decay on a time scale of a few million years[Chan92]:

We turn now to discuss the second question. There are again some suggestions trying to resolve this problem; one suggestion is that accretion of mass from a binary companion is somehow responsible. What motivates this suggestion is the additional observation that the field strength is correlated not only with age, but also with accretion.

This model has the attractive feature in that it can be used to explain the weak magnetic fields found in binary radio pulsars and millisecond pulsars which are assumed to have been spun up by accretion.

There is (at least) one difficulty with this field decay via accretion hypothesis though, namely why do all millisecond pulsars end up with field strengths in the relatively narrow range 10^{8-9}G. That is, if this process is so efficient that it can reduce the field by some four to five orders of magnitude, why should it suddenly and consistently stop once the field reaches 10^{8-9}G. We are motivated therefore to find an alternative mechanisms.

Other researchers said that the amount of field decay should increase with the amount of mass accreted, but the X-ray binary pulsars show that it has accreted large amount of matter, while the recent observations of X-ray binaries do not show any correlation between magnetic field and amount of matter accreted; they are similar pulsars have essentially the same period of 1.6ms, and therefore similar amounts of accreted mass, but have different magnetic fields.

Thus, in the absence of a satisfactory theory for the origin of the magnetic fields of degenerate stars, flux conservation remains an attractive hypothesis. The principal difficulty with this hypothesis is that it is a formidable challenge to estimate quantitatively the magnetic field of the red giant core given an initial main-sequences tar with a prescribed …eld[Kar04]:

Finally, We conclude, from stellar matter to the surfaces of magnetic white dwarfs and NSs, that these stars are very interesting objects from an astronomical point of view, since they o¤er the opportunity to study important astrophysical processes as di¤usion, pulsation, accretion, energies,.... But they are also fascinating for a physicist, because they o¤er conditions that cannot, or not easily be achieved in terrestrial laboratories.We recall that the magnetic …eld (B) can be measured directly by the observation of cyclotron lines, or indirectly by the spin-down rate of pulsars assuming a dipole magnetic con…guration.

Thus, the e¤ect of strong magnetic and electric …elds on atoms, which is the topic of this work, is very imprtant to make a good knowledge about compact object's structure.

Chapter 2

Hydrogen atom in weak external ...elds

2.1 *The hydrogen atom structure*

The origins of atomic physics were entwined with the development of quantum mechanics itself ever since the ...rst model of the hydrogen atom by Bohr. This introductory chapter surveys a classical treatment of the early atomic physics such as the spectrum of atomic hydrogen and the Bohr model, and later we shall describe the quantum theory of one electron atom.

2.1.1 Spectrum of atomic hydrogen

In the following, we shall take up the analysis of the spectra of hydrogen atom, where the most important sources of information about the electronic structure and composition of atoms are spectra in the visible, infrared, ultraviolet, x-ray, microwave and radio frequency ranges.

It has long been known that the spectrum of light emitted by an element is characteristic of that element. This crude form of spectroscopy, in which the colour is seen by eye, formed the basis for a simple chemical analysis.

The most important discovery in the search for regularities in the line spectra of atoms was made by J. Balmer in 1885, who showed that the frequencies of a series of lines in the visible part of the spectrum of atomic hydrogen were among those given by the empirical formula:

$$\nu = R\left(\frac{1}{n^2} - \frac{1}{n'^2}\right) \tag{2.1}$$

where n and n' are whole numbers with $n' > n$; R is a constant that has become known as the Rydberg constant.The corresponding Rydberg constant for hydrogen atom has the value:

$$R(\infty) = \frac{m_e}{4\pi\hbar^3 c}\left(\frac{e^2}{4\pi\varepsilon_0}\right)^2 = (109737.318 \pm 0.012)\,\mathrm{cm}^{-1} \tag{2.2}$$

Here we have written $R(\infty)$ to recall that, we are using the infinite nuclear mass approximation and it is usual in the spectroscopy to give the frequencies in terms of inverse wavelengths (wave numbers): $\tilde{\nu} = \frac{1}{\lambda} = \frac{\nu}{c}$.

In reality both the electron and proton move around the centre of mass of the system. For a nucleus of finite mass M the equations are modified by replacing the electron mass m_e by its reduced mass.

For hydrogen atom

$$R = R_\infty \frac{M_p}{m_e + M_p} \simeq R_\infty\left(1 - \frac{m_e}{M_p}\right) \tag{2.3}$$

The electron-to-proton mass ratio is $m_e/M_p = 1/1836.15$; so because of the nuclear mass effect, there is an isotopic shift between the spectral lines of different isotopes of the same element.

The observed spectral lines in hydrogen can all be expressed as differences between energy levels, where the energies are proportional to $1/n^2$. For a given value of n, the set of transitions from $n' = n+1, n+2, \ldots$ constitutes a series of lines, and these series bear the names of their discoverers or principal investigators as it shows in Fig.$(2-1)$:

The fundamental relation between the terms of an atom and its structure was first recognized by Bohr who postulated that an electron in a stable orbit does not radiate electromagnetic energy, and that radiation can only take place when a transition is made between the allowed energy levels.

A second equation is obtained from Bohr's postulate that the orbital angular momentum is quantized: $L = mvr = n\hbar$ with $n = 1, 2, 3, \ldots$.

Figure 2-1: Energy levels of hydrogen atom [Foo05]:

Then we can easily find the famous Bohr formula:

$$E_n = -\frac{e^2/4\pi\varepsilon_0}{2a_0}\frac{1}{n^2} \tag{2.4}$$

Bohr's theory was a great breakthrough. It was such a radical change that the fundamental idea about the quantization of the orbits was at first difficult for people to appreciate.

2.1.2 Non-relativistic *quantum mechanical study of hydrogen atom*

In the following, we begin our quantum mechanical study of atomic structure by considering the simplest atom, namely the hydrogen atom, which consists of a proton and an electron.

Our starting point is the Schrödinger equation for one-electron atoms. After that we will solve this equation in spherical polar coordinates, and obtain the energy levels and wave functions of the discrete spectrum. We then treat the fine structure and the Lamb shift.

α: *The Schrödinger equation for hydrogen atom*

The simple hydrogen atom had a great influence on the development of quantum theory. The solution of the Schrödinger equation for a Coulomb potential is in every quantum mechanics textbook and only a brief outlines are given here.

The Schrödinger equation for an electron of mass m in a spherically-symmetric potential is:

$$\left(\frac{-\hbar^2}{2m}\Delta + V(r)\right)\psi = E\psi \tag{2.5}$$

In this case the potential energy of a particle is:

$$V(r) = \frac{-e^2}{4\pi\varepsilon_0 r}$$

We recall that in equation (2.5), we are using the infinite nuclear mass approximation.

In spherical polar coordinates we have:

$$\nabla^2 = \frac{1}{r^2}\frac{\partial}{\partial r}\left(r^2\frac{\partial}{\partial r}\right) - \frac{1}{r^2}L^2 \tag{2.6}$$

where the angular momentum square operator L^2 contains the terms that depend on θ and φ.

As far as operators L^2 and L_z commute, they have a common set of eigenfunctions (with $\hbar = 1$):

$$L^2\psi_{lm}(r;\theta;\varphi) = l(l+1)\psi_{lm}(r;\theta;\varphi); \qquad L_z\psi_{lm}(r;\theta;\varphi) = m_l\psi_{lm}(r;\theta;\varphi) \tag{2.7}$$

The analysis has shown that in the case of particle motion in the spherically symmetric potential the wave function can be taken in the form:

$$\psi_{E;l;m}(r;\theta;\varphi) = R_{E;l}(r)Y_{lm}(\theta;\varphi) \tag{2.8}$$

Here $Y_{\ell m}(\theta;\varphi)$ are the standard spherical harmonics and $R_{El}(r)$ the radial wave functions;

solution of the radial equation:

$$\left(\frac{-\hbar^2}{2m}\left(\frac{1}{r^2}\frac{d}{dr}\left(r^2\frac{d}{dr}\right)-\frac{l(l+1)}{r^2}\right)-\frac{e^2}{(4\pi\varepsilon_0)\,r}\right)R_{E;l}(r)=E R_{E;l}(r) \tag{2.9}$$

We can simplify eq(2.9) by introducing the new unknown function $U_{E\ell} = rR_{E\ell}(r)$: where we find that:

$$\frac{d^2U_{E;l}}{dr^2}+\frac{2m}{\hbar^2}\left[E-V_{eff}\right]U_{E;l}(r)=0 \tag{2.10}$$

With

$$V_{eff}=\frac{-e^2}{(4\pi\varepsilon_0)\,r}+\frac{l(l+1)\hbar^2}{2mr^2} \tag{2.11}$$

The effective potential is given in the following figure (Fig $2-2$).

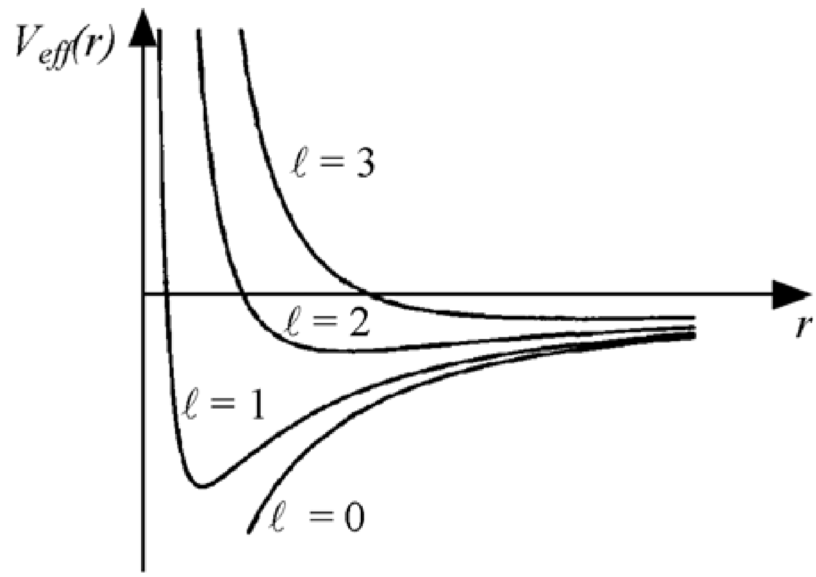

Figure 2-2: The effective potential ($l = 0;1;2;3$)[Bra83]:

It is clear that since V_{eff} tends to zero for large r, the solution $U_{E;l}(r)$ for $E > 0$ will have an oscillatory behaviour at infinity and will an acceptable eigenfunction for any positive value of E (unbound states).

For the moment, we will only be concerned with the bound states corresponding to $E < 0$ (discrete spectrum).

After calculations, we find that the energy levels predicted by the Schrödinger theory for hydrogen atom agree with those already obtained using Bohr model, i.e; $E_n = -\frac{e^2/4\pi\epsilon_0}{2a_0}\frac{1}{n^2}$. However, the Schrödinger theory has much more predictive power than the old quantum theory since it also yields the eigenfunctions of the discrete spectrum[Ana06].

The energy does not depend on l; this accidental degeneracy of wavefunctions with different l is a special feature of Coulomb potential, it is removed if the dependence of the potential on r is modified. In contrast, degeneracy with respect to the magnetic quantum number m_l arises because of the system's symmetry (central potential), i.e. an atom's properties are independent of its orientation in space, in the absence of external fields. The total degeneracy of the energy level E_n (neglecting spin) is:

$$\sum_{l=0}^{n-1}(2l+1) = 2\frac{n(n-1)}{2} + n = n^2 \tag{2.12}$$

The normalized radial functions for the bound states of hydrogen atom may be written as:

$$R_{n,l}(r) = -\left[\left(\frac{2}{na_0}\right)^3 \frac{(n-l-1)!}{2n[(n+l)!]^3}\right]^{\frac{1}{2}} e^{-\frac{\rho}{2}}\rho^l L_{n+l}^{2l+1}(\rho) \tag{2.13}$$

We note that $L_{n+l}^{2l+1}(\rho)$ is the associated Laguerre polynomial, a_0 is the first Bohr radius and $\rho = \frac{2r}{na_0}$. [Blo04].

β: *Electromagnetic transitions*

β:1: ***Electric dipole transitions:*** The theory of atomic spectra divides itself rather sharply into two parts: the theory of the energy levels and the corresponding states, and the theory of the radiative process whereby the spectral lines arise through transitions between states.

We shall now consider how transitions between the stationary states occur when the atom interacts with an electromagnetic radiation that produces an oscillating electric field $\mathbf{F}$.

The result of time-dependent perturbation theory is encapsulated in the golden rule (or Fermi's golden rule); this states that the rate of transitions is proportional to the square of the matrix element of the perturbation.

The Hamiltonian that describes the time-dependent interaction with the field F is:

$$H' = e\vec{r}.\vec{F} \tag{2.14}$$

This interaction with the radiation stimulates transitions from state $|1\rangle$ to state $|2\rangle$ at a rate:

$$W \propto |eF_0|^2 . |\langle 2|\vec{r}.\hat{e}_{rad}|1\rangle|^2 \tag{2.15}$$

$|F_0|$ is the constant of amplitude and $\hat{e}_{rad}$ is the polarization vector.

We denote that, the dipole approximation involves that the exponential function, occured in field F expression, equals to the unity:

We write the dipole matrix element as the product:

$$\langle 2|\vec{r}.\hat{e}_{rad}|1\rangle = D_{12} \times I_{ang} \tag{2.16}$$

here the radial integral is:

$$D_{12} = D_{21} = \int_0^{\infty} R_{n',l'}(r) r R_{n,l}(r) r^2 dr \tag{2.17}$$

and the angular integral is:

$$I_{ang} = \int_0^{2\pi}\int_0^{\pi} Y^*_{l',m'}(\theta,\varphi)\, \hat{r}.\hat{e}_{rad} Y_{l,m}(\theta,\varphi) \sin\theta\, d\theta\, d\varphi \tag{2.18}$$

where $\hat{r} = \vec{r}/r$.

β.2.*Selection rules:* Not all transitions between states are allowed. The selection rules for electric dipole transitions are based on an examination of the transition dipole moment between the two states of interest. They are established by identifying the conditions under which the transition dipole moment is non-zero, corresponding to an allowed transition, or zero, for a forbidden transition.

The transition dipole moment for a transition between states $|i\rangle$ and $|f\rangle$ is defined as:

$$\mu_{if} = \langle f|\mu|i\rangle \tag{2.19}$$

where $\mu = -e.\mathbf{r}$ is the electric dipole operator.

The selection rules that govern allowed transitions arise from the angular integral I_{ang} which contains the angular dependence of the interaction for a given polarization of the radiation[Foo05].

In order to study the expression $|\mathbf{r}.\hat{e}_{rad}|$ in eq.(2.15), it is convenient to induce the spherical components of the vectors $\hat{\epsilon}$ and $\mathbf{r}$ (more details will express in chapter 4), with the scalar product can be expressed in terms of spherical components as:

$$\hat{e}.\mathbf{r} = \sum_{q=0,\pm1} \hat{e}_q . I^q_{n'l'm';n,l,m} \tag{2.20}$$

where

$$I^q_{n'l'm';nlm} = \left(\frac{4\pi}{3}\right)^{\frac{1}{2}} \int_0^\infty dr\, r^3 R_{n'l'}(r) R_{nl}(r) . \int d\Omega\, Y^*_{l'm'}(\theta,\varphi) Y_{1,q}(\theta,\varphi) Y_{lm}(\theta,\varphi) \tag{2.21}$$

The angular integrals are only non-zero for certain values of (l,m) and (l',m') , giving rise to selection rules.

We can prove that this quantity is only non-vanishing if $l' = l \pm 1$ which is the orbital angular momentum selection rule for electric dipole transition.

We shall consider separately the two cases $q = 0$ and $q = \pm1$, which correspond respectively to radiation polarized parallel and perpendicular to the Z-axis.

- $q = 0$ (polarization vector in the Z direction):

The matrix element $I^q_{n',l',m';n,l,m}$ vanishes unless: $m = m'$ i.e. $\Delta m = 0$, for this polarization, the magnetic quantum number does not change, this transition called π-transition.

- $q = \pm1$ (propagation vector $\mathbf{K}$ in the Z direction)

For this case, the matrix element $I^q_{n',l',m';n,l,m}$ vanishes unless: $m' = m \pm 1$, thus the selection rule for this σ-transitions is $\Delta m = \pm1$. Then, the selection rules are determined by the properties of the matrix element for the angular wave function which give $\Delta l = \pm1; \Delta m = 0, \pm1$ [Smi03].

¯:3:***Oscillator strength:*** **The concept of the oscillator strength arises from a model of the electric properties of matter in which we suppose that the atomic electrons are in equilibrium positions. Thus, the electrons execute simple harmonic motion around their equilibrium positions. Actually, electrons do not have …xed equilibrium positions in atoms.**

It is of interest to remark that the oscillator strength, as the name suggests, has its origin in the classical theory where an atom emitting or absorbing radiation is modelled by a set of oscillators interacting with the classical …elds:

The oscillator strength f_{ki} for a transition $k \rightarrow i$ is de…ned by:

$$f_{ki} = \omega_{ki} \, |\langle \mathbf{k} | \mathbf{r} | \mathbf{i} \rangle|^2 \text{ in a.u.} \tag{2.22}$$

where $\omega_{ki} = (E_k - E_i)$ in a.u. (i.e; $m_e = a_0 = \hbar = e = 1$).

If the transition is from a lower state to an upper state (absorption), then the oscillator strength is positive.

The oscillator strength is a dimensionless quantity and it satis…es the following important identity, known as the *Thomas-Reiche-Kuhn (TRK) sum rule*:

$$\sum_k f_{ki} = Z \tag{2.23}$$

Where Z is the total number of atomic electrons. In this equation, the sum is over all levels (states) permitted by the dipole selection rules, including the continuum. If the sum is restricted only to those transitions in which valence electrons take part, then Z is the number of valence electrons in the atom[V la97] .

2.1.3 *Breaking the accidental degeneracy*

To this point, our discussion of the hydrogen atom has centred on the eigenstates and their energies,but there are, however, corrections to these energies that are caused by e¤ects not included in the Schrödinger equation.

These corrections are conveniently characterized by their magnitudes in terms of the …ne-

structure constant α, then may write the total energy of the hydrogen atom as:

$$E_{TOTAL} = E_n + E_{FS} + E_{Lamb} + E_{hfs} \tag{2.24}$$

where E_n is the Bohr energy: $E_n = -\left(\frac{1}{2}\right) m_e c^2 \alpha^2 / n^2$.

The remaining terms in Eq.(2.24) are referred to as fine-structure, the Lamb shift and the hyperfine structure respectively , where the last term will not be treated here due to its small contribution[Bur06]:

α: *Fine structure of hydrogen atom*

The most rigorous way of obtaining the relativistic corrections to the Schrödinger energy levels of hydrogen atom is to solve the Dirac equation for an electron in the central field. On the other hand, neither the Lamb shift nor the hyperfine corrections are inherent in the Dirac equation. The Lamb shift requires quantization of the electromagnetic field, whereas the proton spin is absent from the Dirac Hamiltonian.We deal with these corrections later.

Now we look at how to calculate fine structure by treating relativistic effects as a perturbation to the solutions of the Schrödinger equation. This approach requires the concept that electrons have spin.

We shall therefore start from the Hamiltonian $H = H_0 + H'$ where

$$H_0 = \frac{p^2}{2m} - \frac{e^2}{4\pi\varepsilon_0 r} \tag{2.25}$$

The perturbation term can be written as:

$$H' = H'_{rel} + H'_{so} + H'_D \tag{2.26}$$

With:

• $H'_{rel} = -\frac{p^4}{8m^3c^2}$ is a relativistic correction to the kinetic energy due to the relativistic motion.

By using the perturbation theory, the energy correction due to this term is given by:

$$\Delta E_{rel} = -E_n \frac{\alpha^2}{n^2}\left[\frac{3}{4} - \frac{n}{l+\frac{1}{2}}\right] \tag{2.27}$$

$\varepsilon H'_{so} = \dfrac{1}{2m^2c^2}\dfrac{1}{r}\dfrac{dV}{dr}\vec{L}.\vec{S}$: represents the spin-orbit interaction. It results from a magnetic interaction between the orbital moment and the intrinsic moment of the electron. After introducing the total electron momentum, as a new quantum number (sum of the orbital and spin momentum), we find the energy correction due to this term as:

$$\Delta E_{so} = -E_n \frac{\alpha^2}{2nl\left(l+\frac{1}{2}\right)(l+1)} \begin{cases} l \text{::::::::::::::::for} & j = l+\frac{1}{2} \\ -l-1\text{:::::::::::for} & j = l-\frac{1}{2} \end{cases} \tag{2.28}$$

$\varepsilon H'_D = \dfrac{\pi\hbar^2}{2m^2c^2}\left(\dfrac{e^2}{4\pi\varepsilon_0}\right)\delta(r)$: is the Darwin term.

The spin-orbit interaction is proportional to $\vec{S}.\vec{L}$; accordingly; there is no correction when the orbital angular momentum is zero. There is, however, an additional correction term that pertains only when the orbital angular momentum is zero. This effect, which arises naturally in the solution to the Dirac equation, has no classical analogue; it is caused by the singularity of the potential in $r = 0$.Using the perturbation theory we get the energy correction:

$$\Delta E_D = -E_n \frac{\alpha^2}{n};\text{::::::}l = 0 \tag{2.29}$$

If we examine the limit of ΔE_{so} for $j = +1/2$ as approaches zero, we obtain:

$$\begin{aligned} \lim_{l \to 0} \Delta E_{so} &= -\frac{1}{2}\alpha^2 E_n \lim_{l\to 0}\left[\frac{1}{n(l+1/2)(l+1)}\right] \\ &= -\alpha^2 E_n \frac{1}{n} = \Delta E_D \end{aligned} \tag{2.30}$$

For the hydrogen atom, all these corrections, which are of comparable magnitude, are small compared to the Energy E_n. One can therefore combine the three effects to obtain the total energy:

$$E_{nj} = E_n\left[1 + \frac{\alpha^2}{n^2}\left(\frac{n}{j+1/2} - \frac{3}{4}\right)\right]\text{:::::::::::::;}\, j = l \pm 1/2 \tag{2.31}$$

The Fig.(2 − 3) shows the theoretical positions of the hydrogen's energy levels calculated by the fully relativistic theory of Dirac for $n = 3$.[Foo05] .

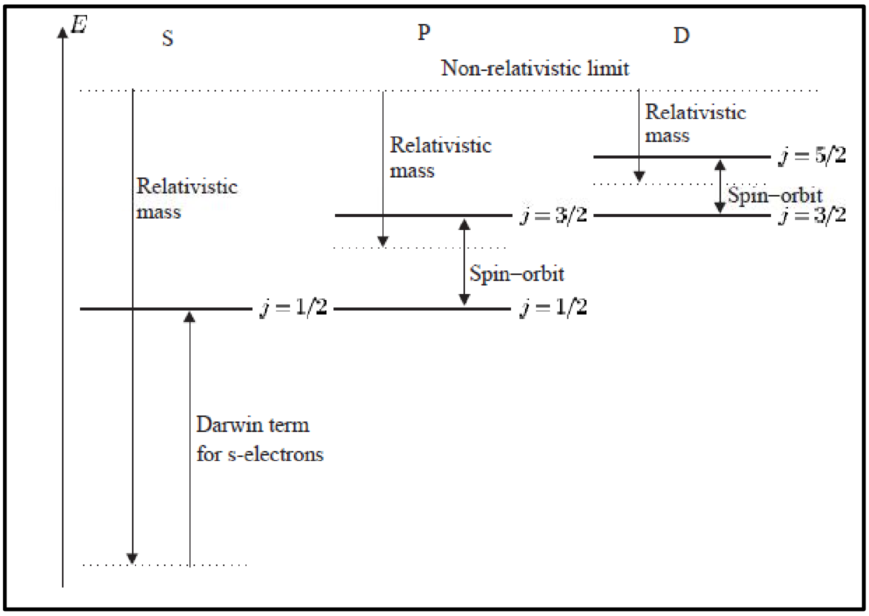

Figure 2-3: The theoretical positions of the energy levels [Foo05]:

There is also an additional rule that prevents some transitions; this rule depends on the change of the total angular momentum quantum number in an electric dipole transition which obeys to $\Delta j = 0; \pm 1$ and $\Delta m_j = 0; \pm 1$.

¯: *The Lamb Shift*

In the years 1947 -1952, *Lamb* and *Rutherford* showed that even the relativistic Dirac theory do not completely describe the hydrogen atom. They used the methods of high-frequency and microwave spectroscopy to observe very small energy shifts and splitting in the spectrum of atomic hydrogen. In other words, they used microwave techniques to stimulate a direct radio-frequency transition between the $2S_{1/2}$ and $2P_{1/2}$ levels.

They could, in this way, observe energy differences between terms with the same j, namely differences of $0.03 cm^{-1}$, this corresponds to a difference of 900 MHz between $2S_{1/2}$ and $2P_{1/2}$.

The Fig(2 − 4) represents the fine structure of the $n = 2$ level in the hydrogen atom according to Bohr, Dirac and quantum electrodynamics taking into account the Lamb shift.

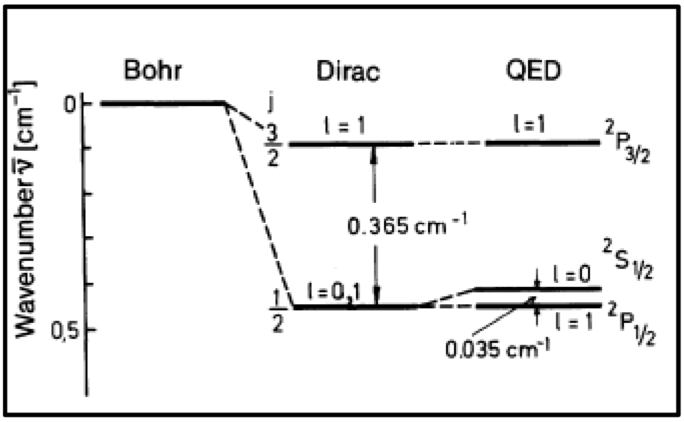

Figure 2-4: Splitting of the doubled $2p_{1/2}$ - $2s_{1/2}$ [Gor06].

Like the fine structure, this small energy shift was not observable by means of optical spectroscopy of hydrogen, because the Doppler broadening of the spectral lines due to the motion of the atom exceeded the magnitude of the splitting.

The explanation of this Lamb shift goes beyond relativistic quantum mechanics and requires quantum electrodynamics (QED). An intriguing feature of QED is so-called vacuum fluctuations-regions of free space are not regarded as being completely empty but are permeated by fluctuating electromagnetic fields.

In a mathematical treatment, these vacuum fluctuations correspond to the zero-point energy of quantum harmonic oscillators, i.e. the lowest energy of the modes of the system is not zero but $\hbar\omega/2$ .In other words, when quantizing the electromagnetic field, the basis set is that of a harmonic oscillator for which there is a zero-point energy. Thus, the absence of any field, the vacuum state, has non-zero energy. This means that even in the vacuum state charged particles are affected by an electromagnetic field.

The principal significance of the Lamb shift is such that it was one of the first real confirmations of the vacuum nature and allows one to present a vacuum as a set of zero oscillations of electromagnetic waves, where in this theory, the corrections to the Dirac theory are obtained by taking into account the interaction of the electron with the quantized electromagnetic field.

2.2 *The Hydrogen atom in external weak fields*

In practical terms, an atom's spectrum acts as its signature, so it is important to understand how magnetic and electric fields alter the structure's characteristics of an atom .

In this section, a summary of the basic non-relativistic theory of electrons and hydrogen atom in external magnetic and electric fields is given. Extensions to the case of very strong fields are then treated for both types of fields in the next chapter.

In this section, we shall consider how the application of magnetic and electric fields can affect the energy levels and hence, the spectra of hydrogen atom. We shall describe two effects: the Zeeman effect is the response to a uniform magnetic field and the Stark effect is the response to a static electric field.

2.2.1 *Charged particle in external electromagnetic field*

The non-relativistic Hamiltonian for an electron in an external field is:

$$H = \frac{1}{2m}\left(\mathbf{P} + e\mathbf{A}\right)^2 - \boldsymbol{\mu}_S.\mathbf{B} + eV \qquad (2.32)$$

Where $\mathbf{A}$ is the vector potential and V is the scalar potential. The second term in this equation must be included to account for the interaction of the electron magnetic moment with an external magnetic field.

We choose the gauge $\nabla.\mathbf{A} = 0$ in which, the momentum operator $\mathbf{P} = -i\hbar.\nabla$ and the vector potential $\mathbf{A}$ commute.

Here, $\mathbf{B}$ is an uniform magnetic field with vector potential $\mathbf{A} = \frac{1}{2}\mathbf{B}\wedge\mathbf{r}$ and $\boldsymbol{\mu}_S$ is the magnetic moment of the electron in which: $\boldsymbol{\mu}_S = -g_e\mu_B.\mathbf{S}/\hbar$ where $\mu_B = \frac{e\hbar}{2m}$ is the Bohr magneton and g_e is the electron g-factor.[Gor06].

The time-independent Schrodinger equation for a hydrogen atom in an electromagnetic field reads:

$$H\psi(\mathbf{r}) = \left[-\frac{\hbar^2}{2m}\nabla^2 - \frac{e^2}{(4\pi\varepsilon_0)\,r} - \frac{i\hbar e}{m}\mathbf{A}.\nabla + \frac{e^2}{2m}\mathbf{A}^2\right]\psi(\mathbf{r}) \qquad (2.33)$$

where we have neglected the reduced mass effects.

We shall treat the weak field case in which, the term in $\mathbf{A}^2$ is small compared with the term in $\vec{A}$. Accordingly, we shall drop the term in $\vec{A}^2$ and treat the linear term as a small perturbation.

2.2.2 *Hydrogen atom in an external uniform magnetic field (*Zeeman effect)

In 1896, *P.Zeeman* observed that the spectral lines of atoms split in the presence of an external magnetic field. We shall now divide the discussion of magnetic field effects into two parts: uniform strong and weak magnetic fields.

From the last equation, the linear term and the quadratic term in $\vec{A}$ can be written respectively as:

$$\frac{e}{2m}\vec{B}.\vec{L} \qquad \text{and} \qquad \frac{e^2}{8m}\left[B^2r^2 - \left(\vec{B}.\vec{r}\right)^2\right].$$

We can prove that the ratio of the quadratic to the linear term is about: $B.10^{-6}$ where B is expressed in tesla(T). In the laboratory, the fields encountered do not exceed $\sim 50T$, so that for most purpose the quadratic term is negligible.

The atom's magnetic moment has orbital and spin contributions:

$$\vec{\mu} = -\mu_B\vec{L}/\hbar - g_e\mu_B\vec{S}/\hbar \tag{2.34}$$

The interaction of the atom with an external magnetic field is described by:

$$H_{ZE} = -\vec{\mu}.\vec{B} \tag{2.35}$$

the energy associated with the coupling of the magnetic moment to an external magnetic field is given by:

$$-\vec{\mu}.\vec{B} = \frac{e}{2m}\left(\vec{L} + 2\vec{S}\right).\vec{B} \tag{2.36}$$

The complete Schrödinger equation for hydrogen atom in a constant magnetic field , including the spin-orbit interaction, but neglecting the reduced mass effect, the relativistic kinetic energy correction, the Darwin term and the quadratic ($\vec{A}^2$) term, is (with $g_e = 2$):

$$\left[-\frac{\hbar^2}{2m}\vec{\nabla}^2 - \frac{e^2}{(4\pi\varepsilon_0)\,r} + \xi(r)\vec{L}.\vec{S} + \frac{\mu_B}{\hbar}\left(\vec{L} + 2\vec{S}\right).\vec{B}\right]\Psi(\vec{r}) = E\,\Psi(\vec{r}) \tag{2.37}$$

where the term $\xi(r)$ is written as:

$$\xi(r) = \frac{1}{2m^2c^2}\frac{e^2}{4\pi\varepsilon_0}\frac{1}{r^3}.$$

The nature of the solution depends on whether the magnetic field is greater or less than the spin-orbit interaction. We shall first discuss the case of strong magnetic field and then analyse the so-called 'anomalous Zeeman effect' which corresponds to weak fields[Lor03].

α.Strong fields

If the magnetic field is high enough so that the magnetic field splitting is large as compared to the fine structure splitting, the atomic quantum numbers in this case are l, s, m_l, m_S; where m_l and m_S are the projections of the angular and spin momentum onto the direction of the magnetic field.[Gar76]

Taking **B** to be along the Z- axis, we find that the level shift is given by:

$$\Delta E = \mu_B.(m_\ell + 2m_S).B_Z \tag{2.38}$$

The introduction of the magnetic field does not remove the degeneracy in l, but it remove the degeneracy in m_l and m_S, where each level with a given n splits into equally spaced terms.

In the strong-field limit, we are considering here (no spin-orbit coupling) the orbital and the spin angular momentum are constants of the motion.

In the following figure, we see the splitting of a p level into five equally spaced by a strong magnetic field.

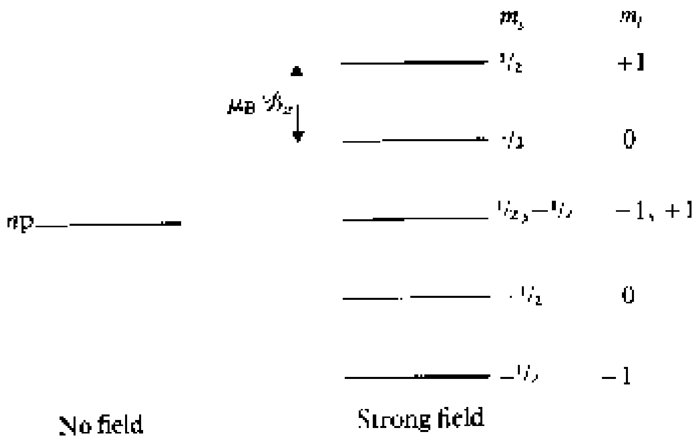

Figure 2-5: The splitting of a 'p' level [Bra83].

β: *The Paschen-Back effect*

The Paschen-Back effect arises when the interaction with an external magnetic field is stronger than the spin-orbit interaction in which we shall treat it as a perturbation . We add now to the results of the last section the first order perturbation caused by the spin-orbit term.

We see that the perturbation is just : $\xi(r)\mathbf{L}\cdot\mathbf{S}$, and its contribution to the total energy is therefore (with $\ell \neq 0$):

$$\Delta E = \int r^2 dr\,[R_{nl}(r)]^2\,\xi(r)\langle l\tfrac{1}{2}m_l m_s\,|\,\mathbf{L}\cdot\mathbf{S}\,|\,l\tfrac{1}{2}m_l m_s\rangle = \zeta_{nl}m_l m_s \qquad (2.39)$$

The quantity ζ is given by:

$$\zeta_{nl} = \hbar^2\int r^2 dr\,[R_{nl}(r)]^2\,\xi(r).$$

γ. Weak field: the anomalous Zeeman effect

One speaks of the anomalous Zeeman effect when the interaction caused by the external magnetic field is small compared with the spin-orbit term, therefore, the unperturbed Hamiltonian can be taken to be:

$$H_0 = -\frac{\hbar^2}{2m}\nabla^2 - \frac{e^2}{(4\pi\varepsilon_0)\,r} + \xi(r)\,\mathbf{L}.\mathbf{S} \tag{2.40}$$

and the perturbation term is (taking the magnetic field to be along the Z-axis):

$$H' = \frac{\mu_B}{\hbar}(L_z + 2S_z).B_z = \frac{\mu_B}{\hbar}(J_z + S_z).B_z \tag{2.41}$$

here, J_z is the projection of the total angular mamentum onto the direction of the magnetic field.

Using the *Wigner-Eckart* theorem, we obtain that:

$$\langle lsjm_j \mid J_z + 2S_z \mid lsjm_j\rangle = gm_j\hbar \tag{2.42}$$

where g is called *the Landé g factor* and is given by:

$$g = 1 + \frac{j(j+1) + s(s+1) - l(l+1)}{2j(j+1)}$$

The energy shift due to the weak magnetic field is given by:

$$\Delta E_{m_j} = \mu_B g m_j B_z \tag{2.43}$$

and the total energy of the level with quantum number $n; j; m_j$ of hydrogen atom in a constant magnetic field is therefore:

$$E_{n;j;m_j} = E_n + \Delta E_{n;j} + \Delta E_{m_j}$$

where E_n is the non-relativistic energy, $\Delta E_{n;j}$ is the fine structure correction and ΔE_{m_j} is the correction due to the weak magnetic field[Blo04]:

The selection rules for the splitting of spectral lines are $\Delta m_j = 0$ for components polarized parallel to the field (π components), and $\Delta m_j = \pm 1$ for those perpendicular to the field (σ components).

As a result, the anomalous Zeeman effect gives way to the normal Zeeman effect. This switch from the anomalous effect to the normal effect is called the Paschen-Back effect. In other words, when the magnetic field is steadily increased, a gradual transition takes place from the anomalous to the normal Zeeman effect; the transitional zone is referred to as that of the Paschen-Back effect.

2.2.3 *Hydrogen atom in the presence of an external electric field*

Electric fields may also have an effect on the states of an atom. This effect was studied by J.Stark and also by A. Lo Surdo in 1913 and it is known as the Stark effect.

We shall assume that the external electric field is constant over a region of atomic dimensions and its strength is large enough for fine structure effects to be unimportant (the treatment given here must be modified for electric fields $F < 10^5 V/m$; since in this case the stark splitting is the same order of magnitude as the fine structure splitting) .

If the coordinate system is chosen so that the z-axis coincides with the direction of the electric field, the Hamiltonian for the interaction is:

$$\begin{aligned} H' &= eFz = eFr\cos\theta \\ &= eFr\sqrt{4\pi/3}\,Y_{10}(\theta,\varphi) \end{aligned} \tag{2.44}$$

The internal field in an atom being of the order of a few volts over a few nm, even an external field of $10^5 V/cm$ is weak in comparison. Therefore, we expect the additional interaction to be a small perturbation[Rau03].

Since H' does not depend on the electron spin we shall use the Schrödinger hydrogenic wave functions $\psi_{nlm}(r)$ where we have set $m = m_l$.

α: *The linear Stark effect*

The linear Stark effect is a modification of the spectrum that is proportional to the strength of the applied electric field. It arises when there is degeneracy between the two wavefunctions that the perturbation mixes.

We can evaluate the action of the electric field on the basis of the perturbation theory where the electric field strength is a small parameter. Thus, a first-order perturbation calculation for the energy $E_n^{(1)} = \langle n \mid H' \mid n \rangle$ yields null results unless the unperturbed states are degenerate with states of opposite parity. So that for the ground state there is no energy shift that is linear in the electric field. In fact, we see that atomic hydrogen in the ground state cannot possess a permanent electric dipole field moment.

As in the case of high magnetic fields, the uncoupled representation is the appropriate one; we shall therefore calculate matrix elements of H' in the $\mid nlm_l m_s \rangle$ representation.

Consider the case $n = 2$, this consists of four degenerate states: $l = 0; m_l = 0; l = 1; m_l = 0 \pm 1$. Within this manifold of states there will be non-vanishing matrix elements of Y_{10} between the state with $l = 0$ and states with $l = 1$. Then a first order Stark effect in hydrogen is therefore expected.

The only non vanishing matrix elements of this perturbation are those connecting the 2s (200) and $2p_0$(210) states.

We find that the matrix element of the perturbation is:

$$\langle 2p_0 \mid H' \mid 2s \rangle = \pm 3ea_0 F$$

where the two states with $m_l = 0$ are shifted up and down symmetrically, while the states with $m_l = \pm 1$ are not affected by the electric field, thus the m degeneracy is only partially lifted.

For the hydrogen atom, assuming $F = 10^4 V/cm$, we get:

$$3ea_0 F = 1.3\ cm^{-1}$$

which is considerably larger than the fine structure splitting.

In particular, because the operator H' has a non-vanishing matrix element between the 2s and $2p_0$ states, these two states are mixed by this perturbation with the result that the metastable 2s state is contaminated by the unstable 2p state.

Figure 2-6: Splitting of the degenerate $n = 2$ levels of hydrogen atom due to the linear Stark effect [Bra83].

β. *Quadratic Stark effect*

The linear Stark effect depends on the degeneracy characteristic of hydrogenic atoms, and is not observed for many-electron atoms where that degeneracy is absent. In these atoms, it is replaced by the quadratic Stark effect, which is even weaker. The origin of the effect is the same, but now the resulting shifts in energy are proportional to F^2.

The linear term in the electric field F yields no contribution to non-degenerate states (e.g., the ground state; $n = 1$, $m = 0$). In this case, the lowest order contribution comes from the quadratic Stark effect, the contribution of the order of F^2. The quadratic perturbation to a level $E_n^{(0)}$ caused by a general electric field F can be written as:

$$E_{100}^{(2)} = e^2F^2 \sum_{\substack{n\neq 1\\ l;m}} \frac{|\langle \psi_{nlm}|Z|\psi_{100}\rangle|^2}{E_1 - E_n} \tag{2.45}$$

Upon differentiation of this expression with respect to the electric field strength, we obtain for the magnitude of the dipole moment the result:

$$D = \frac{-\partial E_{100}^{(2)}}{\partial F} = \alpha . F \tag{2.46}$$

where

$$\alpha = 2e^2 \sum_{\substack{n\neq 1\\ l;m}} \frac{|\langle \psi_{nlm}|Z|\psi_{100}\rangle|^2}{E_n - E_1}$$

is called the dipole polarizability of the atom in the state (100).

So, the energy shift under the action of the electric field is:

$$\Delta E = \frac{-\alpha F^2}{2} \tag{2.47}$$

where $\alpha = 4.50(4\pi\varepsilon_0)a_0^3$ for a free hydrogen atom, but for this atom in an electric field strength of $F = 10^8 V/m$, the corresponding shift due to the quadratic Stark effect is approximately $0.02 cm^{-1}$.

We have restricted our discussion to the ground state of hydrogen atom; similar calculations may be carried out for excited states, where the quadratic Stark effect is a correction to the linear Stark effect studied above[Smi03]:

γ. *Stark Ionization*

We shall now consider another effect due to the presence of an external electric field, namely the removal of the electron from the atom.

Consider a hydrogenic atom in a static electric field $\mathbf{F} = F.\hat{\mathbf{z}}$. The total potential acting on the electron is then:

$$V_{tot}(\mathbf{r}) = -\frac{e^2}{4\pi\varepsilon_0 r} + eFz \tag{2.48}$$

i.e. the total potential V of the electron is obtained by adding the potential energy arising from the external field to the coulomb potential of the nucleus. A schematic drawing of V is shown in the next Figure as a function of z, for x and y fixed.

Consider the z-dependence of this potential. Call $\rho = \sqrt{(x^2 + y^2)}$ and $V(z;\rho) \equiv V(x;y;z)$. Unlike the Coulomb case in which $V_{Coul}(\pm\infty;\rho) = 0$ resulting in an infinite number of bound states, now $V_{tot}(\pm\infty;\rho) = \pm\infty$.

On the z-axis, the maximum occurs at $z_{max} = -\sqrt{\frac{|e|}{(4\pi\varepsilon_0 F)}}$ for which $V(z_{max};0) = 0$.

There is then a potential barrier through which the electron can tunnel, in which the electron has a finite probability of escaping from the atom by means of the tunnel effect, and being accelerated toward the anode, so that ionization will occur[Cla05].

We note that this possibility of ionization was first pointed out by *J.Oppenheimer* in 1928. Experimentally it can be observed when the external electric field is very strong and (or) for levels with high principal quantum number.

Moreover, in the presence of an external electric ...eld, the width of the spectral lines is increased because the tunnel e¤ect, this is known as Stark broadening. The following ...gure (Fig 2-9) shows the potential V experienced by an electron interacting with a nucleus in a uniform electric ...eld, as a function of z, for $x = x_0$ and $y = y_0$ ...xed.

Figure 2-7: the total potential in the presence of an electric ...eld[Bra83]:

Chapter 3

Hydrogen atom in strong (stellar) magnetic and static electric …elds

In chapter 2, we considered the e¤ect of weak …elds (magnetic and electric …elds) on hydrogen's atomic structure. In recent decades, strong and ultrastrong magnetic and electric …elds have been observed on astronomical objects where the magnetic white dwarfs have surface …elds of $10^{2\,i\,5}$T and electric …elds of the order of $10^{6\,i\,7}$V/m, and the neutron stars have stronger magnetic …elds of the order of 10^{9}T in radio pulsars and somewhat smaller $(10^{5\,i\,7})$T in binary pulsars. These strong …elds can transform atoms into new species.

The designation of "strong …elds" applies to external static magnetic, and/or electric …elds that are su¢ciently intense to cause alterations in the atomic or molecular structure and dynamics; i.e. The term "strong …eld" characterizes a situation for which the Lorentz force is of the order of magnitude or greater than the Coulomb binding force. For a hydrogen atom in the ground state, the corresponding …eld strength cannot be reached in the laboratory, but it only exists in astrophysical objects as white dwarfs or neutron stars[Huj00]:

Our knowledge of the astronomical world is derived from the emission, absorption, and scattering of electromagnetic radiation from atoms and molecules. We touch and discern the material content of these distant objects only through such absorptions and emissions. As a result, there is a strong coupling between the subjects of astronomy and atomic physics.

We will consider in this chapter that the …eld is strong, which is associated with magnetic white dwarfs and neutron stars. They provide the impetus to understanding atoms under strong perturbations that can even alter basic structure. Thus, particularly, white dwarfs are very interesting objects from an astronomical point of view, since they are the most common end-product of stellar evolution, and they offer the opportunity to study important astrophysical processes. But they are also fascinating for a physicist, because they offer conditions that cannot, or not easily be achieved in terrestrial laboratories[Sch02].

Primary, we shall represent the units that adopted in this chapter, then we will expose the treatment of hydrogen structure in strong magnetic field; in addition, we investigate the hydrogen atom in both magnetic and electric fields.

3.1 *Hydrogen atom in stellar (strong) magnetic field*

From a physical point of view, the first appearances of the influence of a magnetic field on the atom are: i/ changes in binding energies, including the Zeeman level splitting and ii/ the development of a non vanishing quadrupole moment as a sequence of the deformation of the spherical-symmetrical atomic shape which undergo dramatic changes in comparison with the field-free case.

In this section we show some results on the binding energies of hydrogen atom in an external uniform magnetic fields, where we try to estimate its ground state and first few excited states energies focussing on the case of strong magnetic fields as are believed to exist in the atmospheres of neutron stars and white dwarfs which are the only best possibility to observe the behaviour of hydrogen atom in such fields and to compare binding energies shifts with the predictions of the theory.

3.1.1 *Atomic units*

Atomic and molecular calculations based on the Schrödinger equation are most conveniently done in atomic units (a.u.), introduced by Hartree, to avoid carrying too many numerical factors[beth57]:

In atomic units, $\hbar = m_e = e = 4\pi\varepsilon_0 = 1$:

the atomic units of length, velocity, time, and energy are then:

Length: $a_0 = \frac{4\pi\varepsilon_0\hbar^2}{m_e e^2} = \frac{\hbar}{\alpha m_e c} = 1.$

Velocity: $v_B = \frac{e^2}{4\pi\varepsilon_0\hbar} = \alpha c = 1.$

Time: $\tau_0 = \frac{16\pi^2\varepsilon_0^2\hbar^3}{m_e e^4} = \frac{\hbar}{\alpha^2 m_e c^2} = 1.$

Energy: $E_h = \frac{e^2}{4\pi\varepsilon_0 a_0} = \alpha^2 m_e c^2 = 1.$

From the definition $\alpha = \frac{e^2}{4\pi\varepsilon_0\hbar c}$, the numerical value of c is: $\alpha^{-1} = 137.03599911.$

For the lowest 1s state of hydrogen (with infinite nuclear mass), a_0 is the Bohr radius, v_B is the Bohr velocity, $2\pi\tau_0$ is the time to complete a Bohr orbit, and E_h (the *Hartree* energy) is twice the ionization energy.

So, in atomic units we have for hydrogen: $E_n = -\frac{1}{2n^2}$ a.u. and the ground state energy $(n = 1)$ is: $-1/2$ a.u.

3.1.2 *Free electrons in strong magnetic fields*

The motion of a free charged particle in an uniform magnetic field is well-known classically and quantum mechnically. In the former, the charges may be regarded as "beads on a wire", free to slide along the field lines, but confined to cyclotron orbits in their transverse motion:

Consider the non-relativistic motion of a particle (charge e and mass m) in a uniform magnetic field $\mathbf{B}$ (assumed to be along the z-axis). In classical physics, the particle gyrates in a circular orbit around the field direction with radius and (angular) frequency are given as: $r = \frac{mv}{eB}$, $\omega_c = \frac{|e|B}{m}$

If the energetic contribution of magnetic field term is large in comparison to the one made by coulomb potential then we are dealing with the motion of free electrons (Landau regime).

It is well-known that a strong magnetic field confines the particles to Landau orbits orthogonal to the field, leaving only their behaviour in the direction of the field subject to significant influence by a static potential[Ray03].

The non-relativistic Hamiltonian for an electron in an external field $\vec{A}$ is:

$$H = \frac{1}{2m}\left(\mathbf{P} + e\vec{A}\right)^2 - \mu_s.\mathbf{B} + eV \tag{3.1}$$

Where $\vec{A}$ is the vector potential , V is the scalar potential and $\mu_s = -g_e\mu_B.\mathbf{S}/\hbar$ is the

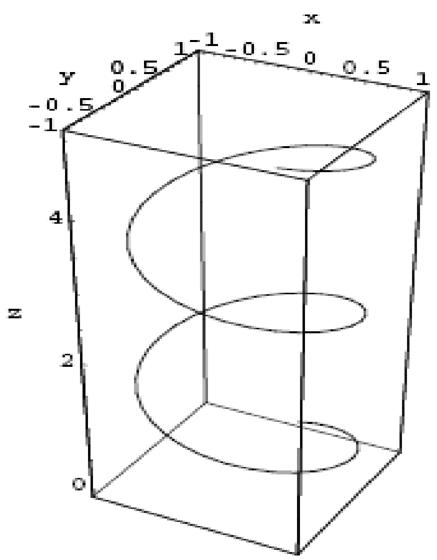

Figure 3-1: Classical orbit of an electron in magnetic field $\mathbf{B}$

magnetic moment of the electron.

Consider now the case of a free electron in a constant uniform field in the z-direction with no scalar potential, i.e., $V = 0$; this case describes an atom in the limit of strong magnetic fields such that the Coulomb interactions are negligible. For a given field, say $\mathbf{B}$ along the z-direction, different choices of $\vec{A}$ are possible.

In this case, we have: $\mathbf{B} = B.\hat{z}$ with

$$\begin{aligned} A_x &= -By \\ A_y &= A_z = 0 \end{aligned} \tag{3.2}$$

For this field, the operators $\hat{\mu}_z$ (the projection of $\vec{\mu}_s$ onto the magnetic field direction), $\hat{p}_x$ and $\hat{p}_z$ commute with the Hamiltonian and are, therefore, conserved. Calling their respective eigenvalues μ_z, p_x and p_z, with $-\infty \leq p_x; p_z \leq +\infty$; the eigenstates can be written as:

$$\Psi = e^{i(p_x x + p_z z)/\hbar}\,\varphi(y) \tag{3.3}$$

Calling $y_0 = -P_x/eB$ we get that $\varphi(y)$ satisfies:

$$-\frac{\hbar^2}{2m}\frac{d^2}{dy^2}\varphi + \frac{1}{2}m\omega_B^2(y-y_0)^2\varphi = \left(E + B_z.\mu_z - \frac{P_z^2}{2m}\right)\varphi \tag{3.4}$$

which is the Schrödinger equation for a one-dimensional harmonic oscillator with angular frequency $\omega_B = |e|B/m$.

The solutions to the last equation give the eigenstates for an electron in an external homogeneous magnetic field. They are called Landau levels with energies given by:

$$E = E_n^{\perp} + E_{p_z}^{\parallel} = \left(n + \frac{1}{2} + m_s\right)\hbar\omega_B + \frac{P_z^2}{2m} \tag{3.5}$$

with wave functions:

$$\varphi_n(y) = \frac{1}{\sqrt{\pi^{\frac{1}{2}} a_B 2^n n!}} \exp\left(-\frac{(y-y_0)^2}{2a_B^2}\right) H_n\left(\frac{y-y_0}{a_B}\right) \tag{3.6}$$

here $a_B = \sqrt{\frac{\hbar}{m\omega_B}} = \sqrt{\frac{\hbar}{eB}}$ is the cyclotron radius (or magnetic length) and the H_n are Hermite polynomials[Rau03]:

Landau energy levels $E_n^{\perp}$ correspond to a discrete set of round orbits of electron which are projected to the transverse plane. The energy $E_{p_z}^{\parallel}$ corresponds to the free motion of electron in parallel to the magnetic field (continuous spectrum), with a conserved momentum p_z along the magnetic field.

An alternative, more symmetric, choice for $\vec{A}$ is:

$$\vec{A} = (-By/2; Bx/2; 0)$$

this symmetric, cylindrical gauge, is the one of the choice in most studies of atoms in magnetic fields[Zac07]:

We may write the equation for a free electron in an external magnetic field which is satisfied by a function of the form:

$$\Psi_{nm\gamma}(r) = R_{nm}(\rho;\varphi)Z_{m\gamma}(z)\chi(s) \tag{3.7}$$

The adiabatic approximation, which is proposed by *Schiff* and *Snyder*, assumes a decoupling between the motions of the electrons parallel and perpendicular to the field. This is the case if, in classical terms, the gyration of the electron in the plane perpendicular to the field is fast in comparison with the motion along the field direction, which is caused by the Coulomb interaction with the positively charged nucleus[Eng09]:

Thus, in this adiabatic approximation, the one-electron wave function can be separated into a transverse (perpendicular to the external magnetic field) component and a longitudinal (along the magnetic field) component and the spin component, therefore we can use the ground Landau state:

$$\psi_{0m\nu}(r) = R_{0m}(\rho;\varphi)Z_{m\nu}(z)\chi(s)$$

where $Z_{m\nu}(z)$ remains to be determined. ν counts the number of nodes in the z- wavefunction, and we expect the axial wavefunctions to be different for different values of the magnetic quantum number m.

For $n = 0$, the function (the ground-state Landau wave function) has been assumed to have the form:

$$R_{0m}(\rho;\varphi) = \frac{1}{a_B^{|m|+1}\sqrt{2^{|m|+1}\pi\,|m|!}}\exp\left(-\frac{\rho^2}{4a_B^2}\right)\rho^{|m|}e^{im\varphi} \tag{3.8}$$

with these assumptions, the functions $Z_{m\nu}(z)$ must satisfy a one-dimensional Schrödinger equation[Lai01]:

We note that, for the ground level, i.e; at $n = 0$ and $m = 0$ and zero momentum of the electron in the z-direction, i.e. $p_z = 0$, $E_0^{\perp} = \frac{eB\hbar}{m}$ if $m_s = \frac{1}{2}$, and the corresponding normalized ground state wave function is:

$$R_{00} = \sqrt{\frac{1}{2\pi a_B^2}}\,e^{\frac{-\rho^2}{4a_B^2}} \tag{3.9}$$

It is convenient to define a critical field where the energy of the Landau ground state $\hbar\omega_B$ equals the characteristic energy of hydrogen. The transition to the intense magnetic field regime (IMF) occurs at:

$$B_0 = 2m_e^2\left(\frac{e}{\hbar}\right)^3 = 4.701 \times 10^9 G \tag{3.10}$$

This critical value of the magnetic field B_0 is naturally taken as an atomic unit for the strength of the magnetic field, and corresponds to the case when the pure Coulomb interaction energy of electron with nucleus is equal to the interaction energy of a single electron with the external magnetic …eld, $|E_0^{Bohr}| = E_0^{\perp} = 13.6eV$, or equivalently, when the Bohr radius a_0 is equal to the Landau radius a_B.

Equivalently, the deformation condition $a_B < a_0$ corresponds to the case when the binding energy of the hydrogen atom is smaller than the ground Landau energy $E_0^{\perp}$ [Ari02].

We note that the non-relativistic treatment of bound states is valid for two reasons:

(i): For electrons in the ground Landau level, the free electron energy reduces to

$E = m_e^2c^2 + \frac{p^2}{2m}$ for $pc << m_ec^2$; the electron remains non-relativistic in the z-direction (along the …eld axis) as long as the binding energy E_B is much less than m_ec^2.

(ii): The shape of the Landau wave function in the relativistic theory is the same as in the non-relativistic theory[Ali06].

The so-called Landau spacing of the levels in a strong …eld is the parameter β which is de…ned in the usual way as: $\beta = B/B_0$, where it is convenient to classify the …eld strength as low ($\beta \leq 10^{-3}$), intermediate or strong($10^{-3} < \beta < 1$), and intense or high ($1 \leq \beta \leq \infty$)[Thi08].

3.1.3 *Overview on some previous works on Hydrogen atom in strong magnetic …elds*

The motivation to study atoms in magnetic …elds of strength beyond the perturbation regime was in a large part due to the discovery of such …elds being present in white dwarf stars and neutron stars. At the high …eld strengths observed in these compact objects, the electron cyclotron energy of an atom becomes equal or greater than the corresponding Coulomb potential energy. In order to facilitate a proper understanding of the spectra of neutron stars and white dwarf stars, one must necessarily have more stringent bounds on the energy levels of atoms in the atmospheres of these compact objects in the intermediate regime of magnetic …eld strengths; this is the aim of the current work.

Since the 1970's the problem of the hydrogen atom in strong magnetic …eld has been tackled by various researchers using di¤erent methods.

Some researches used the …nite element method (FEM) such as Ref.[Iva00] and Ref.[Thi08], in which the Schrodinger equation can be seen as a second order partial di¤erential equation, and it was solved numerically on a computer using …nite-element techniques.

Moreover, some works used the variational method like Ref.[Gar76], and Ref.[Lop07]; while the majority of the treatises employed Landau orbitals to describe the motion of the electron perpendicular to the field. The electrons were required to reside in the ground Landau state, thereby simplifying calculations somewhat by restricting the wave functions to the so called adiabatic approximation such as: Ref.[Hey96];Ref.[Hey98];Ref.[Khr03];Ref.[Pot01], and Ref.[Bac00].

Ref.[Hey96] and Ref.[Hey98] discussed this subject by using the variational method for very strong magnetic field $\beta \gg 1$, where they found that the properties of matter are significantly modified by strong magnetic fields, as are typically found on the surfaces of neutron stars. In such strong magnetic fields, the Coulomb force on an electron acts as a small perturbation compared to the magnetic force.

Atoms attain a much greater binding energy compared to the zero-field case, because of the strong magnetic confinement of electrons perpendicular to the field.

Heyl consider that the perpendicular wave function has the same form as Landau wave function for an electron in a magnetic field, while along the direction of the magnetic field, the electron experiences an effective (averaged) potential:

$$V_{eff}(z) = \langle R | V(r) | R \rangle = \int_0^\infty -\frac{e^2}{\sqrt{z^2+\rho^2}} |R_{0m}(\rho)|^2 \, 2\pi\rho \, d\rho \tag{3.11}$$

Using the variational principle, which constrains the ground-state wave function ($\nu = 0$) along the magnetic field for a given values of m, Heyl takes the axial wave function to be a Gaussian as :

$$Z(z) = \frac{1}{\sqrt[4]{2\pi}\sqrt{a_z}} \exp\left(-\frac{z^2}{4a_z^2}\right) \tag{3.12}$$

The minimization yields the values of the binding energy for the ground state $1s_0$ of the hydrogen atom for several magnetic field strengths ($\beta \gg 1$):

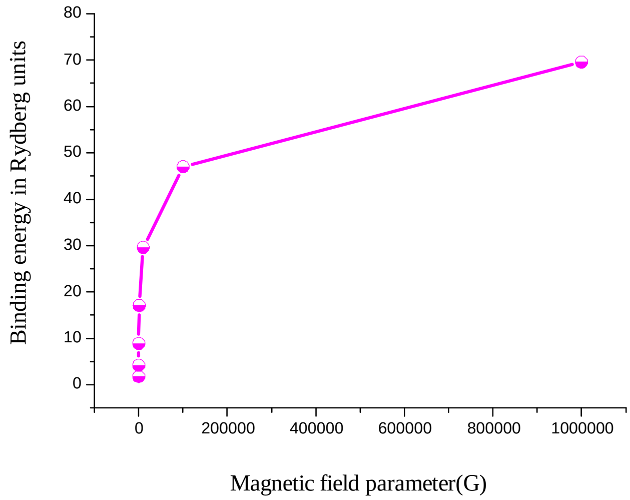

Figure 3-2: Binding energies for the ground state of hydrogen atom from [Hey96] .

—	$E_{m=0}$(Ry)
1	1:77
10	4:18
100	8:91
1000	17:1
10000	29:6
10^5	47:0
10^6	69:6

Table:1:Binding energies for the ground state of the hydrogen atom in strong magnetic …eld calculated with the axial wave function (eq.3-12) as in the Ref:[Hey96]:

From table.1 and Fig.(3 ¡ 2), we conclude that the binding energy of the ground state increases with the magnetic …eld.

3.1.4 *The diagonalization of the Hamiltonian of Hydrogen atom in strong magnetic fields*

α: *The problem of the basis choice*

The three prototypes of spectra (the discrete, the continuous and the mixed spectrum, as well as the corresponding wave functions), contain important information about the physical systems that they describe.

In section 1 of chapter 2, we restricted the treatment of hydrogen spectrum to bound states ($E < 0$); however, an attractive coulomb Hamiltonian has also unbound states ($E > 0$).

States with positive energy can escape to infinity, therefore the solution $R_{E;l}(r)$ for $E > 0$ have an oscillatory behaviour at infinity, and will be an acceptable eigenfunction for any positive value of E; so, we have a continuum spectrum.

States with negative energy, in turn, must be fully localized; thus, these states must be bound states. Therefore the spectrum of hydrogen possess a mixed spectrum consisting of a discrete series where it involves discrete values (labeled by n), and a continuous spectrum, in which the radial wave function $R_{E;l}(r)$ is characterized by a positive value E of the total energy and by the orbital quantum number l.

If the energy is positive, the wave number k, that is associated to the electron whenever it moves far from the origin, is in atomic units equal to $\sqrt{2E}$.

The radial function obtained has an asymptotic behaviour :

$$U_l(\rho = 2kr) = N_l e^{\frac{-i\rho}{2}} \rho^{l+1} \, {}_1F_1(l + 1 + i\gamma; 2l + 2; i\rho) \tag{3.13}$$

where $\gamma = -\frac{1}{\sqrt{2E}} \equiv \frac{1}{k}$ is the dimensionless constant.

$$N_l = \frac{|\Gamma(l + 1 - i\gamma)|}{2\Gamma(2l + 2)} e^{\frac{-\pi\gamma}{2}}$$

is the normalization factor, and $U_l(r) = rR_l(r)$:

We recall that

$$|\Gamma(l + 1 - i\gamma)| = \sqrt{\pi\gamma} \prod_{s=1} \sqrt{s^2 + \gamma^2} \, (\sinh \pi\gamma)^{\frac{-1}{2}}$$

The complete wave function with positive energy and with definite values of l and m reads:

$$\psi_{lm}(E;\theta;\varphi) = R_l(E;r)Y_{lm}(\theta;\varphi) \equiv \frac{1}{r}U_l(E;r)Y_{lm}(\theta;\varphi) \tag{3.14}$$

Only the combined set of wave functions $R_{n;l}(r)$; as we have seen in eq.(2.13) with negative eigenvalues and eq.(3.13) with positive energies, are complete.

The completeness relation then reads $(x \equiv (r;\theta;\varphi))$:

$$\sum_{n=1}^{\infty}\sum_{l=0}^{n-1}\sum_{m=-l}^{l}\psi_{nlm}(x)\psi^{*}_{nlm}(x') + \int_{0}^{\infty} dE \sum_{l=0}^{\infty}\sum_{m=-l}^{l}\psi_{lm}(E;x)\psi^{*}_{lm}(E;x') = \delta\left(x - x'\right) \tag{3.15}$$

β: The Quadratic Zeeman term

The work described here extends previous works and presents an analytical and numerical treatment of hydrogen in magnetic field, yielding accurate results for the eigenvalues and eigenvectors of the first few low-lying states over a wide range of field strengths in the intermediate field regime, focusing on the basic physical picture derived from the Schrödinger equation.

In the case of external weak magnetic field B (as showed in the previous chapter), one can ignore the quadratic term in the field B; because its small contribution in comparison with the other terms in Schrodinger equation, hence, the wave function of electron remains unperturbed, with the only effect being the well known Zeeman splitting of the energy levels of the hydrogen atom. In both Zeeman effects, the energy of interaction of electron with the magnetic field is assumed to be much smaller than the binding energy of the hydrogen atom, $e\hbar B/2m << me^4/2\hbar^2 = 13.6eV$. Thus, the action of a weak magnetic field can be treated as a small perturbation of the hydrogen atom.

In the case of strong magnetic field, the quadratic term in the field B makes a great contribution and can not be ignored. Calculations show that a considerable deformation of the electron charge distribution in the hydrogen atom occurs.

In the present work, the Hamiltonian is diagonalized, as a first step, in a truncated basis including only bound states.

We shall begin with the non-relativistic Hamiltonian for the hydrogen atom in a strong magnetic field using the spherical coordinates:

$$H = \underbrace{\frac{p^2}{2m}}_{\text{Kin}} - \underbrace{\frac{e^2}{4\pi\varepsilon_0 r}}_{\text{Coul}} + \underbrace{\frac{e}{2m}\mathbf{B}.(\mathbf{L} + 2\mathbf{S})}_{\text{Linear}} + \underbrace{\frac{e^2}{8m}\left(\mathbf{B}\wedge\mathbf{r}\right)^2}_{\text{Quadratic}} \tag{3.16}$$

We recall that the ratio of the quadratic to the linear term is about: $B.10^{-6}$ where B is expressed in Tesla. So, for strong magnetic field, which can occur in certain astrophysical situation such as in neutron stars or white dwarf stars, the quadratic term can not be negligible.

To obtain an estimate, we need the quantum mechanical mean value of a Bohr orbit corresponding to the principal quantum number n. The mean value will be estimated by replacing r by the Bohr radius a_n and $r^2\sin^2(\theta)$ by $\frac{2}{3}a_n^2$,thus:

$$\frac{e^2}{4\pi\varepsilon_0 a_n} \approx \frac{2}{3}\frac{e^2B_z^2}{8m}a_n^2 \tag{3.17}$$

Solving the equation for B_z and inserting the Bohr radius

$$a_n = \frac{n^2\hbar^2(4\pi\varepsilon_0)}{e^2m}$$

leads us to:

$$B_z \approx \sqrt{12}\frac{m^2e^3}{(4\pi\varepsilon_0)^2\hbar n^3} \tag{3.18}$$

This formula is in agreement with similar estimates except for a numerical factor ($\sqrt{12}$ in this case).

The essential term for this approach is the $1/n^3$ dependence. For sufficiently large quantum numbers, i.e. for Rydberg atoms, the required magnetic fields of several Teslas can be obtained in the laboratory, where the highest static magnetic field produced in a terrestrial laboratory is $\approx$ 50 T; this strength has recently been generated during high-intensity laser interactions with dense plasma[Zac07].

For low quantum numbers n; the required field strengths can not be obtained in laboratory.

°: Analytic expression of matrix elements

We can write the Hamiltonian for hydrogen atom in magnetic field and spherical coordinates using atomic unit as:

$$H = \underbrace{-\Delta - \frac{2}{r}}_{H_0} + \underbrace{\beta\,(L_z + 2S_z)}_{H_{LZ}} + \underbrace{\beta^2 r^2 \sin^2\theta}_{H_{QZ}} \tag{3.19}$$

With the magnetic field β is in units of :

$$B_0 = 4.701 \times 10^5 T$$

and the electron is moving around a fixed proton (Born-Oppenheimer approximation)[Sch02]:

We mentioned that the Spin $-$ orbit coupling is neglected in actual calculations since it is weak compared to the effect of the external magnetic fields.

We have : $H\,\psi(r;\theta;\varphi) = \epsilon\,\psi(r;\theta;\varphi)$ in which, the energy parameter ϵ is defined as:

$$\epsilon = \frac{E}{E_1} \tag{3.20}$$

where

$$E_1 = \frac{\alpha^2 m_e^2 c^2}{2}$$

is the Rydberg energy and the quantity $\alpha \simeq 1/137$ is the fine structure constant.

In the case of relatively weak fields, the main features of the geometry of the wavefunction are determined by the dominating Coulomb term, whereas the effect of the magnetic field can be consider as a perturbation of the Coulomb wavefunctions. For the opposite situation of strong magnetic fields and dominating cylindrical symmetry, the adiabatic approximation was the main theoretical tool during the last four decades. This approximation separately considers the fast motion of the electron across the field and its slow motion in a Coulomb potential along the field direction. Both early and more recent works on the hydrogen atom have used different approaches for these regimes of the magnetic field. All these calculations had problems when considering the hydrogen atom in fields of *intermediate strength* which is the subject of our work.

We can see, from the eq.(3.19), that H_0 and H_{LZ} are diagonal in the basis $\{|nlm_lm_s\rangle\}$:

$$(H_0 + H_{LZ})|nlm_lm_s\rangle = \left[\varepsilon_n^0 + 2\beta(m_l + 2m_s)\right]|nlm_lm_s\rangle \tag{3.21}$$

Here $\varepsilon_n^0 = \frac{-1}{n^2}a.u$ is the energy of a free hydrogen atom .

Since we have $[H; S_z] = 0$, the eigenvectors depend only on one of the projection of S_z; i.e; $S_z|nlm_lm_s\rangle = m_s|nlm_lm_s\rangle$; therefore, we shall assume that the electron has spin anti-aligned with the magnetic field; $m_s = \frac{-1}{2}$.

One has to diagonalize the quadratic Zeeman term in $\{|nlm_lm_s\rangle\}$ basis. The matrix elements of H_{QZ} are:

$$\begin{aligned}\langle nlm_lm_s|\, H_{QZ}\, |n'l'm_l'm_s'\rangle &= \beta^2\langle nlm_lm_s|\, r^2\sin^2\theta\, |n'l'm_l'm_s'\rangle \\ &= \beta^2\underbrace{\int_0^\infty R_{nl}(r)r^2R_{n'l'}(r)r^2dr}_{Radial-Part}\times\underbrace{\int Y^*_{l,m_l}(\theta,\varphi)\sin^2\theta\, Y_{l',m_l'}(\theta,\varphi)\,d\Omega}_{Angular-part}\end{aligned} \tag{3.22}$$

In order to calculate the angular integral, we start from the spherical harmonic

$$Y_{20}(\theta) = \sqrt{\frac{5}{16\pi}}\left(3\cos^2\theta - 1\right)$$

and we obtain:

$$\sin^2\theta = \frac{2}{3} - \frac{1}{3}\sqrt{\frac{16\pi}{5}}Y_{2,0}(\theta) \tag{3.23}$$

Using some appropriate properties of these spherical harmonics, we find that the matrix elements of H_{QZ} are diagonal in m_l and m_s but not in n and l. Δn may have any value, and Δl may be 0 or ± 2; i.e; we get the selection rules as: $\Delta m_l = 0$; $\Delta l = 0; \pm 2$ and of course $\Delta m_s = 0$. For more details, see appendix A.

We can, therefore, write the one-electron matrix elements of H_{QZ} in $\{|nlm_lm_s\rangle\}$ basis, whose radial wavefunctions are $R_{nl}(r)$ and $R_{n',l'}(r)$; and whose angular wave- functions are the usual spherical harmonics, as:

$$\langle n l m_l m_s | H_{QZ} | n' l' m_l' m_s' \rangle =$$

$$\begin{cases} -2\, \dfrac{2\left[l^2 + l - 1 + m_l^2\right]}{(2l+3)(2l-1)}\, \sigma(nl;n'l') & \text{if} \quad l' = l \\[2ex] -\,{-2} \left[\dfrac{(l_< + m_l + 2)(l_< + m_l + 1)(l_< - m_l + 2)(l_< - m_l + 1)}{(2l_< + 5)(2l_< + 3)^2 (2l_< + 1)}\right]^{\frac{1}{2}} \sigma(nl;n'l') & \text{if} \quad l' = l \pm 2 \\[2ex] 0 & \text{Otherwise} \end{cases} \tag{3.24}$$

Here $l_< = \min(l; l')$ and n, n' may have any values.

The radial integral σ is:

$$\sigma\left(nl;n'l'\right) = \int_0^{\infty} R_{nl}(r) r^2 R_{n'l'}(r) r^2 dr \tag{3.25}$$

In order to evaluate this radial integral, we use the normalized radial functions for the bound states of hydrogen atom which is written as:

$$\begin{aligned} R_{n,l}(r) &= \frac{1}{(2l+1)!} \sqrt{\left(\frac{2}{n}\right)^3 \frac{(n+l)!}{(n-l-1)!2n}}\, \rho^l e^{\frac{-\rho}{2}}\, {}_1F_1(-(n-l-1); 2l+2; \rho) \\ &= -\left[\left(\frac{2}{n}\right)^3 \cdot \frac{(n-l-1)!}{2n[(n+l)!]^3}\right]^{\frac{1}{2}} e^{\frac{-\rho}{2}} \rho^l L^{2l+1}_{n+l}(\rho) \end{aligned} \tag{3.26}$$

with $\rho = \dfrac{2r}{n}$ in a.u. and

$$L^{2l+1}_{n+l}(\rho) = \sum_{k=0} (-1)^{k+1} \frac{[(n+l)!]^2 \rho^k}{(n_r - k)!(2l+1+k)!k!}; \qquad n_r = n - l - 1 \tag{3.27}$$

is the associated Laguerre polynomial.

In practical calculations, one often uses this polynomial instead of the confluent hypergeometric, because there are many recurrence relations for them which are useful in simplifying integrals;

$$L^{2l+1}_{n+l}(\rho) = -\frac{[(n+l)!]^2}{(n-l-1)!(2l+1)!} \cdot {}_1F_1(-(n-l-1); 2l+2; \rho) \tag{3.28}$$

So, from eq.(3.25) and eq.(3.26) we obtain:

$$\sigma\left[nl;n'l'\right] = \frac{4}{n^2n'^2}\sqrt{(n+L)!\,(n'+l')!\,(n-l-1)!\,(n'-l'-1)!}\times$$
$$\times\left(\frac{2}{n}\right)^{l}\left(\frac{2}{n'}\right)^{l'}\cdot\sum_{k=0}^{n_r}\sum_{k'=0}^{n'_r}(-1)^{k+k'}\times$$
$$\times\frac{\left(\frac{2}{n}\right)^{k}\left(\frac{2}{n'}\right)^{k'}(4+l+l'+k+k')!}{(n_r-k)!\,(2l+1+K)!k!\,(n'_r-k')!\,(2l'+1+k')!k'!\left[\frac{1}{n}+\frac{1}{n'}\right]^{5+l+l'+k+k'}} \tag{3.29}$$

where we have used the integral (See more in appendix A):

$$\int_0^\infty r^m e^{-ar}dr = \frac{\Gamma(m+1)}{a^{m+1}} = \frac{m!}{a^{m+1}}$$

Measuring lengths in Bohr radii, energies in Rydberg, and magnetic fields in units of $B_0 = 4.7\times10^5\mathrm{T}$, we get that the non-vanishing matrix elements of the quadratic Zeeman term in the hydrogenic basis for $l = l'$ and $n = n'$ read:

$$\Delta E_{QZ} = \gamma^2\frac{n^2\left[5n^2+1-3l(l+1)\right]\left(l^2+l-1+m_l^2\right)}{(2l-1)(2l+3)} \tag{3.30}$$

But the challenge occurs for the case $n \neq n'$ with both values of l, l'. (See [Gar76] and [Wun85])

In our work, we calculated the σ integral numerically for $l' = l$ and $l' = l \pm 2$ with Δn may have any value.

As a result, we can write the general form of the matrix elements in atomic units with $m_s = -\frac{1}{2}$ as:

$$\langle nlm_lm_s\,|\,H\,|\,n'l'm'_lm'_s\rangle = \left(-\frac{1}{n^2}+2\beta(m_l-1)\right)\delta_{nn'}\delta_{ll'}\delta_{m_lm'_l}\delta_{m_sm'_s} + \gamma^2\delta_{m_lm'_l}\delta_{m_sm'_s} \tag{3.31}$$
$$\times\left\{\begin{array}{ll}\left(\frac{2\left(l^2+l-1+m_l^2\right)}{(2l+3)(2l-1)}\right)\sigma(nl;n'l') & \text{if } l' = l\\ -\left[\frac{(l_<+m_l+2)(l_<+m_l+1)(l_<-m_l+2)(l_<-m_l+1)}{(2l_<+5)(2l_<+3)^2(2l_<+1)}\right]^{\frac{1}{2}}\sigma(nl;n'l') & \text{if } l' = l\pm2\\ 0 & \text{otherwise}\end{array}\right\},$$

¾: *Numerical calculations*

In order to find the energy levels of hydrogen atom in strong magnetic field, we must diagonalize the matrix elements showed above in eq.(3.31).

Therefore, we have written a program for diagonalizing the square, symmetric and off-diagonal matrix, where we calculate the numerical values of the radial integrals σ and then the quadratic Zeeman term (eq.(3.24)).

Some results of σ are given in table.2 for the first lowest states (the selection rules $\Delta l = 0; \pm 2$ are taken into account):

$\vert i\rangle$	1s	1s	2s	2s	2p	2p	3s
$\langle f\vert$	ns	nd	ns	nd	np	nf	ns
n = 1	3.00	$-$	-2.9797	$-$	$-$	$-$	-1.0960
2	-2.9797	$-$	42.00	$-$	30.00	$-$	-29.906
3	-1.0960	1.7330	-29.906	-52.632	-25.480	$-$	207.000
4	-0.6291	1.1254	-9.7117	-7.8967	-7.8967	24.1250	-123.093
5	-0.4260	0.7970	-5.3412	-2.5735	-4.2556	14.8584	-36.5556
6	-0.3146	0.6017	-3.5621	-1.1462	-2.8077	10.3166	-19.2409
7	-0.2453	0.4751	-2.6200	-0.6055	-2.0520	7.73873	-12.5349
8	-0.1985	0.3875	-2.0437	-0.3564	-1.5943	6.10547	-9.104217

Table.2: Numerical values of the radial integral σ with $\sigma\left(nl;n'l'\right) = \int_0^\infty R_{nl}(r)r^2R_{n'l'}(r)r^2dr$

The Hamiltonian is diagonalized numerically using the Jacobi method. For this purpose, a Fortran program has been written. The Jacobi method gives accurate eingenvalues as well as the corresponding eigenvectors in short time.

±: *Results and discussion*

We have calculated energy levels of hydrogen atom under magnetic field strengths in the range $0 \leq \beta \leq 0.5$ which corresponding to $0 \leq B \leq 2.35 \times 10^9$G.

We restrict in our work the results to the ground state and the first few excited states of this atom in strong magnetic fields, while our program can give the energy levels of other states.

First, we must note that, we take , in our work, the binding energy as a positive value; it is defined as the energy must be given for removing the electron (ionization), and the energy, in all curves, is reported in units of Rydberg energy.

The calculations of eigenstates show, for $0 \leq \beta \leq 0.5$; only a small basis states mixing. So we continue using the spectroscopic labels used for a free atom. We can give an example for showing the new eigenstates and proving that there is a small mixing in which, we can conserve the spectrocopic labels used for a free atom.

Let us consider that the new eigenstates of hydrogen atom in magnetic field are labeled as $|v_k\rangle$; thus, we can write it as a linear combination of the eigenstates for a free atom using the numerical parameters a_i :

$$|v_k\rangle = \sum_i a_i \, |n_i; l_i; m_{l_i}; m_{s_i}\rangle$$

This small state mixing can be shown by two examples:

- $\beta = 0.01$ ($\equiv B = 4.7 \times 10^7 G$) :

$|v_1\rangle = 100\% \, |100 - \tfrac{1}{2}\rangle$ corresponding to $1s_0$ $\left(\text{with } m_s = -\tfrac{1}{2}\right)$ in a free atom.

$|v_2\rangle = 6.9696 \times 10^{-6}\% \, |100 - \tfrac{1}{2}\rangle + 99.9718\% \, |200 - \tfrac{1}{2}\rangle + 0.016887\% \, |300 - \tfrac{1}{2}\rangle$ $+ 0.0113444\% \, |320 - \tfrac{1}{2}\rangle + \ldots$ corresponding to $2s_0$ $\left(\text{with } m_s = -\tfrac{1}{2}\right)$ in a free atom.

$|v_3\rangle = 0\% \, |100 - \tfrac{1}{2}\rangle + 0\% \, |200 - \tfrac{1}{2}\rangle + 99.9818\% \, |211 - \tfrac{1}{2}\rangle + 0.0182412\% \, |311 - \tfrac{1}{2}\rangle + \ldots$ corresponding to $2p_1$ $\left(\text{with } m_s = -\tfrac{1}{2}\right)$ in a free atom.

$|v_4\rangle = 0\% \, |100 - \tfrac{1}{2}\rangle + 0\% \, |200 - \tfrac{1}{2}\rangle + 0\% \, |211 - \tfrac{1}{2}\rangle + 99.9951\% \, |210 - \tfrac{1}{2}\rangle$ $+ 0.0494772\% \, |310 - \tfrac{1}{2}\rangle + \ldots$ corresponding to $2p_0$ $\left(\text{with } m_s = -\tfrac{1}{2}\right)$ in a free atom.

- $\beta = 0.07$ ($B \approx 0.33 \times 10^9 G$) :

$|v_1\rangle = 99.991\% \, |100 - \tfrac{1}{2}\rangle + 0.0127268\% \, |200 - \tfrac{1}{2}\rangle + 0.00107465\% \, |300 - \tfrac{1}{2}\rangle +$ $3.99620955 \times 10^{-4}\% \, |320 - \tfrac{1}{2}\rangle + \ldots$ corresponding to $1s_0$ $\left(\text{with } m_s = -\tfrac{1}{2}\right)$ in a free atom.

$|v_2\rangle = 0.0120012\% \, |100 - \tfrac{1}{2}\rangle + 95.9594\% \, |200 - \tfrac{1}{2}\rangle + 0.676391\% \, |300 - \tfrac{1}{2}\rangle$ $+ 3.35223\% \, |320 - \tfrac{1}{2}\rangle + \ldots$ corresponding to $2s_0$ $\left(\text{with } m_s = -\tfrac{1}{2}\right)$ in a free atom.

$|v_3\rangle = 0\%\,|100\ {-\frac{1}{2}}\rangle + 0\%\,|200\ {-\frac{1}{2}}\rangle + 98.2124\%\,|211\ {-\frac{1}{2}}\rangle + 1.78757\%\,|311\ {-\frac{1}{2}}\rangle + \ldots$
corresponding to $2p_1$ $\left(\text{with } m_s = -\frac{1}{2}\right)$ in a free atom.

$|v_4\rangle = 0\%\,|100\ {-\frac{1}{2}}\rangle + 0\%\,|200\ {-\frac{1}{2}}\rangle + 0\%\,|211\ {-\frac{1}{2}}\rangle + 98.7199\%\,|210\ {-\frac{1}{2}}\rangle + \ldots$

Figure $(3-3)$ presents the variation in the binding energy of the hydrogen's ground state $1s_0$, where the magnetic field strength parameter is in the range $10^{-3} \le \beta \le 5 \times 10^{-1}$.

It is clearly seen in the figure that the binding energy of hydrogen's ground state with quantum numbers $m_l = 0$ increases monotonically with the magnetic field strength; i.e; the electron becomes more and more bound as the magnetic field strength increases. The computation results for this magnetic field region are in good agreement with the results in the published works such as [Thi08], [Lop07].

In Fig $(3-4)$, a comparison with [Thi08] is given for the ground state of hydrogen atom, where we can see good agreements for magnetic field $B < 2.35 \times 10^9$G. We mention that the two results have been obtained using different methods.

The variation in the binding energies of the three lowest states corresponding to $1s_0, 2p_{-1}$ and $3d_{-2}$, with the magnetic field strength parameter in the range $10^{-2} \le \beta \le 5 \times 10^{-1}$ are shown in the Fig $(3-5)$ They are results of the numerical calculation which uses finite-element method[Thi08].

Figure $(3-6)$ presents the variation of binding energies for the four low states $1s_0; 2p_{-1}; 2p_0; 3d_{-2}$ of the hydrogen atom as a function of magnetic field strength with $10^{-3} \le \beta \le 5 \times 10^{-1}$ in which we prove that the binding energy increases at an increasing rate with increasing magnetic field strengths.

Our results are similar to [Lop07], where we have shown that the three most lowest states of hydrogen are $1s_0$; $2p_{-1}; 2p_0$. However, there is a difference between our results and those of [Thi08], where we obtained that $2p_0$ level is more tightly bounded than $3d_{-2}$ level, as showed in the Fig.$(3-5)$ and Fig.$(3-6)$.

In addition, from the Fig.$(3-6)$, we see that $3d_{-2}$ increases faster than $2p_0$, especially for high magnetic field. Thus, we expect that the $3d_{-2}$ level will be more bounded than $2p_0$ for high magnetic field strengths.

Fig.$(3-7)$ shows a comparison between our results for the three states $1s_0$; $2p_{-1}; 3d_{-2}$ and those of [Thi08] which used the FEM method.

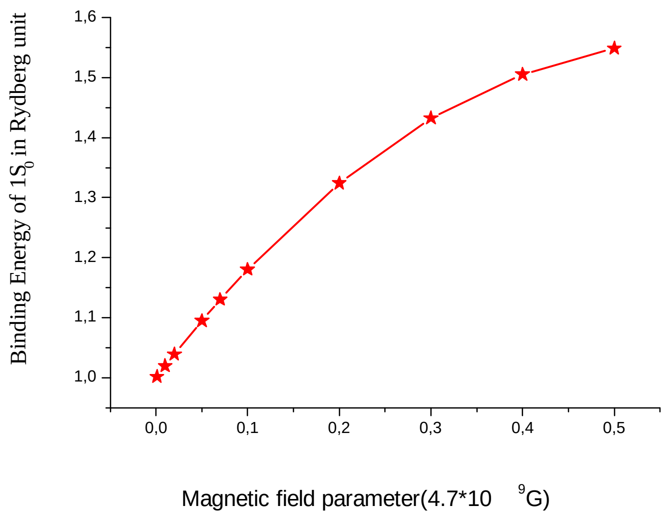

Figure 3-3: Th ground state's binding energies of hydrogen atom in strong magnetic ...eld.

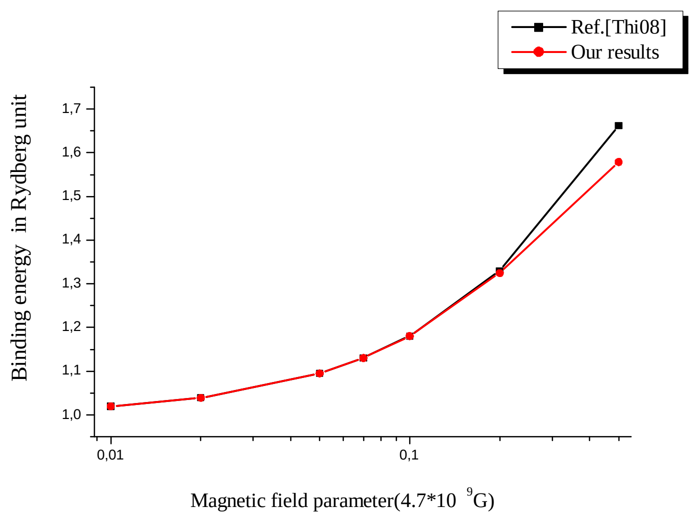

Figure 3-4: Comparison between our results and those of [Thi08] for $1s_0$ state.

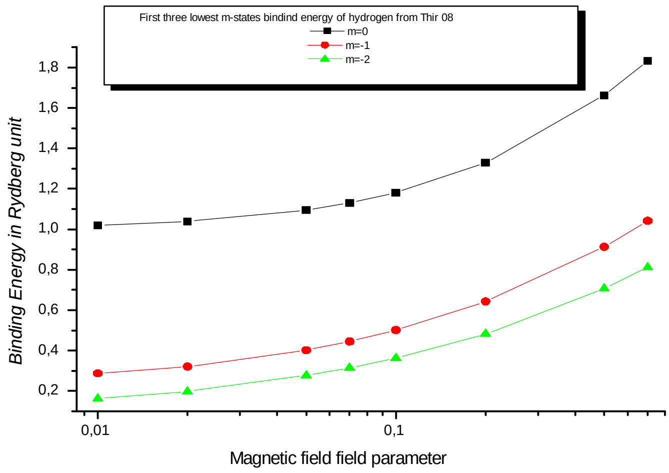

Figure 3-5: First three lowest m-states binding energy of [Thi08] as a function of the ...eld strengths in atomic units on a logarithmic scale.

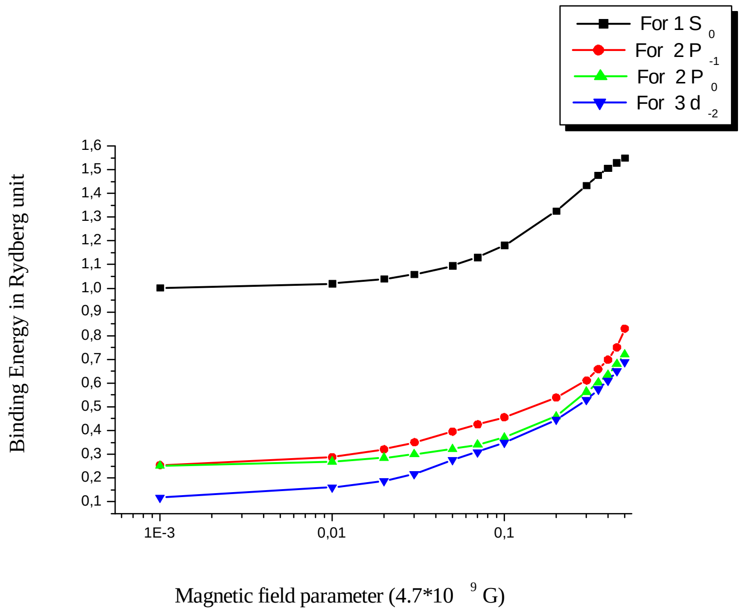

Figure 3-6: Our results for binding energies of the four most tightly bound states as a function of the ...eld strengths in atomic units on a logarithmic scale.

A global agreement is obtained except for $2p_{-1}$. The differences appeared for the highest magnetic field strength considered here.

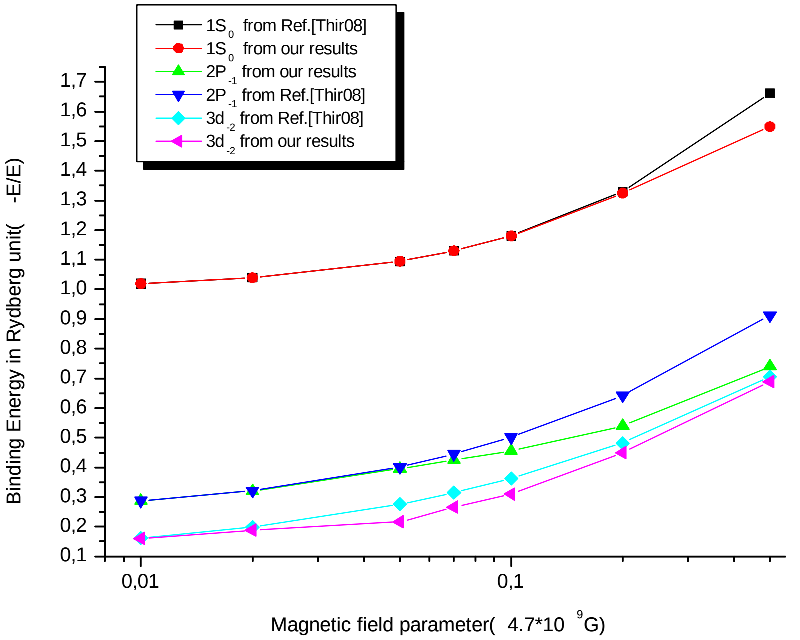

Figure 3-7: Comparison between our results with those in [Thi08] as a function of magnetic field strengths.

We recall that the Ref.[Thi08] used another method to calculate the eigenvalues(the finite-element method (FEM)) and also did [Iva00]; while [Lop07] used the variational method.

In Fig.(3 − 8), the binding energies are reported in Rydberg units, where we remark the tendency of the $2p_1$ state to become unbound with the increasing of the magnetic field.

Having such accurate analytical forms for the energies of atoms in strong magnetic fields obviates the need for performing laborious calculations for the energy estimates.

In addition, it becomes possible to analyze observed spectra of neutron and white dwarf stars with relative ease at arbitrary field strengths within the intermediate field regime.

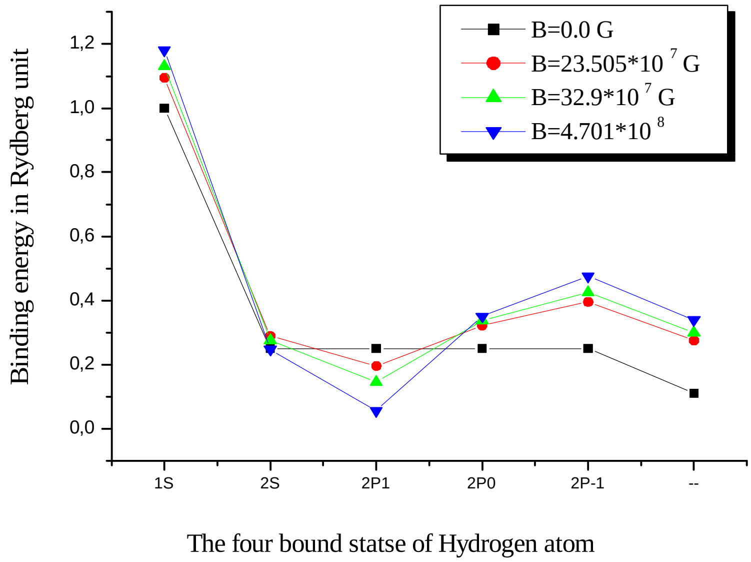

Figure 3-8: Comparison of the binding energies for the …rst lowest states as a function of magnetic …eld.

3.2 *Hydrogen atom in strong electric …elds*

As it is known from the spectra of DA white dwarfs, there exist strong electric …elds caused by free electrons and ions in the stellar atmospheres which lead to the appearance of Stark broadened lines.

In addition to their in‡uence on the wavelengths and oscillator strengths these electric …elds might be responsible for evidental changes of transitions probabilities.

In the atmosphere of a white dwarf, an atom feels an electric …elds whose mean values are presumed to be of the order of $\approx 10^6 - 10^9 V/m$.

We consider the ground state energy of the hydrogen atom in an uniform static electric …eld assumed to be in the z-axis direction:

$$\Big[\underbrace{-\nabla^2 - \frac{2}{r}}_{H_0} + \underbrace{2fz}_{H_{st}}\Big]\psi = \varepsilon\psi \tag{3.32}$$

In what follows, the energy ε and the …eld strength f are measured respectively by: Rydberg unit ($\varepsilon = \frac{E}{E_1}$) and $F_0 = 1a.u. = m_e^2 e^5/(4\pi\varepsilon_0)^3 \hbar^4 = 5.142 \times 10^{11} V/m$, with $f = \dfrac{F}{F_0}$.

The unit of electric …eld intensity is the …eld produced by a proton at a distance equal to the radius of the …rst hydrogen's Bohr orbit.

Under realistic conditions in laboratory, the maximum electric …eld strength that can be produced is: $F \leq 10^{-4}(a.u.)$; i.e. $F \leq 10^7 V/m$.

3.2.1 *Analytical treatment*

We will brie‡y present the e¤ect of strong electric …eld in the intermediate regime $0 \leq f \leq 0.1$.i.e; later on, the electric …eld strength will be smaller than $5.142 \times 10^{11} V/m$.

The matrix elements of H will be calculated using spherical coordinates system where $z = r\cos\theta$ and $\cos\theta = \sqrt{\dfrac{4\pi}{3}}\, Y_{10}(\theta)$.

The matrix elements can then be written:

$$\langle nlm_lm_s \,|\, H_{st} \,|\, n'l'm_l'm_s' \rangle = 2f\, \langle nl \,|\, r \,|\, n'l' \rangle \delta_{m_l m_l'} \delta_{m_s m_s'} \times \sqrt{\frac{4\pi}{3}} \int Y^{*}_{lm_l}(\theta;\varphi)\, Y_{10}(\theta)\, Y_{l'm_l'}(\theta;\varphi)\, d\Omega \tag{3.33}$$

Using some properties of spherical harmonics and $3j$ symbols, we conclude that the H_{st} is diagonal in m_l and m_s but not in l. The involved $3j$ symbols vanishe unless $\Delta l = \pm 1$. Details of calculations are given in appendix B.

Thus, we can write the matrix elements in the form:

$$\langle nlm_lm_s \,|\, H_{st} \,|\, n'l'm_l'm_s' \rangle = 2f\, \langle nl \,|\, r \,|\, n'l' \rangle \delta_{m_l m_l'} \delta_{m_s m_s'} \times \left\{ \begin{array}{ll} \sqrt{\dfrac{(l+m_l+1)(l-m_l+1)}{(2l+1)(2l+3)}} & \text{for} \quad l' = l+1 \\ \sqrt{\dfrac{(l-m)(l+m)}{(2l+1)(2l-1)}} & \text{for} \quad l' = l-1 \end{array} \right\} \tag{3.34}$$

3.2.2 *Numerical calculations*

The square symmetric matrix is diagonalized numerically to obtain the eigenvalues(energies).

In the beginning, we have calculated the radial integral $\langle nl \,|\, r \,|\, n'l' \rangle = \int_0^\infty R_{nl}(r) R_{n'l'}(r) r^3 dr$ with the selection rules $\Delta l = \pm 1$; $\Delta m_l = 0$; $\Delta m_s = 0$.

We give below some numerical values, obtained by our program (Fortran language), for the radial integrals; the radial wave function is given in the last section.

$\lvert i \rangle$	1s	2s	2p	2p	3s	3p	3p
$\langle f \rvert$	np	np	ns	nd	np	ns	nd
$n = 1$	−	−	1.29026	−	−	0.51668	−
2	1.29026	5.19615	5.19615	−	0.938407	3.06481	−
3	0.51668	3.06481	0.93840	4.74799	12.72788	12.7279	10.062
4	0.30458	1.28227	0.38230	1.70970	5.469332	2.44353	7.5654
5	0.20870	0.77343	0.22802	0.97508	2.25959	0.96960	2.9683
6	0.15513	0.54036	0.15820	0.66181	1.36026	0.57232	1.7411

Table:3 : Nnumerical values of the radial integral: $\int_0^\infty R_{nl}(r) R_{n'l'}(r) r^3 dr$

3.2.3 *Results and discussion*

Our results in the Fig.(3 ¡ 9) have an agreement with those of [Dav83] and of [Ken95] which used the expansion of the Weak ...eld series.

Fig.(3 ¡ 10) shows a comparison of the binding energies for the ground state of hydrogen atom in an electric and magnetic ...elds. We can see that the in‡uence of the magnetic ...eld ¯ is larger than the in‡uence of the electric ...eld of the same strength f . This is normal because we know that the magnetic ...eld presses the atom in its direction, while the strong electric ...eld tries to act in the opposit way. i.e., atomic levels become quasi-discrete levels if an electric ...eld acts on it.

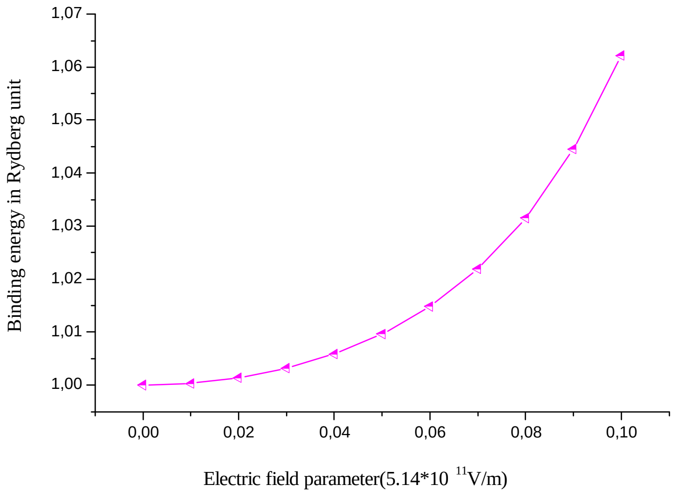

Figure 3-9: Our results for ground state's binding energy of hydrogen atom in a uniform static electric …eld.

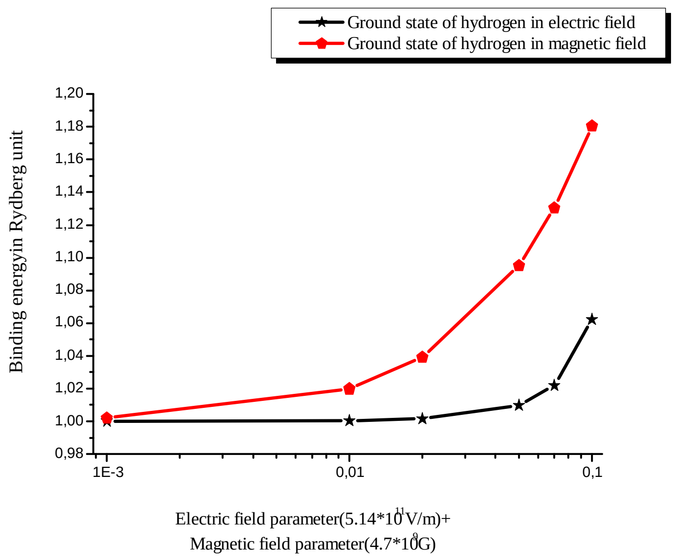

Figure 3-10: Comparison between the energy of ground state in an electric and magnetic …elds separately of the same strengths.

3.3 *Hydrogen atom in combined stellar magnetic and electric …elds*

'The e¤ects of an external electric and magnetic …elds on atomic spectra' is a fundamental question of atomic physics. However, up to now most investigations have concentrated on atoms in only one of the two …elds, or on selected mutual orientations. In our work, we will …rst study the e¤ects of an external parallel static electric and magnetic …elds. In a second step, we will discuss the case in which the electric and magnetic …eld, will be in arbitrary mutual orientations, for a wide …eld range.

3.3.1 *Hydrogen atom in the combination of strong magnetic and parallel static electric …elds*

Despite its long history, the problem of a hydrogen atom in an external uniform magnetic and static electric …elds still have a signi…cant interest. Besides the fundamental questions associated with this non-integrable system, decisive stimulus came from the discovery of huge magnetic and electric …elds in compact astrophysical objects, such as white dwarf stars with …eld strengths of the order of B t 10^2 ¡ 10^5T and F t 10^6 ¡ 10^9V=m:

We start this work by considering that both magnetic and electric …elds are directed along z-axis; i.e; the in‡uence of the electric …eld component perpendicular to the magnetic …eld is negligible.

®:*Hamiltonian of hydrogen atom in magnetic and parallel static electric …elds*

To examine the e¤ect of the additional electric …eld on the hydrogen atom in the atmosphere of magnetic white dwarf stars, we will solve the Schrödinger equation for a hydrogen atom in strong parallel magnetic and static electric …elds; thus, obtaining the energy values for the low-lying bound states.

The non-relativistic Hamiltonian of a hydrogen atom in parallel static electric and magnetic …elds reads:

$$H = -\underbrace{\Delta}_{kin} - \underbrace{\frac{2}{r}}_{coul} + \underbrace{2\beta\,(l_z + 2S_z)}_{paramag} + \underbrace{\beta^2 r^2 \sin^2\theta}_{diamag} + \underbrace{2f_q\, r\cos\theta}_{electr} \tag{3.35}$$

We assume that the Spin-Orbit coupling is neglected in actual calculations since it is weak compared to the effect of the external fields. On the other hand, the treatment given here must be modified for electric fields $F < 10^3 V/cm$, since in this case the Stark splitting are in the same order of magnitude as the fine structure splitting.

We can show also that the electric term in the last expression is of the same order of the quadratic Zeeman term; so we can't treat it as a perturbation. The relative magnitude of the two terms can be estimated by assuming that the dimensions of the atomic system are of the order of a_0, the Bohr radius of hydrogen. The quadratic term is of the order $\frac{e^2a_0^2B^2}{8m}$, while the electric term is approximately given by eFa_0. Thus,the ratio of the quadratic term to the electric term is: $\frac{ea_0}{8m}\frac{B^2}{F} \sim \frac{B^2}{F}$. A ratio $\simeq 1$ can be obtained with the values given above.

¯: *Results and comments*

In this case, we can't continue to use the spectroscopic labels for a free atom, because there are a considerable basis states mixing, thus, in the following, we shall use the $|v_k\rangle$ labels for the energy levels. Thus, the labels will be $|v_1\rangle$ for the ground state, $|v_2\rangle$ corresponds to 2s in a free atom, $|v_3\rangle$ corresponds to $2p_1$; $|v_4\rangle$ to $2p_0$ and $|v_5\rangle$ to $2p_{-1}$ in a free atom and so on. We shall give the details in chapter 4.

In Fig.$(3-11)$;we see that the magnetic field have larger influence on the energy levels of hydrogen atom in comparison to the case of the electric field effect. The joint influence is almost identical to the effect of the magnetic field alone for low strengths. However, for large values a net effect is observed.

Fig.$(3-12)$ showed also that when the magnetic field increases with the variation of the electric field, its influence becomes more and more significant.

Fig.$(3-13)$ shows that once the hydrogen atom is under magnetic field strength $B = 3.3 \times 10^5 T$, the binding energy of the ground state increases with the electric field. But if the electric field strength reaches 1a.u. a sudden decreasing appears, i.e; a new effect of the electric field occurs when $f \geq 1$.

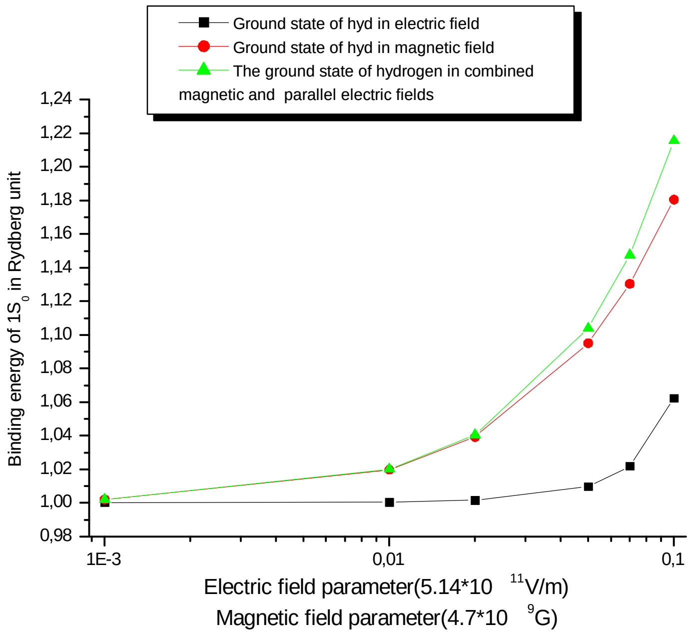

Figure 3-11: Comparison between the three cases of the ground state energy; in electric, magnetic and both ...elds of the same strengths.

In Fig.(3 ¡ 14), the binding energy of hydrogen's ground state increases with the increasing of both magnetic and parallel electric ...elds.

From the Fig.(3 ¡ 15), we can see that for the lowest electric ...eld strengths, the binding energy of j v_5 i level increases with the increasing of magnetic ...eld strengths, but for 4:7 £ 10^6G; 4:7 £ 10^7G and 2:35 £ 10^8G curves, a maximum seems to be reachs respectively for 0:045a:u:, 0:05a:u: and 0:08a:u.

For the two remaining curves corresponding to 0:33 £ 10^9G;and 0:47 £ 10^9G , we see that the binding energies continue to at least for f · 1: Thus the in‡uence of the increased strong magnetic ...eld becomes signi...cant.

Fig.(3 ¡ 16) presents similar behaviour as in Fig.(3 ¡ 15) corresponding to j v_5 i. The difference being in the energy values that are now weaker. We know that the degenerecy is partly removed by the Stark e¤ect where the energies of the j v_5 i ´ $2p_{¡1}$ and j v_3 i ´ $2p_1$ states remaining unaltered (see Fig.(2 ¡ 7)). By comparing the two ...gures Fig.(3 ¡ 15) and Fig.(3 ¡ 16)),

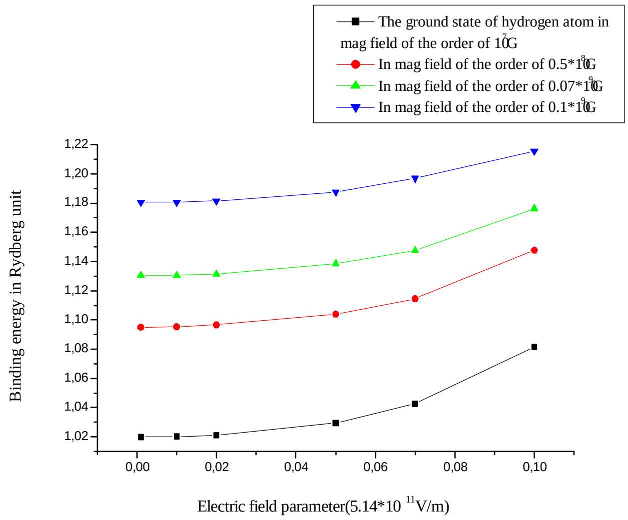

Figure 3-12: Binding energies of the ground state in both magnetic and electric …elds.

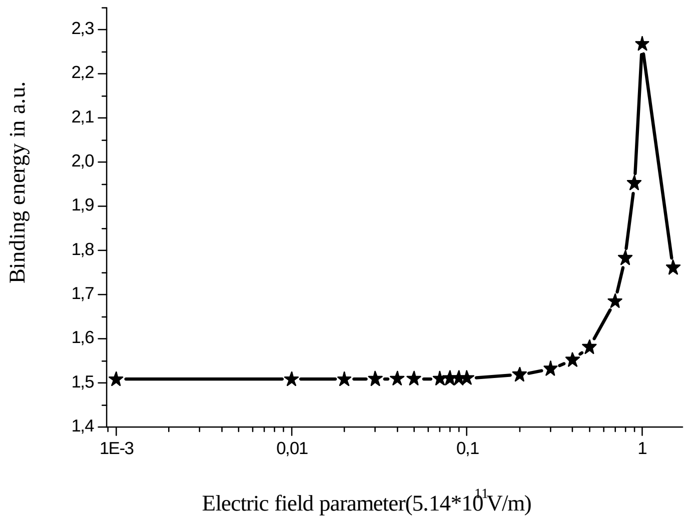

Figure 3-13: The ground state energy in magnetic …eld of the order of $3{:}3 \pounds 10^5$T as a function of an electric …eld strengths.

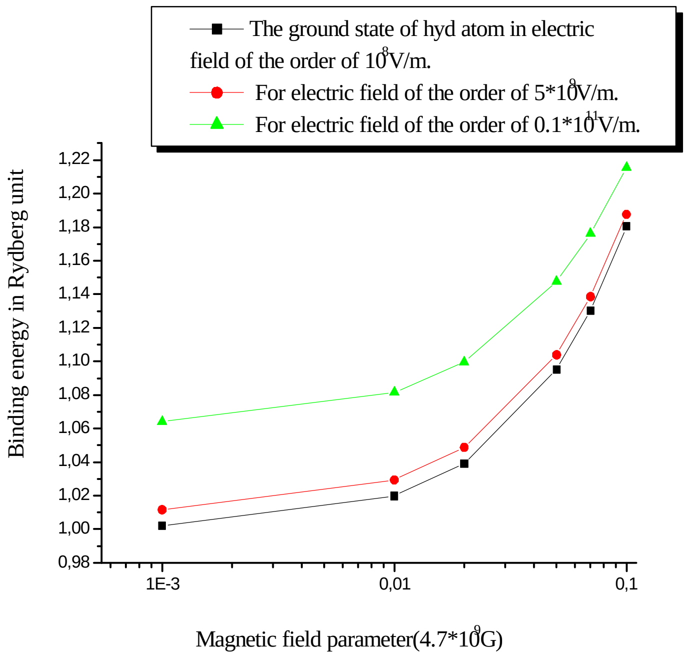

Figure 3-14: Variation in binding energies of the ground state in an electric …eld plus a variable magnetic …eld.

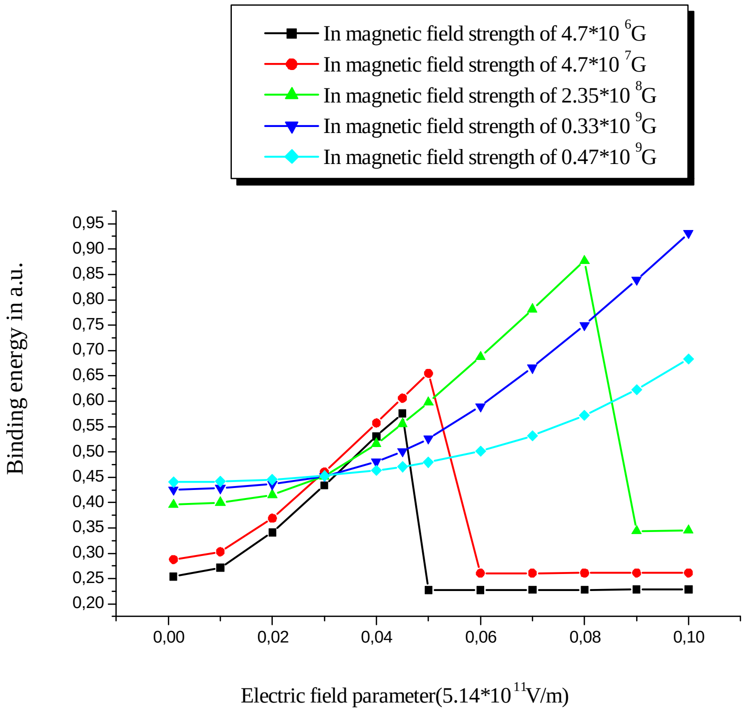

Figure 3-15: Variation in binding energies for j v5 i level(corresponding to 2p ¡ 1 for a free atom) in both electric and magnetic …elds:

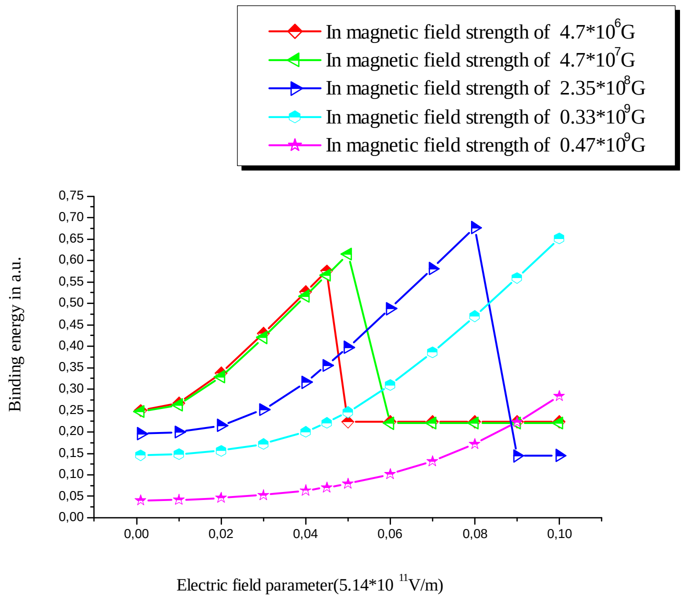

Figure 3-16: Variation in binding energies for $|v_3\rangle$ level (corresponding to $2p_1$ for a free atom) in both electric and magnetic …elds.

we see that the degeneracy is removed by the external magnetic field.

3.3.2 *Hydrogen atom in combined strong magnetic and static electric fields with arbitrary mutual orientations*

For the hydrogen atom in combined magnetic and static electric fields, we investigate the dependence of the quantum spectra (energy levels), on the mutual orientation of the two external fields.These energies are obtained by a diagonalization of the Hamiltonian in our basis set in the intermediate regime .i.e; $10^{-3} \leq \gamma \leq 0.5$ for magnetic field; and $0 \leq f \leq 0.1$ for electric field.

The effects of an external static electric and magnetic fields on atomic spectra is a fundamental question of atomic physics. However, most investigations have focused on atoms in only one of the two fields. The case of arbitrary field orientation is the most general situation for atoms in uniform external fields, and therefore it needs such interest.

α: *Numerical calculations*

The Hamiltonian of the hydrogen atom in uniform magnetic and static electric fields with arbitrary mutual orientations[in atomic units, $f = F/(5.14 \times 10^9 V/cm)$, and $\gamma = B/(4.701 \times 10^9 G)$] reads:

$$H = -\underbrace{\Delta}_{kin} - \underbrace{\frac{2}{r}}_{coul} + \underbrace{2\gamma(l_z + 2S_z)}_{paramag} + \underbrace{\gamma^2 r^2 \sin^2\theta}_{diamag} + \underbrace{2[f_\parallel z + f_\perp x]}_{H_{St}} \tag{3.36}$$

in which, we considered the most general direction of $\vec{F}$ where:

$$\vec{F} = \vec{F}_\parallel + \vec{F}_\perp = F_z \hat{k} + F_\perp \hat{u}.$$

One can choose $\hat{i} \equiv \hat{u}$; this gives: $\vec{F} = F_z \hat{k} + F_\perp \hat{i}$.

We recall that the magnetic field is oriented in the z-direction and the electric field in the (x, z)-plane with $f_\parallel$ and $f_\perp$ the components of the static electric field parallel and perpendicular to the magnetic field axis, respectively[Jor97].

We neglected relativistic and effects due to the finite nuclear mass, which yield only very small contributions in the energy-field regions we examine.

The Hamiltonian H_{St} can be written as:

$$H_{St} = 2[f_z z + f_{\perp} x] = 2r[f_z \cos\theta + f_{\perp} \sin\theta \cos\varphi] \tag{3.37}$$

Using the spherical harmonics

$$Y_{10}(\theta) = \sqrt{\frac{3}{4\pi}} \cos\theta; \; Y_{1,1} = -\sqrt{\frac{3}{8\pi}} \sin\theta e^{i\varphi}; \; Y_{1,-1} = \sqrt{\frac{3}{8\pi}} \sin\theta e^{-i\varphi}. \tag{3.38}$$

We can write the Stark term as:

$$H_{St} = 2r \times \underbrace{\left\{ \sqrt{\frac{2\pi}{3}} f_{\perp} [Y_{1,-1}(\theta,\varphi) - Y_{1,1}(\theta,\varphi)] + \sqrt{\frac{4\pi}{3}} f_z Y_{10}(\theta) \right\}}_{\mathrm{Ang}} \tag{3.39}$$

The angular term in the Hamiltonian H_{St} is calculated in the chosen basis and we obtain:

1= For $\Delta l = +1$:

$$\begin{cases} -\frac{1}{2} f_{\perp} \sqrt{\frac{(l+m_l+2)(l+m_l+1)}{(2l+3)(2l+1)}} & \text{if} \quad m_l^0 = m_l + 1; \\ -\frac{1}{2} f_{\perp} \sqrt{\frac{(l-m_l+2)(l-m_l+1)}{(2l+3)(2l+1)}} & \text{if} \quad m_l^0 = m_l - 1; \\ f_z \sqrt{\frac{(l-m_l+1)(l+m_l+1)}{(2l+3)(2l+1)}} & \text{if} \quad m_l^0 = m_l. \end{cases} \tag{3.40}$$

2=For $\Delta l = -1$:

$$\begin{cases} \frac{1}{2} f_{\perp} \sqrt{\frac{(l-m_l)(l-m_l-1)}{(2l-1)(2l+1)}} & \text{if} \quad m_l^0 = m_l + 1; \\ \frac{1}{2} f_{\perp} \sqrt{\frac{(l+m_l)(l+m_l-1)}{(2l-1)(2l+1)}} & \text{if} \quad m_l^0 = m_l - 1; \\ f_z \sqrt{\frac{(l-m_l)(l+m_l)}{(2l-1)(2l+1)}} & \text{if} \quad m_l^0 = m_l. \end{cases} \tag{3.41}$$

We note that the matrix elements $\langle nl | r | n^0 l^0 \rangle$ have been calculated in the previous section by a numerical method using the Fortron language for any value of the principal quantum number n, then it must diagonalize the total Hamiltonian which contains the paramagnetic and diamagnetic terms, and also the Stark term due to strong arbitrary electric fields.

β: *Results and Outlooks*

As in the case of parallel electric and magnetic fields, we can't use the spectroscopic labels for a free atom, instead, we shall label our new eigenstates by $|v_k\rangle$.

We conclude, from the two figures (Fig.$(3-17)$ and Fig.$(3-18)$), that the non-parallel static electric field has a large contribution of the ground state binding energies, in comparison with the influence of the parallel elctric field.

If the electric field augments, we get that the binding energy of the hydrogen's ground state increases also in all region of selected magnetic field values , but we remark, from the Fig.$(3-19)$, that for strong electric field strength ($F = 0.514 \times 10^{11} V/m$) , the ground state's binding energy starts to decrease with magnetic field strength $\beta = 0.2$ .i.e; $B \sim 10^9 G$. In addition; the increasing of magnetic field strength also has a contribution to the decreasing of the hydrogen's binding energies leading probably to an ionization of the atom.

We denote that the ionization of a hydrogen atom in an electric field plus a variable magnetic field has been examined by "*DehuaWanga, Kaiyun Huanga, Hui Zhoub, Shenglu Linb*" [Deh09] in their paper. They studied this subject with a particular discussion of the influence of the magnetic field on the escape dynamics of the electron. The results show that when the magnetic field is weak, its influence on the ionization of hydrogen atom is very small. However, the ionization of hydrogen atom increases with the increasing magnetic field.

In Fig $(3-20)$, we remark that the energy level $|v_3\rangle$ experience an evident decreasing with the augmented fields (see the second curve corresponding to $f = 0.01$)

As showing in Fig: $(3-21)$, we remark that for an electric field strength in the order of $10^{-3} a.u$; the binding energies of $|v_5\rangle$ state increase as a function of magnetic field strengths, while for $f \geq 0.02 \equiv F \geq 10^{10} V/m$, we find that its binding energies suffer an evident decreasing with magnetic field strengths.

The Fig.$(3-23)$ shows that the influence of strong non-parallel static electric field of the order of $5.14 \times 10^{10} V/m$ exhibits an extreme when the magnetic field strength reachs $0.2 a.u$, i.e; $B \sim 10^9 G$.

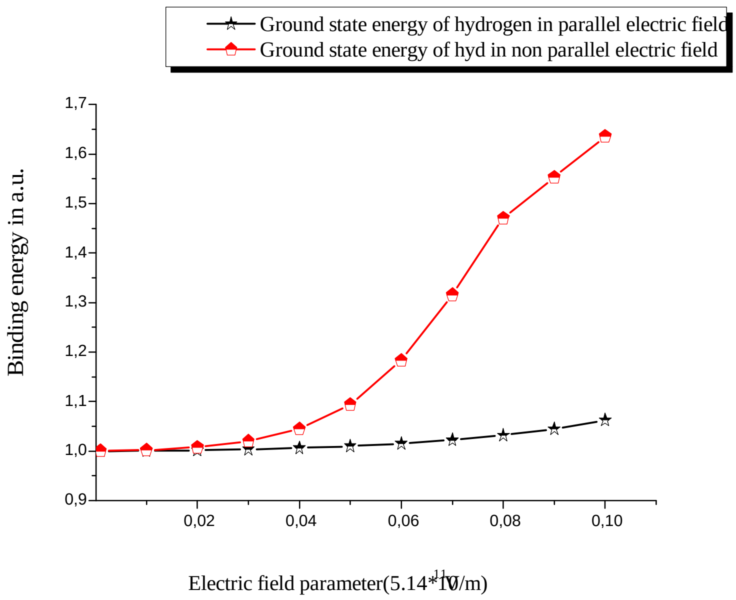

Figure 3-17: Comparison of the ground state's energies in parallel elec ...eld and those in non-parallel elec ...eld.

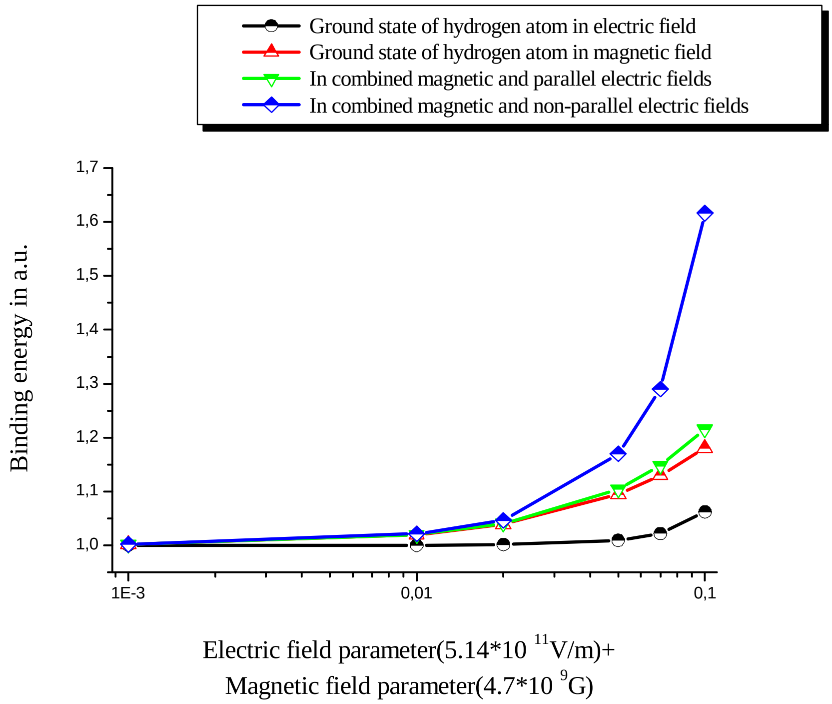

Figure 3-18: Comparison between the ground state's energy in an electric, magnetic ...elds, magnetic and parallel electric ...elds and magnetic and non-parallel electric ...elds of the same strengths.

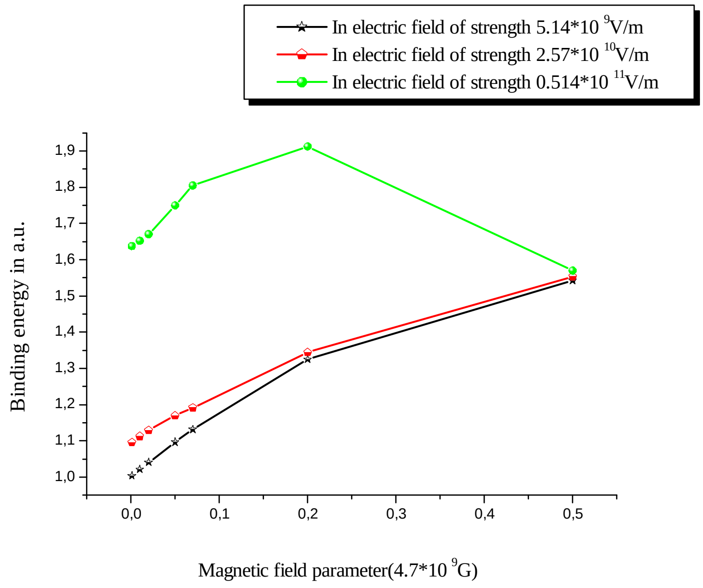

Figure 3-19: Variation of binding energies for the ground state in speci…ed electric and variable magnetic …eld strengths.

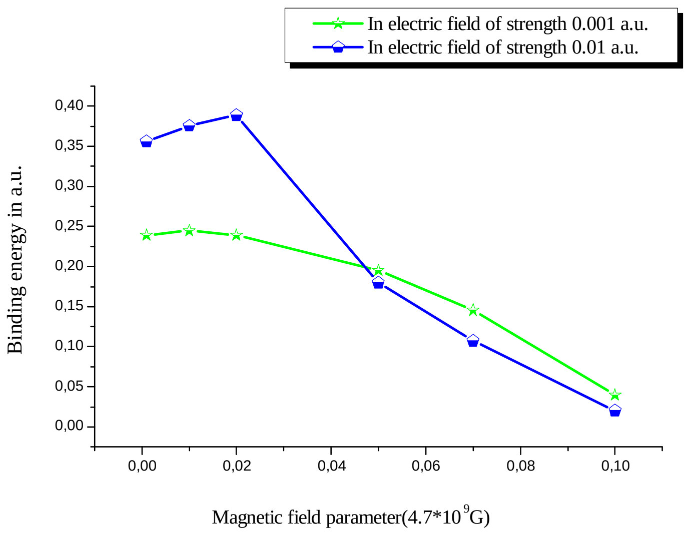

Figure 3-20: Variation of binding energies for j v_3 i state(corresponding to $2p_1$ for a free atom) in speci…ed electric and variable magnetic …eld strengths.

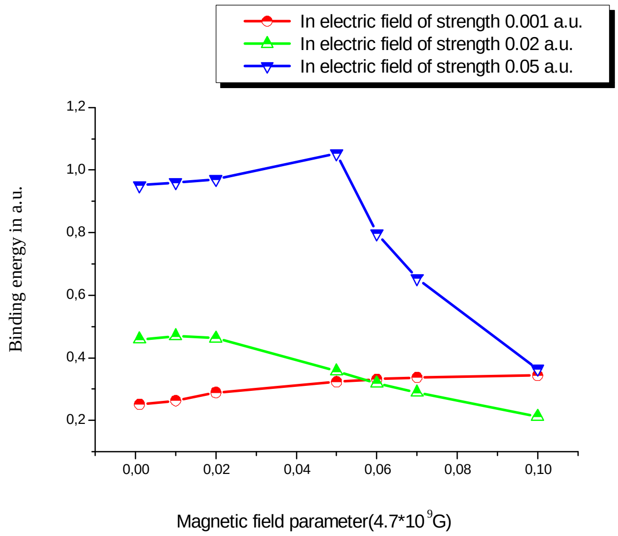

Figure 3-21: Variation of binding energies for $|v_4\rangle$ state (corresponding to $2p_0$ for a free atom) in specified electric and variable magnetic field strengths.

On the other hand, this ground state binding energy of hydrogen under a strong parallel static electric field is continuously increasing all over the chosen magnetic field strengths.

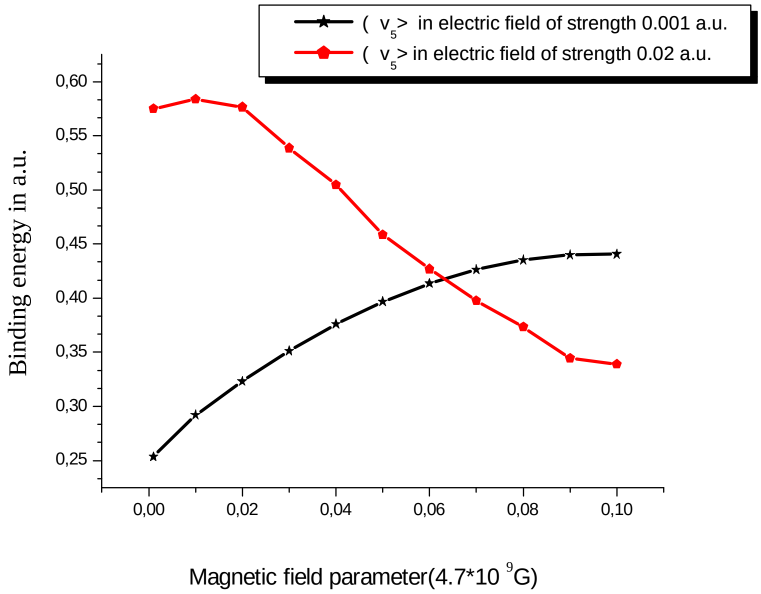

Figure 3-22: Variation of binding energies for j v_5 i state (corresponding to 2p $_{¡\,1}$ for a free atom) in speci…ed electric and variable magnetic …eld strengths.

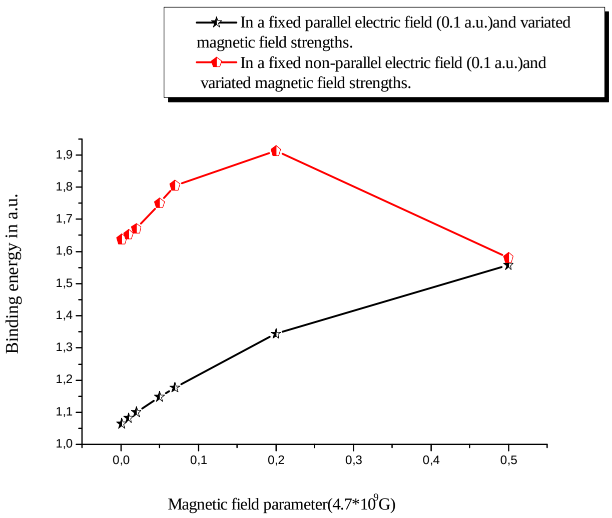

Figure 3-23: Comparison of the ground state's energies in a …xed strength of parallel electric …eld and those in non-parallel one.

Chapter 4

Electromagnetic transition probabilities

Recent observations of thermally emitting isolated neutron stars revealed spectral features that could be interpreted as radiative transitions of H and He in a magnetized neutron star atmosphere.

The detection and detailed studies of surface emission from a large number of isolated neutron stars (NSs), radio pulsars, magnetars... were possible by X-ray telescopes. Such studies can provide invaluable information on the physical properties and evolution of NSs (e.g., surface magnetic …eld, composition,...).

Because the strong magnetic and electric …elds greatly change the binding energies of atoms, we can conclude that the transition probabilities will be su¤er a di¤erence by comparison with the free-…elds case.

This work is organized as follows: …rstly,we will describe our numerical calculations of eigenvectors bound states of the hydrogen atom in strong magnetic …elds, secondly, we shall present our numerical results for the dipole strengths, the oscillator strengths of the transitions and the transition probabilities between two levels of hydrogen atom; …nally, we repeat these steps for hydrogen atom under the combination of magnetic and electric …elds in which the labels of the new eigenestates will be di¤erent due to the basis-states mixing.

Our detailed study of the energies of the hydrogen's lowest states placed in magnetic and electric field strengths $B \sim (0 - 2.35 \times 10^9 G)$ and $F \sim (0 - 5.14 \times 10^{10} V/m)$ are given in chapter 3.

In this study our goal is the treatment of the electromagnetic transitions between the lowest bound states $1s_0$, $2p_{-1}$ and $2p_0$ i.e.; ($1s_0 \leftrightarrow 2p_{-1}$ and $1s_0 \leftrightarrow 2p_0$).

Our consideration is non-relativistic, it is based on a numerical treatment of the eigenstates, and on Born-oppenheimer approximation: the proton is assumed to be infinitely massive.

4.1 *Electromagnetic transition probabilities of the lowest states of hydrogen atom in strong magnetic field*

In a magnetic field, the m-degeneracy of the hydrogen energy levels is fully removed and electromagnetic transitions depend explicitly on the magnetic quantum numbers of the initial and final states in the transition.

A consideration of an electromagnetic transitions in *the electric dipole approximation* is valid even in the case of high magnetic fields where in this case characteristic of wavelengths are always much larger than the size of the system. The atomic wave functions extend over distances of the first Bohr radius of the atom; on the other hand, the wavelengths associated with optical transitions are of the order of several thousand Angstroms. Thus we can replace the exponential function occured in the oscillating electric field F in eq (2.14) by unity; this is known as *the electric dipole approximation*.

In the electric dipole approximation, we are interested in the square of the matrix element (called *dipole strength*):

$$d^{(q)}_{v',v} = |p^{(q)}_{v',v}|^2 = |\langle \mathbf{v}' | \hat{\epsilon} \cdot \mathbf{r}^{(q)} | \mathbf{v} \rangle|^2 \tag{4.1}$$

Where v', v label the final and initial states in the transition, $p^{(q)}_{v',v}$ is the matrix element (in atomic units) of a dipole transition between two states v and v', and $r^{(q)} = \vec{r}/a_r$ are the spherical components of the electric dipole operator.

The modulus squared $d^{(q)}_{v',v}$ is called the dipole strength of the transition, which when multiplied by the energy difference (in Rydberg units) of the two states yields the oscillator strength of the transition[Lop07]:

$$f^{(q)}_{v',v} = (E_{v'} - E_v)\, d^{(q)}_{v',v} \qquad (4.2)$$

where $(E_{v'} - E_v)$ is the (binding) energy difference of the initial and final states in a.u.

In order to evaluate the above expressions, we use the spherical components $r^{(q)}\,(q = 0, \pm 1)$ defined as:

$$\begin{aligned} r^{(1)} &= -\frac{1}{\sqrt{2}}(x + iy) = -\frac{1}{\sqrt{2}} r \sin\theta e^{i\varphi} = r\left(\frac{4\pi}{3}\right)^{\frac{1}{2}} Y_{1,1}(\theta,\varphi). \qquad (4.3)\\ r^{(0)} &= z = r\cos\theta = r\left(\frac{4\pi}{3}\right)^{\frac{1}{2}} Y_{1,0}(\theta,\varphi).\\ r^{(-1)} &= \frac{1}{\sqrt{2}}(x - iy) = \frac{1}{\sqrt{2}} r \sin\theta e^{-i\varphi} = r\left(\frac{4\pi}{3}\right)^{\frac{1}{2}} Y_{1,-1}(\theta,\varphi).\end{aligned}$$

Similarly, the spherical components ε_q are given in terms of its Cartesian components $(\varepsilon_x, \varepsilon_y, \varepsilon_z)$ by:

$$\varepsilon_1 = -\frac{1}{\sqrt{2}}(\varepsilon_x + i\varepsilon_y);\quad \varepsilon_{-1} = \frac{1}{\sqrt{2}}(\varepsilon_x - i\varepsilon_y);\quad \varepsilon_0 = \varepsilon_z.$$

The scalar product $\varepsilon \cdot \mathbf{r}_{v',v}$ can be expressed in terms of spherical components as:

$$\varepsilon \cdot \mathbf{r}_{v',v} = \sum_{q=0,\pm 1} \varepsilon^*_q \cdot (\mathbf{r}_{v',v})_q = \sum_{q=0,\pm 1} \varepsilon^*_q \cdot \mathcal{I}^q_{v',v} \qquad (4.4)$$

where $\mathcal{I}^q_{v',v}$ is given as:

$$\mathcal{I}^q_{v',v} = \left(\frac{4\pi}{3}\right)^{\frac{1}{2}} \int_0^\infty dr\, r^3 \Phi'_{n'l'}(r)\Phi_{nl}(r) \cdot \int d\Omega\, Y^*_{l'm'}(\theta,\varphi) Y_{1,q}(\theta,\varphi) Y_{lm}(\theta,\varphi) \qquad (4.5)$$

In this formula, we have written the radial wavefunctions for final and initial levels of the hydrogen atom as $\Phi'_{n'l'}(r), \Phi_{nl}(r)$ respectively and not as $R'_{n'l'}(r), R_{nl}(r)$, because they are different from the free-field case; we shall detail this idea later.

The radial integral is always non-zero, but the angular integrals are only non-zero for certain values of (l, m) and (l', m'), giving rise to selection rules which we can calculate in the same way as in the previous chapter. These rules are: $\Delta l = \pm 1$; $\Delta m_s = 0$; $\Delta m = 0, \pm 1$ which implies $q = \Delta m = 0, \pm 1$.

We can show, in our study, that the polarization vector of the emitted photon in the z-direction $\vec{\Pi}^{q}_{v',v}$ vanishes unless: $m = m'$. This transition called π-transition. Circularly polarized radiation with $\Delta m = +1$(for right polarization) can also be emitted. This transition called σ-transition; but for $\Delta m = -1$ neither $2p_{-1}$, nor $2p_0$ have an excitation (de-excitation) mode to the ground state via left-polarized radiation.

Thus, we can write $\Pi^{q}_{v',v}$ in term of the matrix element $\langle v' \mid r \mid v \rangle$ as:

- for $\Delta l = 1$:

$$\Pi_{v',v} = \langle \psi' \mid r \mid \psi \rangle \times \delta_{m_s m_s'} \times \left\{ \delta_{0} \sqrt{\frac{(l+m_l+1)(l+1-m_l)}{(2l+3)(2l+1)}} - \frac{1}{2}\delta_{1} \sqrt{\frac{(l+m_l+1)(l+m_l+2)}{(2l+3)(2l+1)}} - \frac{1}{2}\delta_{-1} \sqrt{\frac{(l-m_l+1)(l-m_l+2)}{(2l+3)(2l+1)}} \right\}; \tag{4.6}$$

- for $\Delta l = -1$:

$$\Pi_{v',v} = \langle \psi' \mid r \mid \psi \rangle \times \delta_{m_s m_s'} \times \left\{ \delta_{0} \sqrt{\frac{(l+m_l)(l-m_l)}{(2l-1)(2l+1)}} + \frac{1}{2}\delta_{1} \sqrt{\frac{(l-m_l-1)(l-m_l)}{(2l-1)(2l+1)}} + \frac{1}{2}\delta_{-1} \sqrt{\frac{(l+m_l-1)(l+m_l)}{(2l-1)(2l+1)}} \right\} \tag{4.7}$$

4.1.1 *Calculation of the new wave functions*

Now, we need to know the new eigenfunctions corresponding to the eigenvalues obtained in chapter 3 with strong magnetic field. We note that these new eigenfunctions $\mid v_k \rangle$ are linear combinations of the free hydrogen eigenvectors $\{\mid n; l; m_l; m_s \rangle\}$:

$$\mid v_k \rangle = \sum_i a_i \mid n_i; l_i; m_{l_i}; m_{s_i} \rangle \tag{4.8}$$

For this goal we have added some instructions to our program for calculating the different values of the parameter a_i. These new eigenfunctions are, evidently, orthogonal.

In the following tables, we give some numerical values of the parameter a_i for few magnetic field strengths:

1/ For $\beta = 0.01 (B = 4.701 \times 10^7 G)$;

$\frac{\text{States}}{\text{Eigenvalues}}$	$1s_0$	$2s_0$	$2p_1$	$2p_0$	$2p_{-1}$	$3s_0$...
$\lvert v_1\rangle \to 1.01980$	1.00	-2.64×10^{-4}	0.0	0.0	0.0	-8.2×10^{-5}
$\lvert v_2\rangle \to 0.26724$	2.64×10^{-4}	0.99985	0.0	0.0	0.0	-0.012995
$\lvert v_3\rangle \to 0.24762$	0.0	0.0	0.99990	0.0	0.0	0.0
$\lvert v_4\rangle \to 0.26880$	0.0	0.0	0.0	0.99975	0.0	0.0
$\lvert v_5\rangle \to 0.28762$	0.0	0.0	0.0	0.0	0.99909	0.0
$\lvert v_6\rangle \to 0.115409$	4.7×10^{-5}	0.016184	0.0	0.0	0.0	0.915152

Table:4 : Numerical values of the parameter a_i for $\beta = 0.01$

2/ For $\beta = 0.07 (B \simeq 0.33 \times 10^9 G)$;

$\frac{\text{States}}{\text{Eigenvalues}}$	$1s_0$	$2s_0$	$2p_1$	$2p_0$	$2p_{-1}$	$3s_0$...
$\lvert v_1\rangle \to 1.130327$	0.99992	-0.01128	0.0	0.0	0.0	-3.27×10^{-3}
$\lvert v_2\rangle \to 0.27525$	0.010955	0.97958	0.0	0.0	0.0	-0.083343
$\lvert v_3\rangle \to 0.14585$	0.0	0.0	0.99102	0.0	0.0	0.0
$\lvert v_4\rangle \to 0.336887$	0.0	0.0	0.0	0.99357	0.0	0.0
$\lvert v_5\rangle \to 0.42587$	0.0	0.0	0.0	0.0	0.99102	0.0

Table:5 : Numerical values of the parameter a_i for $\beta = 0.07$

Example of detailed calculation

Once the a_i parameters are known, we can calculate the dipole strength of the transition $d^{(q)}_{v',v} = |\langle v' | r^{(q)} | v\rangle|^2$: An example of details of our calculation is given in this section:

For $\beta = 0.05$; we can write the eigenvectors corresponding to the eigenvalues $E_{|v_1\rangle \equiv 1s_0}$ and $E_{|v_5\rangle \equiv 2p_{-1}}$ respectively , in the form:

$$|v_1\rangle = 99.9957\% \, |100 - \tfrac{1}{2}\rangle - 0.00377979\% \, |200 - \tfrac{1}{2}\rangle - 3.3856 \times 10^{-4}\% \, |300 - \tfrac{1}{2}\rangle$$

$-1.45202 \times 10^{-4}\% \, |320 - \tfrac{1}{2}\rangle + \dots$

$|v_5\rangle = 98.704\% \, |21 - 1 - \tfrac{1}{2}\rangle - 1.29604\% \, |31 - 1 - \tfrac{1}{2}\rangle + \dots;$

Therefore, The dipole strength is:

$$d^{(1)}_{|v_5\rangle \to |v_1\rangle} = |p^{(1)}_{|v_5\rangle \to |v_1\rangle}|^2 = |\langle v_5| r^{(1)} |v_1\rangle|^2 = 0.6400$$

and the oscillator strength is given by:

$$f^{(1)}_{|v_5\rangle \to |v_1\rangle} = \left(E_{|v_1\rangle \equiv 1s_0\rangle} - E_{|v_5\rangle \equiv 2p_{-1}}\right) d^{(1)}_{v_5, v_1} = 0.44753794$$

We recall that, we obtain a positive value because we take the binding energies as positive values.

The transition probability is calculated according to the relation:

$$W^{(q)}_{v', v} = \frac{1}{3\tau_0} (E_{v'} - E_v)^3 \, |p^{(q)}_{v', v}|^2; \tag{4.9}$$

where $\frac{1}{\tau_0} = 8.03 \times 10^9 s^{-1}$[Eng09].

The transition probability between the two levels ($|v_5\rangle \to |v_1\rangle$) is:

$$W^{(1)}_{|v_5\rangle \to |v_1\rangle} = \frac{1}{3\tau_0} \left(E_{|v_1\rangle \equiv 1s_0} - E_{|v_5\rangle \equiv 2p_{-1}}\right)^3 |p^{(1)}_{|v_5\rangle \to |v_1\rangle}|^2 = 5.8562657 \times 10^8 s^{-1}.$$

With the wavefunctions found in the procedure described above, we carried out a study of the electromagnetic transitions between the states $2p_{-1}$, $2p_0$and the ground state $1s_0$, i.e. $1s_0 \leftrightarrow 2p_{-1}$ ($m = 1$), and $1s_0 \leftrightarrow 2p_0$ ($m = 0$), where we are conserved the labels of the eigenstates for a free atom.

The transition $1s_0 \leftrightarrow 2p_{-1}$ occurs by emission (absorption) of circular-right-polarized radiation ($q = +1$), while the transition $1s_0 \leftrightarrow 2p_0$ occurs by emission (absorption) of linearly-polarized (along the magnetic field direction) radiation.

4.1.2 *Results and discussion*

Having obtained wavefunctions and energies of initial $|i\rangle$ and final $|f\rangle$ bound states, one can calculate dipole strengths, oscillator strengths of radiative transitions and the transition probabilities of $2p_0 \to 1s_0$ and $2p_{-1} \to 1s_0$.

In Fig.$(4-1)$; the dipole strengths $d^{(q)}_{v',v}$ for the transitions $2p_0 \to 1s_0$, and $2p_{-1} \to 1s_0$ as a function of magnetic field strength β are exposed. The curves show the calculated values of the dipole strengths $d^{(+1)}_{2p_{-1} \to 1s_0}$ and $d^{(0)}_{2p_0 \to 1s_0}$.

In the Fig$(4-2)$; the oscillator strengths that are, by convention, negative values in the emission case have been calculated with the binding energies as positive values (they are defined as the energy of ionization).

The oscillator strengths of the bound-bound radiative transitions undergo radical changes when the atom moves across the field of the strength more than $0.07a.u.$

For the both transitions ($2p_{-1} \to 1s_0$, $2p_0 \to 1s_0$);the maximum in the dipole strength $d^{(q)}(\beta)$ and in the oscillator strength $f^{(q)}(\beta)$ approximately coincide at $0.07a.u$ .i.e. 0.33×10^9G.

In Fig.$(4-3)$, the first remarkable observation concerning the electromagnetic transitions is the fact that, for strong magnetic fields the (circularly polarized) transition $2p_{-1} \to 1s_0$ is strongly suppressed in comparison to the transition probability for the (linearly polarized) transition $2p_0 \to 1s_0$ where, from this curve, the transition probability$W^{(0)}_{2p_0 \to 1s_0}(\beta)$ is an increasing function of the magnetic field.

This phenomenon is a consequence of the strong deformation of the electronic distribution due to the enourmous Lorentz force acting on it, being elongated in the direction of the magnetic field.

These results show different behaviours for linearly polarized transitions in which, for the $2p_0 \to 1s_0$ transition, the quantities $d^{(0)}_{2p_0 \to 1s_0}$;and $f^{(0)}_{2p_0 \to 1s_0}$ are increasing functions of β in the fields smaller than 0.7×10^8G; but the transition probability $W^{(0)}_{2p_0 \to 1s_0}$ increases with the increasing of strengths of β.

As we go to higher magnetic fields, the results obtained, using our eigenfunctions, show

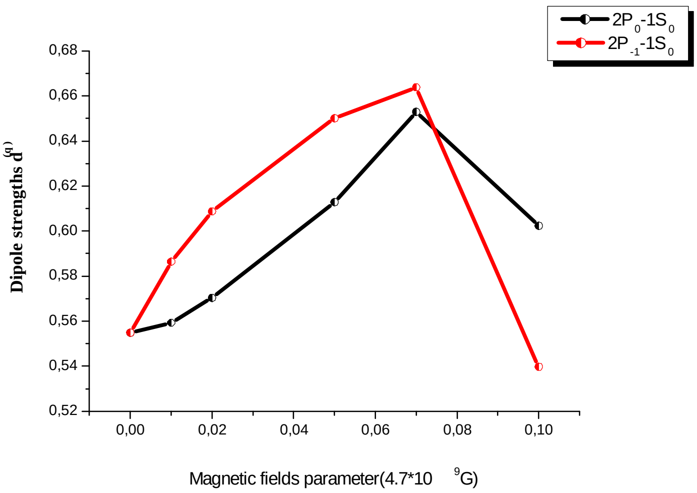

Figure 4-1: Variation in dipole strengthof hydrogen atom in strong magnetic …eld for $2p_0$! $1s_0$ (q = 0)and $2p_{¡1}$! $1s_0$ (q = +1):

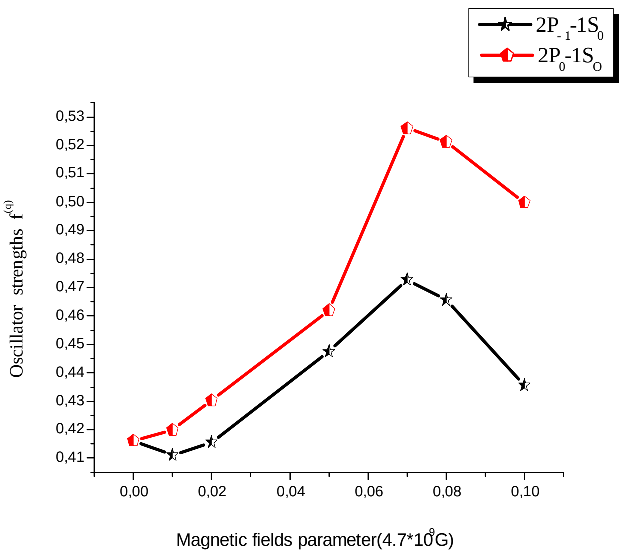

Figure 4-2: Oscillator strength of hydrogen in strong magnetic …eld for $2p_0$! $1s_0$ and $2p_{¡1}$! $1s_0$.

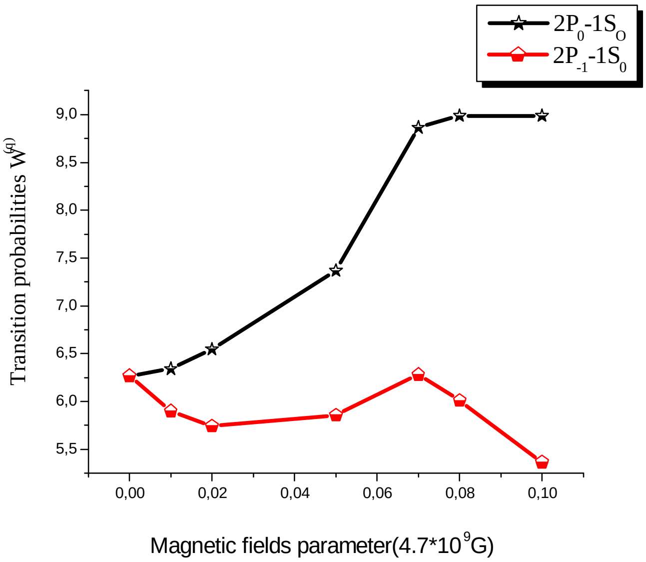

Figure 4-3: Transition probabilitie (in $10^8 s^{-1}$units) for $2p_0 \rightarrow 1s_0$ and $2p_{-1} \rightarrow 1s_0$ of hydrogen in strong magnetic field.

that the dipole strengths and the oscillator strengths of both transitions eventually reach a maximum as the magnetic field grows, after which, they start to decrease monotonously in the region of high magnetic fields $\beta > 0.07$.

Our results for the both transitions are in good agreement with the results for [Lop07] in, roughly, all selected magnetic field strengths. The difference between our results and those of [Lop07] appears in the domain of high magnetic field strengths; where it found that the oscillator strength reach a maximum in $\beta \simeq 1$.

4.2 *Electromagnetic transition probabilities of the lowest states of hydrogen atom in combined strong magnetic and electric fields*

We shall use the same method as in the previous section for the calculation of the new orthogonal wavefunctions, where we divide our work on two subsections: First, we consider the case of hydrogen atom in combined strong magnetic and parallel static electric fields; and second in combined strong magnetic and static electric fields with arbitrary mutual orientations.

4.2.1 *Combined strong magnetic and parallel static electric fields*

In the following tables, we set some numerical values of the parameter a_i for this case:

1/ $\beta = 0.001 (B = 4.701 \times 10^6 G)$ and $f = 0.001 (F = 5.14 \times 10^8 V/m)$.

States / Eigenvalues	$1s_0$	$2s_0$	$2p_1$	$2p_0$	$2p_{-1}$	$3s_0 \ldots$
$\lvert v_1\rangle \to 1.002001$	0.999998	-0.00001	0.0	0.001987	0.0	-0.000009
$\lvert v_2\rangle \to 0.246108$	-0.001402	0.709976	0.0	0.70359	0.0	0.004012
$\lvert v_3\rangle \to 0.250106$	0.0	0.0	0.999529	0.0	0.0	0.0
$\lvert v_4\rangle \to 0.30642$	-0.001404	-0.703756	0.0	0.709674	0.0	0.007201
$\lvert v_5\rangle \to 0.254106$	0.0	0.0	0.0	0.0	0.999529	0.0

Table:6 : Numerical values of the parameter a_i for $\beta = 0.001; f = 0.001$

2/ For $\beta = 0.05 (B \simeq 2.35 \times 10^8 G)$ and $f = 0.05 (F = 2.57 \times 10^{10} V/m)$.

States / Eigenvalues	$1s_0$	$2s_0$	$2p_1$	$2p_0$	$2p_{-1}$	$3s_0 \ldots$
$\vert v_1\rangle \to 1.103898$	0.992668	-0.032528	0.0	0.113238	0.0	-0.0003975
$\vert v_2\rangle \to 0.75532$	-0.047726	0.731060	0.0	0.532668	0.0	0.085867
$\vert v_3\rangle \to 0.397784$	0.0	0.0	0.592375	0.0	0.0	0.0
$\vert v_4\rangle \to 0.551729$	-0.101448	-0.588063	0.0	0.662913	0.0	0.327425
$\vert v_5\rangle \to 0.597784$	0.0	0.0	0.0	0.0	0.592375	0.0

Table:7 : Numerical values of the parameter a_i for $\beta = 0.05$; $f = 0.05$

3/ For $\beta = 0.07 (B \simeq 0.33 \times 10^9 G)$ and $f = 0.07 (F = 0.36 \times 10^{11} V/m)$.

States / Eigenvalues	$1s_0$	$2s_0$	$2p_1$	$2p_0$	$2p_{-1}$	$3s_0 \ldots$
$\vert v_1\rangle \to 1.147556$	0.984848	-0.031665	0.0	0.133762	0.0	0.053938
$\vert v_2\rangle \to 0.645396$	-0.154906	0.581833	0.0	0.659582	0.0	0.317931
$\vert v_3\rangle \to 0.386139$	0.0	0.0	0.643351	0.0	0.0	0.0
$\vert v_5\rangle \to 0.66139$ ………………	0.0	0.0	0.0	0.0	0.643351	0.0

Table:8 : Numerical values of the parameter a_i for $\beta = 0.07$; $f = 0.07$

From these tables, we can see that the a_i parameters have a non-vanishing values for, roughly, the most states, therefore, the new eigenstates are different from the free atom's labels. We can prove this by giving an example:

For $B = 4.701 \times 10^6 G$; $F = 5.14 \times 10^8 V/m$.

$|v_1\rangle = 99.9996\% \, |100 - \tfrac{1}{2}\rangle - 10^{-10}\% \, |200 - \tfrac{1}{2}\rangle + 3.948169 \times 10^{-4}\% \, |210 - \tfrac{1}{2}\rangle$
$- 8.10 \times 10^{-11}\% \, |300 - \tfrac{1}{2}\rangle + \ldots$

$|v_2\rangle = -1.96733 \times 10^{-4}\% \, |100 - \tfrac{1}{2}\rangle + 50.450\% \, |200 - \tfrac{1}{2}\rangle + 49.54739\% \, |210 - \tfrac{1}{2}\rangle$
$+ 0.001611\% \, |300 - \tfrac{1}{2}\rangle + \ldots$

$|v_3\rangle = 100\% \, |211 - \tfrac{1}{2}\rangle.$

$|v_4\rangle = -1.97326 \times 10^{-4}\% \, |100 - \tfrac{1}{2}\rangle - 49.5786\% \, |200 - \tfrac{1}{2}\rangle + 50.416\% \, |210 - \tfrac{1}{2}\rangle$

$+0.0051908\% \, |300 \; -\tfrac{1}{2}\rangle + \ldots$

$|v_5\rangle = 100\% \, |21 \; -1 \; -\tfrac{1}{2}\rangle.$

We remark, therefore, that there are a mixing between the basis states in which we can't neglect.

Thus we prefer to use a new labels to our new eigenvectors $\{|v_k\rangle\}$;where we must realize in our calculations that these new eigenvectors are normalized.

Therefore, we expect a great variation of the transition probabilities comparing to the previous case of magnetic field; that is what we try to prove in this section.

Results and Outlooks

Using the same method as in the case of magnetic field, we calculated the dipole strength, oscillator strength and transition probabilities of $|v_3\rangle \to |v_1\rangle$ (corresponding to $2p_1 \to 1s_0$ for a free atom); $|v_5\rangle \to |v_1\rangle$ (corresponding to $2p_{-1} \to 1s_0$) and $|v_4\rangle \to |v_1\rangle$ (corresponding to $2p_0 \to 1s_0$):

From Fig.$(4-4)$, we see that the dipole sterngth of both $|v_3\rangle \to |v_1\rangle$ and $|v_5\rangle \to |v_1\rangle$ transitions are comparable in magnitude.

As shown in Fig.$(4-5)$, for small magnetic and static electric fields, the oscillator strength for both transitions are comparable in magnitude, while for $\beta \equiv f \geq 0.03$ the oscillator strength of $|v_3\rangle \to |v_1\rangle$ starts to increase faster than the other transition $|v_5\rangle \to |v_1\rangle.$

The first remarkable observation of the electromagnetic transitions, from Fig.(4-6), is that for small magnetic and static electric fields strengths, the transition probabilities for both transitions are comparable in magnitude, but for strong fields ($\beta \equiv f \geq 0.05$). The transition $|v_5\rangle \to |v_1\rangle$ is strongly lowered in comparison to the transition probability of $|v_3\rangle \to |v_1\rangle.$

From Fig.(4-7), the transition $|v_4\rangle \to |v_1\rangle$ decrease rapidely for strengths less than $\beta \equiv f = 0.02.$ While it starts to increase for $\beta \equiv f = 0.03.$

In the following subsection, transition probabilities for hydrogen atom in strong magnetic and static electric fields with arbitrary mutual orientations will be presented.

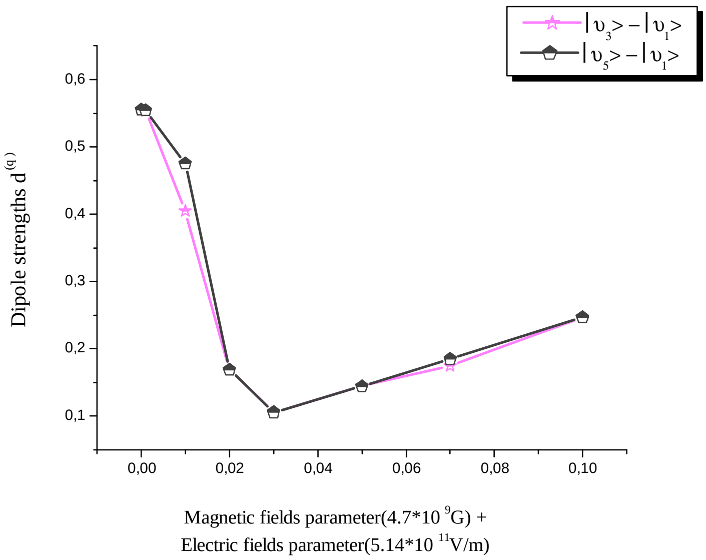

Figure 4-4: Dipole strengths for $|v_3\rangle \to |v_1\rangle$ and $|v_5\rangle \to |v_1\rangle$ as a function of both fields. The horizontal axis gives the common strengths of the magnetic and electric fields.

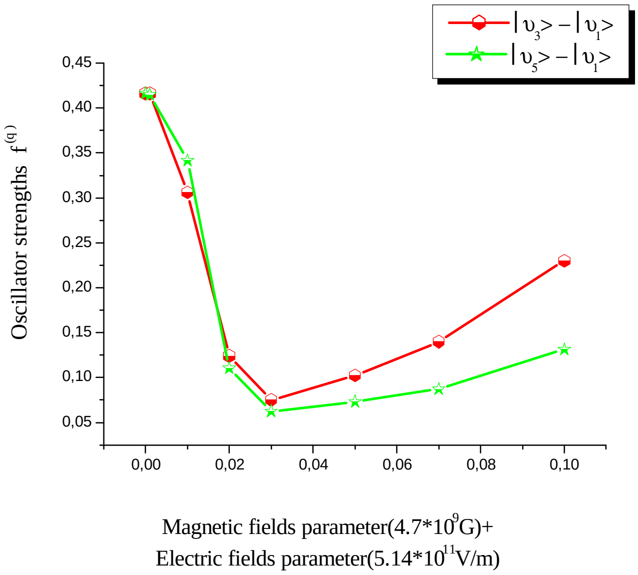

Figure 4-5: Variation in Oscillator strength for $|v_3\rangle \to |v_1\rangle$ and $|v_5\rangle \to |v_1\rangle$. The horizontal axis gives the common strengths of the magnetic and electric fields.

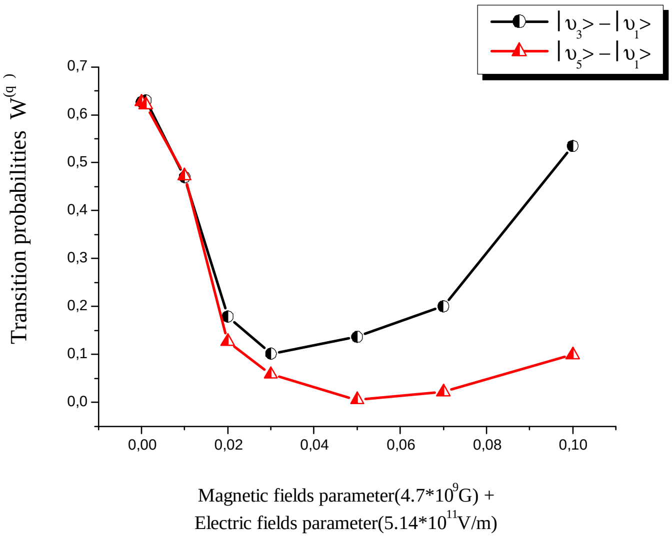

Figure 4-6: Variation in transition probabilities (in $10^9 s^{-1}$units) for $|v_3\rangle \rightarrow |v_1\rangle$ and $|v_5\rangle \rightarrow |v_1\rangle$ of hydrogen atom in combined strong magnetic and parallel electric fields. The horizontal axis gives the common strengths of the magnetic and electric fields.

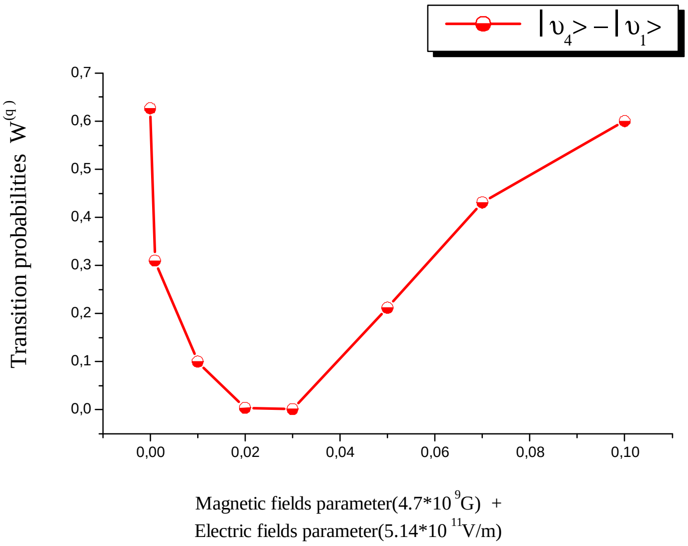

Figure 4-7: Transition probabilities(in $10^9 s^{-1}$units) for $|v_4\rangle \to |v_1\rangle$ of hydrogen atom in combined strong magnetic and parallel electric fields of the same strengths of both fields.

4.2.2 *In combined strong magnetic and static electric fields with arbitrary mutual orientations*

As in the last case, we set some numerical values of the parameter a_i for a few magnetic and electric field strengths:

1/ For $\beta = 0.001 (B = 4.701 \times 10^6 G)$ and $f = 0.001 (5.14 \times 10^8 V/m)$.

States / Eigenvalues	$1s_0$	$2s_0$	$2p_1$	$2p_0$	$2p_{-1}$	$3s_0 \ldots$
$|v_1\rangle \to 1.002015$	0.999989	−0.000061	0.002802	0.001987	0.002817	−0.000043
$|v_2\rangle \to 0.266444$	0.003133	0.689398	−0.383775	−0.323715	−0.514549	−0.022334
$|v_3\rangle \to 0.239172$	−0.003087	0.709602	0.511263	0.294804	0.378503	−0.005685
$|v_4\rangle \to 0.251597$	−0.000026	0.098657	−0.691577	0.678534	0.219012	−0.000640
$|v_5\rangle \to 0.253400$	0.000009	0.089073	−0.327679	−0.585209	0.733598	−0.001855

Table:9 : Numerical values of the parameter a_i for $\beta = 0.001$; $f = 0.001$

2/ For $\beta = 0.02 (B \simeq 9.4 \times 10^{7} G)$ and $f = 0.02 (F = 1.028 \times 10^{10} V/m)$.

States / Eigenvalues	$1s_0$	$2s_0$	$2p_1$	$2p_0$	$2p_{-1}$	$3s_0 \ldots$
$\vert v_1\rangle \to 1.046607$	0.993674	-0.032097	0.061627	0.47867	0.069246	-0.005970
$\vert v_2\rangle \to 1.017027$	0.019413	0.228908	-0.138933	-0.150119	-0.173328	-0.473214
$\vert v_4\rangle \to 0.462560$	0.009314	0.163432	-0.274639	0.382011	-0.135175	-0.070997
$\vert v_5\rangle \to 0.576556$	-0.011538	-0.22805	-0.230399	-0.069228	0.371154	-0.074580

Table:10 : Numerical values of the parameter a_i for $\beta = 0.02; f = 0.02$

From these tables, we see that the values of a_i parameter are more overlapped, thus we conclude that the adding of the non-parallel electric field made great changes, on the hydrogenic wavefunctions, which caused the deformation on the hydrogen's structure.

In order to normalize the new wave functions, we must divide $\langle v_{k'} | v_k \rangle$ by $\sum_i |a_i|^2$.

For example, when we calculate the probability of the transition $|v_3\rangle \to |v_1\rangle$ (corresponding to $2p_1 \to 1s_0$ for a free atom) with magnetic field $B \simeq 9.4 \times 10^7 G$ and a parallel electric field of strength $F = 5.14 \times 10^8 V/m$, we can write:

$|v_1\rangle = 99.9988\% |100 - \tfrac{1}{2}\rangle + 9.6629 \times 10^{-5}\% |200 - \tfrac{1}{2}\rangle - 6.95905 \times 10^{-4}\% |211 - \tfrac{1}{2}\rangle -$
$3.89668 \times 10^{-4}\% |210 - \tfrac{1}{2}\rangle - 8.59664 \times 10^{-4}\% |21 - 1 - \tfrac{1}{2}\rangle + 8.00891 \times 10^{-6}\% |300 - \tfrac{1}{2}\rangle + \ldots\ldots$
$|v_3\rangle = 8.63521 \times 10^{-4}\% |100 - \tfrac{1}{2}\rangle - 4.49619\% |200 - \tfrac{1}{2}\rangle + 95.3824\% |211 - \tfrac{1}{2}\rangle +$
$0.0473422\% |210 - \tfrac{1}{2}\rangle + 0.0408417\% |21 - 1 - \tfrac{1}{2}\rangle - 0.0323428\% |300 - \tfrac{1}{2}\rangle + \ldots\ldots$

The dipole strength $d^{(-1)} = |\langle v_3 | r | v_1 \rangle|^2 = 0.58397$ but, on the other hand, we get that:

$$\sum_i |a_i|^2 = 1.13893$$

Thus, we find that the dipole strength of this transition is:

$$d^{(-1)} = \frac{|\langle v_3 | r | v_1 \rangle|^2}{(1.13893)^2} = 0.450191$$

and the oscillator strength is giving by:

$$f^{(-1)} = 0.450191 \times (1.03217 - 0.239415) = 0.356891$$

Finally, the transition probability of $|v_3\rangle \rightarrow |v_1\rangle$; corresponding to $(2p_1 \rightarrow 1s_0)$ for a free atom, in such conditions is:

$$W^{(-1)} = \frac{8.03}{3} \times 10^9 \times d^{(-1)} \times (1.03217 - 0.239415)^3 = 6.00355 \times 10^8 s^{-1}.$$

®: ***Results and Outlook***

In the following table, we present some results of dipole strengths, oscillator strengths and transition probabilities for giing values of magnetic and static electric fields. We remark a variation comparing to the previous results in the last sections .

Transitions $\beta(a.u);\ f(a.u)$	$\lvert v_3\rangle \rightarrow \lvert v_1\rangle$ $d^{(q)}$	$\lvert v_3\rangle \rightarrow \lvert v_1\rangle$ $f^{(q)}$	$\lvert v_3\rangle \rightarrow \lvert v_1\rangle$ $W^{(q)}(\times 10^9 s^{-1})$
$\beta = f = 10^{-3}$	0.461248	0.351860	0.5480683
$\beta = 10^{-2}; f = 10^{-3}$	0.456912	0.354155	0.56952
$\beta = 0.02; f = 10^{-3}$	0.450191	0.356891	0.600355

Table:11 : Numerical values of $d^{(q)}$; $f^{(q)}$ and $W^{(q)}$ for $|v_3\rangle \rightarrow |v_1\rangle$

Transitions $\beta(a.u);\ f(a.u)$	$\lvert v_5\rangle \rightarrow \lvert v_1\rangle$ $d^{(q)}$	$\lvert v_5\rangle \rightarrow \lvert v_1\rangle$ $f^{(q)}$	$\lvert v_5\rangle \rightarrow \lvert v_1\rangle$ $W^{(q)}(\times 10^9 s^{-1})$
$\beta = f = 10^{-3}$	0.493751	0.369629	0.554469
$\beta = 10^{-2}; f = 10^{-3}$	0.524449	0.381758	0.541444
$\beta = 0.02; f = 10^{-3}$	0.4889514	0.350572	0.481279

Table:12 : Numerical values of $d^{(q)}$; $f^{(q)}$ and $W^{(q)}$ for $|v_5\rangle \rightarrow |v_1\rangle$

Transitions $\beta(a.u);\ f(a.u)$	$\frac{\vert v_4\rangle \to \vert v_1\rangle}{d^{(q)}}$	$\frac{\vert v_4\rangle \to \vert v_1\rangle}{f^{(q)}}$	$\frac{\vert v_4\rangle \to \vert v_1\rangle}{W^{(q)}(\times 10^9 s^{-1})}$
$\beta \equiv f = 10^{-3}$	0.42417	0.318305	0.479782
$\beta = 10^{-2}; f = 10^{-3}$	1.7433	0.98871	1.91975
$\beta = 0.02; f = 10^{-3}$	1.01787	0.76323	1.14862

Table:13 : Numerical values of $d^{(q)}$; $f^{(q)}$ and $W^{(q)}$ for $|v_4\rangle \to |v_1\rangle$

The probabilities of the transition $|v_3\rangle \to |v_1\rangle$ are increased with the magnetic field; while the probabilities of the transition $|v_5\rangle \to |v_1\rangle$ are decreased.

We shall give a comparison of our results in the three cases, as an example, for $B = 4.7\times 10^6 G$ and $F = 5.14 \times 10^9 V/m$:

Transitions $W^{(q)}(\text{in } 10^9 s^{-1})$	free	In mag + paral elect field	In mag + non − paral elect field
$\vert v_4\rangle \to \vert v_1\rangle$	0.626636	0.309966	0.479782
$\vert v_5\rangle \to \vert v_1\rangle$	0.626636	0.620830	0.554469
$\vert v_3\rangle \to \vert v_1\rangle$	0.626636	0.629917	0.5480683

Table:14 : Comparison between our numerical values of $W^{(q)}$ for three transitions.

We denote that the transitions $|v_3\rangle \to |v_1\rangle; |v_4\rangle \to |v_1\rangle$ and $|v_5\rangle \to |v_1\rangle$ are labeled in the free case as $|2p_1\rangle \to |1s_0\rangle; |2p_0\rangle \to |1s_0\rangle$ and $|2p_{-1}\rangle \to |1s_0\rangle$ respectively.

Up to now experimental investigation on atoms in combined electric and magnetic fields have concentrated on parallel and perpendicular field orientation, therefore it is a challange to observe the effect of the fields with arbitrary mutual orientation experimentally.

It is important to emphasize here that there exist no criterion, for binding energies and transition probabilities, to decide about which values are more accurate. Thus, it is not clear so far which results for dipole strengths are better. Therefore, more investigations on the electromagnetic transitions in the hydrogen atom in a magnetic field, specially in the domain of strong magnetic fields, would be desirable in order to answer this question.

Chapter 5

Helium atom in strong magnetic and electric …elds

The properties of matter are signi…cantly modi…ed by strong magnetic …elds as are typically found on the surfaces of neutron stars and white dwarfs.The study of matter in strong magnetic …elds is obviously an important component of these compact objects astrophysics research.

In particular, interpretation of the ever improving spectral data of neutron stars requires a detailed theoretical understanding of the physical properties of highly-magnetized H and He which are the lightest elements and also are likely to be the most important chemical species in the envelope due to their predominance in the accreting gas and also due to quick separation of light and heavy elements in the gravitational …eld of the NS. If the accretion rate is low, gravitational settling produces a pure H envelope. Alternatively, a pure He layer may result if the hydrogen has completely burnt out[Lai01]:

Beyond hydrogen studies, there is signi…cant interest in detailed data on heavier elements, such as He, Na, Fe and even molecules. Especially helium plays an important role in the atmospheres of magnetic white dwarfs and neutron stars.

There are several spectral features and structures which can not be explained by hydrogenic spectra like ,for example, in the spectrum of the magnetic white dwarf GD229, which leads to the conjecture that there are further components in the atmospheres, i.e. atoms with more than one electron.

The simplest atom beyond Hydrogen atom is the helium which contains two electrons, but despite this simplicity, its treatment is difficult as the heavy atoms.

5.1 *A simplified overview on Helium atom*

Helium has only two electrons but this simplicity is deceptive.To treat systems with three particles, it requires new concepts that also apply to multi-particle systems in many branches of physics, and it is very worthwhile to study them carefully using the example of helium. There is truth in the saying that a detailed understanding of the two-electron system is sufficient for much syudies of the atomic structure.

In this section, we shall limit our discussion to the non- relativistic theory of two-electron atom, where the two electrons interact with the nucleus of an atom of a charge Ze, obey a Schrodinger equation of the form (in a.u.) :

$$\left\{\frac{-\nabla_1^2}{2}+\frac{-\nabla_2^2}{2}+\left(-\frac{Z}{r_1}-\frac{Z}{r_2}+\frac{1}{r_{12}}\right)\right\}\Psi(r_1;r_2)=E\,\Psi(r_1;r_2) \tag{5.1}$$

The first two terms are the kinetic energy operators for the two electrons, the following two terms are the potential energies of the two electrons in the field of the nucleus of charge 2e, and the final term is the potential energy arising from the electrostatic repulsion of the two electrons when they are separated by a distance r_{12}, with $r_{12}=|\vec{r}_1-\vec{r}_2|$ is defined in Fig.(5 $-$ 1).

In going beyond hydrogen to other atoms, an additional quantum principle becomes important. Identical particles in quantum physics have to be described by wave functions that are totally antisymmetric (symmetric) under the interchange of any pair of them if they are fermions (bosons), that is, if their intrinsic spins are half-odd integers (integers).

For the electrons in an atom, the "Pauli exclusion principle" about antisymmetric functions acts as a constraint on the states that successive electrons can occupy.

We note that $\Psi(r_2;r_1)=\pm\Psi(r_1;r_2)$;where wave functions which satisfy this formula with the plus sign (that is, whose spatial part remains unchanged upon permutating the spatial coordinates of the two electrons) are said to be space-symmetric which describes the para-states, on the other hand, wave functions with the minus sign (whose spatial part changes sign on interchanging the spatial coordinates of the two electrons) are said to be space-antisymmetric

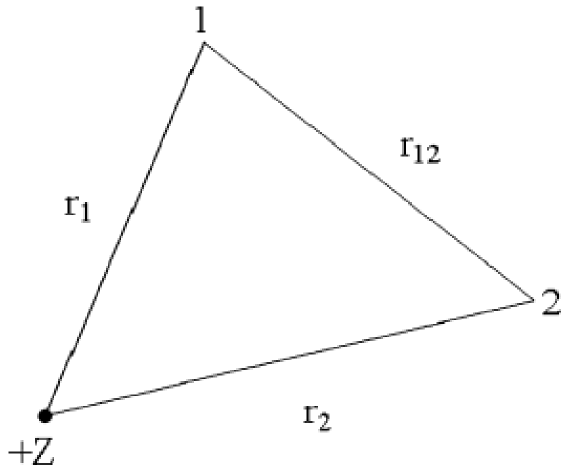

Figure 5-1: The 2-electrons atomic system.

which describes the ortho-states.

In addition, the full eigenfunctions Ψ of the system must be products of the spatial eigenfunctions $\Psi(r_1; r_2)$; satisfying the Schrodinger equation, times spin wave functions $\chi(1;2)$ for the two-electron system. That is:

$$\Psi(q_1; q_2) = \Psi(r_1; r_2)\,\chi(1;2) \tag{5.2}$$

where q_i denotes collectively the space and spin coordinates of electron i:

We have four independent spin states each of which can be represented as the product of two individual spin functions. That is:

$$\begin{aligned} \chi_1(1;2) &= \alpha(1)\alpha(2) \uparrow\uparrow \\ \chi_2(1;2) &= \alpha(1)\beta(2) \uparrow\downarrow \\ \chi_3(1;2) &= \beta(1)\alpha(2) \downarrow\uparrow \\ \chi_4(1;2) &= \beta(1)\beta(2) \downarrow\downarrow \end{aligned} \tag{5.3}$$

We can construct four normalized and orthogonal spin functions which are eigenstates of both operators S^2 and S_z; these are:

The antisymmetric spin function:

$$\chi_{0,0}(1,2) = \frac{1}{\sqrt{2}}[\alpha(1)\beta(2) - \beta(1)\alpha(2)]; \tag{5.4}$$

and the three symmetric spin function are:

$$\begin{aligned} \chi_{1,1}(1,2) &= \alpha(1)\alpha(2); \\ \chi_{1,0}(1,2) &= \frac{1}{\sqrt{2}}[\alpha(1)\beta(2) + \beta(1)\alpha(2)]; \\ \chi_{1,-1}(1,2) &= \beta(1)\beta(2) \end{aligned} \tag{5.5}$$

We know that the Pauli exclusion principle requires that the total wave function $\psi(q_1, q_2, ...q_N)$ of a system of N electrons must be antisymmetric.Then, in order to obtain total antisymmetric wave functions $\psi(q_1, q_2)$ we must multiply space symmetric (para) wave functions by the antisymmetric (singlet) spin state; or multiply space antisymmetric (ortho) wave functions by one of the three symmetric spin functions.

5.1.1 *The independent particle approximation*

It appears to be impossible to find analytical solutions of a complicated partial differential equation in six variables, such as Eq.(5.1); this is due to the presence of the electronic repulsion term.

We shall give in this section a simple approach which yields a qualitative understanding of the main features of 2-electrons atoms spectrum.

Neglecting this mutual repulsion, as a first approximation, we can write the equation as the unperturbed system which is described by a hamiltonian that is the sum of two hydrogenic hamiltonians:

$$H^{(0)}\psi = (\hat{h}_1 + \hat{h}_2)\psi = E^{(0)}\psi \tag{5.6}$$

where

$$\hat{H}_i = \frac{-\nabla_i^2}{2} - \frac{Z}{r_i}; \qquad i = 1; 2:$$

In what follows, we will use the atomic units defined in the first section of chapter 3.

For helium, the wavefunction of the two electrons is the product of two hydrogenic wavefunctions:

$$\Psi(r_1; r_2) = \Psi_{n_1;l_1;m_1}(r_1) \times \Psi_{n_2;l_2;m_2}(r_2) \tag{5.7}$$

Thus, the discrete energy of this atom (neglecting repulsion) in its ground state ($n_1 = 1; n_2 = 1$) is:

$$E^{(0)}_{n_1;n_2} = E_{n_1} + E_{n_2} = -\frac{Z^2}{2}\left(\frac{1}{n_1^2} + \frac{1}{n_2^2}\right) = -108{:}8\mathrm{eV} \tag{5.8}$$

where both electrons have energy $E^{(0)}_1 = E^{(0)}_2 = -54{:}4\mathrm{eV}$:

The experimental value is distinctly different from this value. The total work of removing both electrons is $79\mathrm{eV}$, where $24{:}6$ eV for removing the first electron (ionization of the He to the singly charged positive ion He^+) and $54{:}4\mathrm{eV}$ for the removal of the second electron (ionization of the singly charged He^+ to the doubly charged positive ion He^{++}).

The second value is the same as one would expect from a comparison with the hydrogen atom which the ionizsation energy is $13{:}6\mathrm{eV}$. For helium, one would expect the energy to be four times as great, because the nucleus is doubly charged. The model for the binding energy must therefore be by taking into account the energy of the interaction of the two electrons[Foo05]:

5.1.2 *The ground state of helium atom*

®:*Perturbation theory*

The zero-order wave function can also write as:

$$\Psi^{(0)}(r_2; r_1) = \Psi_{n_2;l_2;m_2}(r_1) \times \Psi_{n_1;l_1;m_1}(r_2) \tag{5.9}$$

which differs from eq.(5.7) only in an exchange of the electron labels, corresponds to the same energy $E^{(0)}_{n_1;n_2}$. This particular case of degeneracy with respect to exchange of electron labels is called *exchange degeneracy.* Thus the exact spatial wave functions of two-electron atoms must be either symmetric or antisymmetric with respect to the interchange of the coordinates r_1 and r_2.

We can write the zero-order spatial wave functions of the simple independent- particle model as:

$$\psi^{(0)}_{\pm}(r_1; r_2) = \frac{1}{\sqrt{2}}\left[\psi_{n_1;l_1;m_1}(r_1) \times \psi_{n_2;l_2;m_2}(r_2) \pm \psi_{n_2;l_2;m_2}(r_1) \times \psi_{n_1;l_1;m_1}(r_2)\right] \qquad (5.10)$$

where the factor $\frac{1}{\sqrt{2}}$ guarantees that the functions $\psi^{(0)}_{\pm}(r_1; r_2)$ are normalized.

The plus sign corresponds to the para wave function while the minus sign corresponds to the ortho wave function.

Now we need to calculate the perturbation produced by the electron-electron repulsion for the ground state of helium. The normalized spatial wave function is therefore given by the simple symmetric(para) wave function:

$$\psi^{(0)}_{1s1s}(r_1; r_2) = R^{Z=2}_{1s}(r_1) \times R^{Z=2}_{1s}(r_2) \times \frac{1}{4\pi} \qquad (5.11)$$

where $\frac{1}{4\pi}$ is the angular part of an s-electron wavefunction, and the corresponding spatial part of the ground state wave function being:

$$\psi_{1s1s}(r_1; r_2) = \frac{Z^3}{\pi} e^{-Z(r_1+r_2)} \qquad (5.12)$$

We can split the Hamiltonian as $H = H_0 + H'$ in which H_0 is the unperturbed term, and $H' = \frac{1}{r_{12}}$ will be treated as perturbation.

Then, the first-order correction to the ground state energy is (in a.u.):

$$\begin{aligned} E^{(1)}_0 &= \langle \psi_{1s1s} | H' | \psi_{1s1s} \rangle \\ &= \int |\psi_{1s1s}(r_1)|^2 \frac{1}{r_{12}} |\psi_{1s1s}(r_2)|^2 \, d^3\mathbf{r}_1 d^3\mathbf{r}_2 \end{aligned}$$

$$= \frac{Z^6}{\pi^2} \int e^{-2Z(r_1+r_2)} \frac{1}{r_{12}} d^3\mathbf{r}_1 d^3\mathbf{r}_2 \tag{5.13}$$

We can expand $\frac{1}{r_{12}}$ in the Legendre polynomials as:

$$\frac{1}{r_{12}} = \sum_{l=0} \frac{(r_<)^l}{(r_>)^{l+1}} P_l(\cos\theta) = \sum_{l=0} \sum_{m_l=-l} \frac{4\pi}{(2l+1)} \frac{(r_<)^l}{(r_>)^{l+1}} Y^*_{lm}(\theta_1, \varphi_1) Y_{lm}(\theta_2, \varphi_2) \tag{5.14}$$

where θ is the angle between the vectors $\mathbf{r}_1$ and $\mathbf{r}_2$, and $r_<$ is the smaller of r_1 and r_2.

We substitute the expression of $\frac{1}{r_{12}}$ in the eq.(5.13) and we calculate the integral using some properties of the spherical harmonics, thus, we get that $E_0^{(1)} = \frac{5}{8} Z \text{ a.u.} = 34\text{eV}$, which is a positive contribution to the energy; Adding this to the (zeroth-order) estimate $E^{(0)}$ gives an energy of $E_{1s} = E_0^{(0)} + E_0^{(1)} = -108.8 + 34 \approx -75\text{eV}$.

It takes an energy of 75eV to remove both electrons from a helium atom leaving a bare helium nucleus He^{++}; the second ionization energy. To go from He^+ to He^{++} takes 54.4eV, so this estimate suggests that the first ionization energy (required to remove one electron from He to create He^+) is $IE(He) = 75 - 54 \approx 21\text{eV}$.

But the expectation value of $E_0^{(1)}$ is not small compared to the binding energy and therefore, the adjustment of the wavefunctions which can be accounted by the variational method will be necessary.

β: *Ritz variational method*

Let Ψ be an arbitrary trial function, the functional

$$E[\Psi] = \frac{\langle \Psi | \mathbf{H} | \Psi \rangle}{\langle \Psi | \Psi \rangle} \tag{5.15}$$

provides a variational principle for the discrete eigenvalues of the Hamiltonian.

If the function Ψ is identical with any one of the exact eigenfunctions ψ, then $E[\Psi]$ is identical with the corresponding exact eigenvalue E. In other words, Schrodinger's variational principle states that any function Ψ for which the functional $E[\Psi]$ has a stationary value is a solution of the equation $H\psi = E\psi$.

Moreover, this functional also yields a minimum principle for the ground state energy. That is:

$$E_0 \le E[\Phi] \tag{5.16}$$

In order to take into account approximately the screening effect on each electron on the other one, we shall therefore select a trial function of the form of (5-12). That is , (in a.u.)

$$\Phi(r_1; r_2) = \frac{Z_e^3}{\pi} e^{-Z_e(r_1+r_2)} \tag{5.17}$$

where Z_e is the effective charge which is considered as a variational parameter.

Then, we can calculate the different terms of the Hamiltonian using the trial function Φ (with $\langle\Phi | \Phi\rangle = 1$) :

$$E[\Phi] = \langle\Phi | T_1 + T_2 - \frac{Z}{r_1} - \frac{Z}{r_2} + \frac{1}{r_{12}} | \Phi\rangle \tag{5.18}$$

where we have set

$$T_i = \frac{-\nabla^2_{r_i}}{2}; \qquad i = 1; 2:$$

We can, easyly, prove that $\langle\Phi | T_i | \Phi\rangle = \frac{1}{2}Z_e^2$; and $\langle\Phi | \frac{1}{r_i} | \Phi\rangle = Z_e$; $i = 1; 2$:

The expression $\langle\Phi | \frac{1}{r_{12}} | \Phi\rangle$ has already been calculated when $Z = Z_e$, in which case it is equal to the correction $E_0^{(1)}$; thus, we get $\langle\Phi | \frac{1}{r_{12}} | \Phi\rangle = \frac{5}{8}Z_e$:

Puting together the above results, we have:

$$E[\Phi] \equiv E(Z_e) = Z_e^2 - 2ZZ_e + \frac{5}{8}Z_e \tag{5.19}$$

Now, we shall minimize $E(Z_e)$ with respect to the variational parameter Z_e: Hence we write:

$$\frac{\partial E}{\partial Z_e} = 2Z_e - 2Z + \frac{5}{8} = 0 \tag{5.20}$$

So that

$$Z_e = Z - \frac{5}{16} \tag{5.21}$$

substituting this value in the equation of $E(Z_e)$; we get

$$E\left(Z_e = Z - \frac{5}{16}\right) = -\left(Z - \frac{5}{16}\right)^2 \text{ a.u.} \tag{5.22}$$

With $Z = 2$, one finds $E = -(\frac{27}{16})^2 = -2.84766$ a.u.

If we substitute Z_e with Z, we find a result identical to those given by the first-order perturbation theory. The variational method gives clearly a better result.

5.2 *Helium atom in strong (stellar) magnetic fields*

Since the astrophysical discovery of strong magnetic fields on the surfaces of white dwarfs ($\leq 10^5$ T) and neutron stars ($\sim 10^9$ T) the interest in the behaviour and the properties of matter in strong magnetic fields has increased enormously.

In order to facilitate a proper understanding of the spectra of neutron stars and white dwarf stars one must necessarily have more stringent bounds on the energy levels of atoms in the atmospheres of these compact objects in the intermediate regime of magnetic field strengths.

Whereas the extensive calculations for the hydrogen atom in strong magnetic fields have resulted in a much better understanding of the spectra of hydrogen-dominated white dwarfs, there are still magnetic white dwarfs like the GD229 with unexplained absorption spectra, for which transitions of neutral He are considered to be important. Therefore the properties of the helium atom in strong magnetic fields are of great relevance.

We investigate the electronic structure of the helium atom in a magnetic field $\beta \leq 1$, the atom is treated as a non-relativistic system with two interacting electrons and a fixed nucleus.

5.2.1 *The ground state of helium atom in strong magnetic field using the variational method*

We note, firstly, that an exception to the equation

$$\Psi_{\pm}(q_1;q_2) = \frac{1}{\sqrt{2}}\left[\psi_{nlm}(r_1)\times\psi_{n';l';m'}(r_2) \pm \psi_{n';l';m'}(r_1)\times\psi_{n;l;m}(r_2)\right]\times\chi(1;2) \qquad (5.23)$$

occurs for the case of the ground state, where both electrons are in the 1s state (that is, $n_1 = n_2 = 1; l_1 = l_2 = 0; m_1 = m_2 = 0$).

The wave function Ψ_{-} for the ortho state is then seen to vanish, in agreement with the original formulation of the Pauli principle, according to which two electrons cannot be exactly in the same state. Indeed, the spatial quantum numbers for both electrons having the same values $n = 1; l = 0$ and $m = 0$; the spin quantum numbers of the two electrons must have antiparallel spin, and only the singlet (para) state is allowed.

It is apparent from the last discussion (perturbation theory) that each electron moves in the fully unscreening effect of each electron on the other one, we shall therefore choose a trial function (as we showed in the paragraph of Ritz variational method) in the form (in a.u.) :

$$\begin{aligned} \Phi(r_1;r_2) &= \psi_{1s}^{Z_e}(r_1)\,\psi_{1s}^{Z_e}(r_2) \\ &= \frac{Z_e^3}{\pi}\exp\left[-Z_e(r_1+r_2)\right] \end{aligned} \qquad (5.24)$$

where the normalized spatial wave function for the ground state of the helium atom (a simple symmetric (para) wave function) is used with taking Z_e (effective charge) as a variational parameter.

we shall neglect all small corrections (motion of the nucleus, relativistic corrections...) and we focus our attention on the discrete states.

We recall that the ground state of helium is a singlet state ($S = 0; M_S = 0$) and possesses no orbital angular momentum ($L = 0$) ; and the linear Zeeman term in the interaction Hamiltonian with a magnetic field is thus zero, so there is no Zemman splitting. Nevertheless, the quadratic term in the hamiltonian produces a shift in the energy, which depends on the magnetic field;

that is what we try to investigate it in this section[Arm06]:

α: ***Analytical calculations***

We consider a system consisting of two electrons and a nucleus in a homogeneous magnetic field **B** along the z-axis. If we use Z-scaled atomic units, i.e. as energy unit Z^2Rydberg and as length unit a_{Bohr}/Z, and if we neglect the finite nuclear mass effect, the Hamiltonian reads:

$$H = \sum_{i=1}^{2}\left[\frac{-\nabla_i^2}{2} - \frac{1}{|\mathbf{r}_i|} + \underbrace{\frac{\gamma_Z^2}{2} r_i^2 \sin^2\theta_i}_{Quadratic-Zeeman}\right] + \underbrace{\frac{1}{Z\,|\mathbf{r}_1 - \mathbf{r}_2|}}_{Interaction-term}; \qquad i = 1;2.$$

But we shall use in this chapter the usual atomic units as in the case of hydrogen atom, i.e. the energy will be measured in Rydberg unit ($E_1 = \frac{-1}{2}a.u.$), thus, the Hamiltonian reads:

$$H = \sum_{i=1}^{2}\left[\underbrace{\frac{-\nabla_i^2}{2}}_{T_i} - \frac{Z}{|\mathbf{r}_i|} + \underbrace{\frac{\gamma^2}{2} r_i^2 \sin^2\theta_i}_{H_{Q-Z}}\right] + \underbrace{\frac{1}{r_{12}}}_{Interact-term}; \qquad i = 1;2. \tag{5.25}$$

Using the variational principle for the discrete eigenvalues of this Hamiltonian, $E[\Psi] = \frac{\langle\Psi|H|\Psi\rangle}{\langle\Psi|\Psi\rangle}$, we get that:

$$E[\Psi] = \langle\Psi(\mathbf{r}_1;\mathbf{r}_2)|\, T_1 + T_2 - \frac{Z}{r_1} - \frac{Z}{r_2} + \frac{1}{r_{12}} + \frac{\gamma^2}{2}(r_1^2\sin^2\theta_1 + r_2^2\sin^2\theta_2)\,|\Psi(\mathbf{r}_1;\mathbf{r}_2)\rangle \tag{5.26}$$

We used the space wave function because all these terms don't depend on spin.

As we showed in the previous section about the Ritz variational method, the first terms were calculated in which we obtained: $\langle\Psi|T_i|\Psi\rangle = \frac{1}{2}Z_e^2$ and $\langle\Psi|\frac{1}{r_i}|\Psi\rangle = Z_e$ with $i = 1;2$.

The expression $\langle\Psi|\frac{1}{r_{12}}|\Psi\rangle$ has already been given above: $\langle\Psi|\frac{1}{r_{12}}|\Psi\rangle = \frac{5}{8}Z_e$.

In the following, we develop the calculation of the remaining term of the Eq.(5.26):

$$\langle\Psi(\mathbf{r}_1;\mathbf{r}_2)| \frac{\gamma^2}{2}(r_1^2\sin^2\theta_1 + r_2^2\sin^2\theta_2)|\Psi(\mathbf{r}_1;\mathbf{r}_2)\rangle = \tag{5.27}$$

$$= \frac{\beta^2}{2}\Big[\langle \varphi_{1s}^{Z_e}(r_1)|\, r_1^2 \sin^2\theta_1 \,|\varphi_{1s}^{Z_e}(r_1)\rangle + \langle \varphi_{1s}^{Z_e}(r_2)|\, r_1^2 \sin^2\theta_2 \,|\varphi_{1s}^{Z_e}(r_2)\rangle\Big]$$

$$= \frac{\beta^2}{2} \times \left[\begin{array}{l} \left(\int_0^\infty R_{10}(r_1)\, r_1^4 R_{10}(r_1)\, dr_1 \times \int Y_{00} \sin\theta_1^2 Y_{00}\, d\Omega_1\right) + \\ \left(\int_0^\infty R_{10}(r_2)\, r_2^4 R_{10}(r_2)\, dr_2 \times \int Y_{00} \sin\theta_2^2 Y_{00}\, d\Omega_2\right) \end{array}\right]$$

thus, using Mathematica, we find that:

$$\langle \Psi(r_1;r_2)|\, \frac{\beta^2}{2}\left(r_1^2 \sin^2\theta_1 + r_2^2 \sin^2\theta_2\right) |\Psi(r_1;r_2)\rangle = \frac{2\beta^2}{Z_e^2}. \tag{5.28}$$

Puting together the above results, we get:

$$E[\Psi] \equiv E(Z_e) = Z_e^2 - 2ZZ_e + \frac{5}{8}Z_e + \frac{2\beta^2}{Z_e^2} \tag{5.29}$$

Now, we shall minimize $E(Z_e)$ with respect to the variational parameter Z_e. Hence we write:

$$\frac{\partial E}{\partial Z_e} = 2Z_e - 2Z + \frac{5}{8} - \frac{4\beta^2}{Z_e^3} = 0 \tag{5.30}$$

We notice here that the effective charge is a function of the magnetic field strength.

β: *Results and outlooks*

Results of our calculations (table 15 and figure 5-2) show the variation helium's binding energies with respect to strong magnetic field.

$Z_e; E(Z_e)$ $\longrightarrow$ $\beta = \frac{B}{4.7 \times 10^9\,G}$	Z_e	$E(Z_e)$ in a.u	$E(Z_e)$ in ev
0	1.6875	2.84766	77.2657
0.2	1.70368	2.81983	76.6994
0.5	1.77666	2.681304	72.9315
0.7	1.84384	2.53496	68.9509
1.0	1.95512	2.25282	61.2767

Table:15 : Variation of the ground state's (1^1S) binding energies for helium atom in strong magnetic

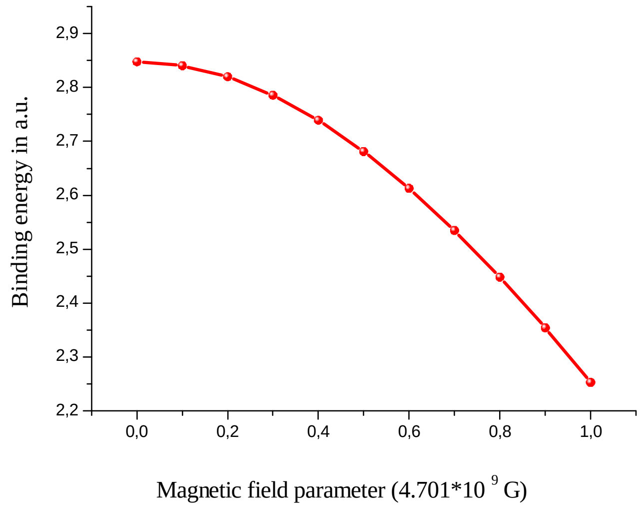

Figure 5-2: The variation of the singlet 1s1s (1^1S) binding energy of helium atom with S=0 and M_S = 0 as a function of the magnetic ...eld.

From Fig.(5:2), we notice that the binding energy of the ground state decreases with the increasing of the magnetic ...eld strengths. However we know that it is very di¢cult to produce these strengths of magnetic ...eld in the laboratories. Thus for small strengths which we can generate in laboratories, these shifts in energy are surely far below the limits of spectroscopic observability.

We observe that the ground state 1^1S becomes monotonically weaker bound with increasing ...eld strength. Below ¯ » 0:15 none of the energies di¤ers considerably from its ...eld free value. Between ¯ » 0:2 and ¯ » 1 a rearrangement takes place which is caused by the increasing dominance of the magnetic forces over the Coulomb forces.

This state is the only state for which both electrons considerably occupy the ground state which forces the two electrons to be close to each other in a narrow domain of space and which thus gives rise to a relatively strong contribution of electronic correlation.

In the Figure(5.3), we present a comparison between our results and those of [Bec99]:We see that we oftain, roughly, a good agreement if we take into a count that we have used a simple trial wave function, while Ref.[Bec99] used a fully numerical method (FEM).

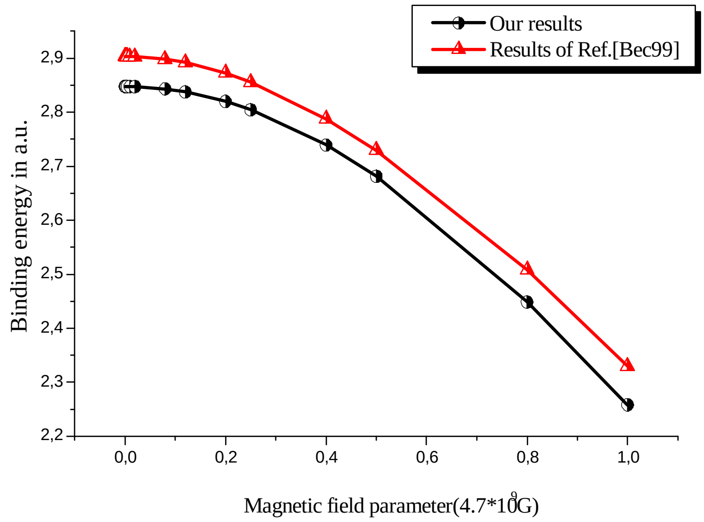

Figure 5-3: Comparison of our results of 1^1S binding energy of helium in strong magnetic field and those of [Bec99].

5.2.2 *Excited states of helium atom in strong magnetic field using the variational method*

5.2.2.*1. Results for the singlet* 2^1P_0 *state (* 1s2p *configuration with* $M_L = 0; S = 0$ *and* $M_S = 0$*)*

For the sake of simplicity, we shall neglect all small corrections (motion of the nucleus, relativistic corrections...) and we focus our attention on the discrete states, for which one of the two electrons remains in the ground state and the other in $2p_{m_l}$ level ,i.e.; $n = 2; l = 1; m_l = 0; \pm 1$.

In the following, we shall use the notation $2^{(2S+1)}P_{M_L}$ for the 1s2p configuration, in which $M_L = m_l^{(1)} + m_l^{(2)}$ and $S = 0$ for the para- state or $S = 1$ for the ortho-state.

We recall that the application of the Rayleigh-Ritz variational method to excited states of a quantum system is in general more difficult than for the ground state. But since para wave functions (which correspond to the value $S = 0$ of the total spin) are orthogonal to ortho wave functions (corresponding to the total spin $S = 1$), we can study separetely the variational determination of the para and ortho energy levels.

α: ***The choice of the trial wave function*** Since the 2^1P and 2^3P states are respectively the para and ortho states corresponding to the configuration 1s2p; simple trial wave functions for these states may be written as:

$$\Psi_{2^{1,3}P} = N_{\pm}\left[u_{1s}(r_1)\,v_{2p}(r_2) \pm v_{2p}(r_1)\,u_{1s}(r_2)\right] \times \chi(1;2) \tag{5.31}$$

where the plus sign refers to the 2^1P state, the minus sign to the 2^3P state, $N_{\pm}$ are normalization constants.

Simple trial wave functions for this state may be written as:

$$u_{1s}(r) = e^{-Z_e r}; \qquad v_{2p}(r) = r e^{-Z_e r/2} Y_{l;m_l}(\theta;\varphi) \qquad \text{with } m_l = 0;\pm 1: \tag{5.32}$$

In the following, we select, as a first step, the spatial symmetric (para state) 2^1P_0; thus, we write the trial wave function for this state as:

$$\Psi(q_1;q_2) = N_{+}\left[u_{1s}(r_1)\,v_{2p_0}(r_2) + v_{2p_0}(r_1)\,u_{1s}(r_2)\right] \times \chi(1;2) \tag{5.33}$$

where $\chi(1;2)$ is antisymmetric (singlet) spin states ($S = 0$ and $M_S = 0$) and q_i denotes collectively the space and spin coordinates of electron i.

β: ***Excited states*** $\left(2^1P_0\right)$ ***of free helium atom*** The Hamiltonian of our system can be written as:

$$H = T_1 + T_2 - \frac{Z}{r_1} - \frac{Z}{r_2} + \frac{1}{r_{12}} \tag{5.34}$$

Substituting our trial wave function in the functional eq.(5.15), we obtain:

$$E[\Psi] = \frac{\left\langle \Psi(r_1;r_2)\right| T_1 + T_2 - \frac{Z}{r_1} - \frac{Z}{r_2} + \frac{1}{r_{12}} \left|\Psi(r_1;r_2)\right\rangle}{\left\langle \Psi(q_1;q_2) \middle| \Psi(q_1;q_2)\right\rangle}: \tag{5.35}$$

Using Mathematica, we calculated these integrals:

$$\left\langle \Psi(r_1;r_2) \middle| \Psi(r_1;r_2)\right\rangle = \int \left[u_{1s}(r_1)\,v_{2p_0}(r_2)\right]^2 + \left[v_{2p_0}(r_1)\,u_{1s}(r_2)\right]^2 + 2 \times \tag{5.36}$$

$$[u_{1s}(r_1)\, v_{2p_0}(r_2) \times v_{2p_0}(r_1)\, u_{1s}(r_2)]\, r_1^2 r_2^2 dr_1 dr_2 d\Omega_1 d\Omega_2 = \frac{48\pi}{Z_e^8}$$

Since:

$$\nabla^2 = \frac{1}{r^2}\frac{\partial}{\partial r}\left(r^2 \frac{\partial}{\partial r}\right) - \frac{1}{r^2} L^2 \tag{5.37}$$

and

$$L^2 = -\left[\frac{1}{\sin\theta}\frac{\partial}{\partial \theta}\left(\sin\theta \frac{\partial}{\partial \theta}\right) + \frac{1}{\sin^2\theta}\frac{\partial^2}{\partial \varphi^2}\right]$$

we find that

$$\begin{aligned} \langle \Psi(r_1; r_2) \mid T_1 \mid \Psi(r_1; r_2)\rangle &= -\frac{1}{2}\langle \Psi(r_1; r_2) \mid \nabla_1^2 \mid \Psi(r_1; r_2)\rangle \\ &= \frac{15\pi}{Z_e^6} \equiv \langle \Psi(r_1; r_2) \mid T_2 \mid \Psi(r_1; r_2)\rangle \end{aligned} \tag{5.38}$$

and

$$\langle \Psi(r_1; r_2) \mid \frac{1}{r_1} \mid \Psi(r_1; r_2)\rangle = \frac{30\pi}{Z_e^7} = \langle \Psi(r_1; r_2) \mid \frac{1}{r_2} \mid \Psi(r_1; r_2)\rangle \tag{5.39}$$

We calculate the interaction term in this case using eq.(5.14) and Mathematica. The result is:

$$\langle \Psi(r_1; r_2) \mid \frac{1}{r_{12}} \mid \Psi(r_1; r_2)\rangle = \frac{8\pi \times 118}{Z_e^7} + \frac{8\pi \times 224}{(3 \times 729)\, Z_e^7} \tag{5.40}$$

Finally, the energy functional is given by:

$$\begin{aligned} E[Z_e] &= \frac{\langle \Psi(r_1; r_2) \mid H \mid \Psi(r_1; r_2)\rangle}{\langle \Psi(r_1; r_2) \mid \Psi(r_1; r_2)\rangle} \\ &= \frac{5}{8} Z_e^2 - \frac{5}{4} Z Z_e + \frac{1705}{6561} Z_e \end{aligned} \tag{5.41}$$

Now, we shall minimize $E(Z_e)$ with respect to the variational parameter Z_e: Hence we write:

$$\frac{\partial E}{\partial Z_e} = \frac{10}{8} Z_e - \frac{5}{4} Z + \frac{1705}{6561} = 0$$

So, the effective charge parameter is:

$$Z_e = 1.7921048 \qquad (5.42)$$

substituting this value in the equation of $E\,(Z_e)$, we get that:

$$E\,[Z_e] = 2.00727 \text{ a.u.} \qquad (5.43)$$

is better result(closer to the exact value 2.124 a.u.) can be obtained by including two effective charges as variational parameters.

γ: ***Excited states (2^1P_0) in strong magnetic field*** In this section, we add to the previous Hamiltonian the terms corresponding to the presence of an external magnetic field. Hence the Hamiltonian can be written as:

$$H = T_1 + T_2 - \frac{Z}{r_1} - \frac{Z}{r_2} + \frac{1}{r_{12}} + \beta\left(\left(l_z^{(1)} + l_z^{(2)}\right) + 2\left(s_z^{(1)} + s_z^{(2)}\right)\right) + \frac{\beta^2}{2}\left(r_1^2 \sin^2\theta_1 + r_2^2 \sin^2\theta_2\right) \qquad (5.44)$$

Using the trial wave function in eq.(5.33), we obtain the functional:

$$E\,[\Psi] = \langle\Psi(q_1; q_2)|\, T_1 + T_2 - \frac{Z}{r_1} - \frac{Z}{r_2} + \frac{1}{r_{12}} + \beta\left(l_z^{(1)} + l_z^{(2)} + 2\left(s_z^{(1)} + s_z^{(2)}\right)\right)$$
$$+ \frac{\beta^2}{2}\left(r_1^2 \sin^2\theta_1 + r_2^2 \sin^2\theta_2\right)\, |\,\Psi(q_1; q_2)\rangle) = \langle\Psi(q_1; q_2)|\Psi(q_1; q_2)\rangle. \qquad (5.45)$$

The first terms were calculated above; now we must calculate the linear and quadratic Zeeman terms using our trial wave function.

Since $\chi(1;2)$ is an antisymmetric (singlet) spin state ($S = 0$; $M_S = 0$), then the linear Zeeman energy is:

$$\langle\Psi(q_1; q_2)|\,\beta\left(\left(l_z^{(1)} + l_z^{(2)}\right) + 2\left(s_z^{(1)} + s_z^{(2)}\right)\right)|\,\Psi(q_1; q_2)\rangle = 0 \qquad (5.46)$$

and the quadratic Zeeman energy is:

$$\langle \Psi(q_1, q_2) | \frac{\beta^2}{2} (r_1^2 \sin^2\theta_1 + r_2^2 \sin^2\theta_2) | \Psi(q_1, q_2) \rangle = \frac{7\beta^2}{Z_e^2} \tag{5.47}$$

Puting together the above results, we have:

$$E[\Psi] \simeq E(Z_e) = \frac{5}{8} Z_e^2 - \frac{5}{4} Z Z_e + \frac{1705}{6561} Z_e + \frac{7\beta^2}{Z_e^2} \tag{5.48}$$

Now, we shall minimize $E(Z_e)$ with respect to the variational parameter Z_e,by using Mathematica language. Hence we write :

$$\frac{\partial E}{\partial Z_e} = \frac{10}{8} Z_e - \frac{5}{4} Z + \frac{1705}{6561} - \frac{14\beta^2}{Z_e^3} = 0 \tag{5.49}$$

Once we change the magnetic field strength, we find a new parameter Z_e and also the binding energy of this system. In order to show the details of our calculations and how we solve the integrals, we will add an appendix D in the end of this thesis.

Binding energies for this system as a function of the magnetic field strength is given in Fig.(5.4) and table 16.

$Z_e, E(Z_e)$ $\longleftrightarrow$ $\beta = \frac{B}{4.7 \times 10^9 \mathrm{G}}$	Z_e	$E(Z_e)$ in a.u	$E(Z_e)$ in ev
0	1.7921	2.00727	54.5977
0.2	1.86155	1.92346	52.3181
0.5	2.09613	1.55121	42.1929

Table:16 : Variation of $1s2p_0$ (singlet state) binding energies for helium atom in strong magnetic field (1-electrons in 1s state and the other in $2p_0$).

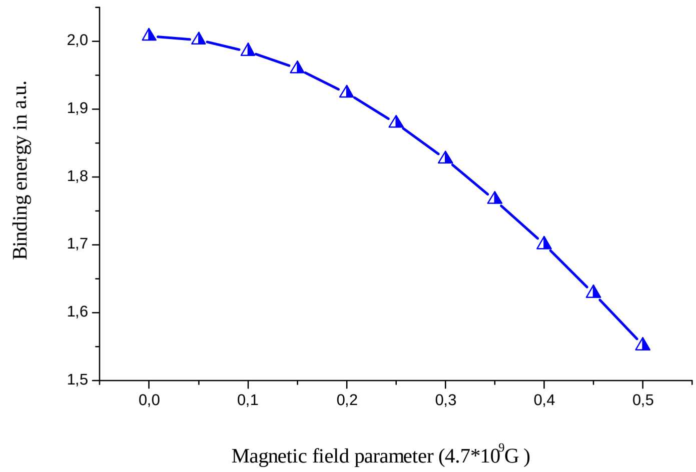

Figure 5-4: Variation of $1s2p_0$ binding energies for helium atom in strong magnetic field (one electron in 1s state and the other in $2p_0$ with $S = 0$ and $M_S = 0$).

5.2.2.2. *Results for the triplet 2^3S_0 state (1s2s configuration with $M_L = 0; S = 1$)*

α: ***The choice of the trial wave function*** **This is the lowest ortho (space-antisymmetric) state, corresponding to the configuration 1s2s.**

It is reasonable to adopt for the spatial part of the wave function a simple trial function which is the antisymmetrized product of an inner 1s orbital u_{1S} corresponding to the effective charge Z_i and an outer 2s orbital v_{2S} corresponding to the effective charge Z_O. That is:

$$\Psi_{2^3S}(q_1; q_2) = N_+ \left[u_{1S}(r_1)\, v_{2S}(r_2) - v_{2S}(r_1)\, u_{1S}(r_2)\right] \times \chi(1; 2) \tag{5.50}$$

where

$$u_{1S}(r) = e^{-Z_i r}; \qquad v_{2S}(r) = (1 - Z_o r/2)\, e^{-Z_o r/2} \tag{5.51}$$

and N_+ is a normalization constant; Â (1; 2) is a symmetric (triplet) spin states (S = 1 and M_S = 0; §1).

¯: ***Excited states*** ¡2^3S_0¢ ***of free helium atom*** Upon substituting Eq.(5.50) into the functional Eq.(5.15) and repeating the steps of calculation for the $1s2p_0$ states, with the variation of the variational parameters Z_i and Z_o to obtain the minimum energy, we found, by using Mathematica, the values Z_i = 1:98417896 and Z_o = 1:209613; which yield the energy:

$$E_{2^3S} = 2:151389a:u: \qquad (5.52)$$

We denote that the exact value obtained in this way is E_{2^3S} = 2:175a:u: The agreement between our result and this exact value is seen to be good, considering the simplicity of the trial function Eq(5.51).

°:***Excited states (***2^3S_0***) in strong magnetic …eld*** Now, we add to the Hamiltonian of the free helium atom the terms corresponding to the presence of an external magnetic …eld, hence the Hamiltonian can be written as:

$$H = T_1 + T_2 \;¡\; \frac{Z}{r_1} \;¡\; \frac{Z}{r_2} + \frac{1}{r_{12}} + \overline{\ }\left(l_z^{(1)} + l_z^{(2)} + 2\left(s_z^{(1)} + s_z^{(2)} \right) \right) + \frac{-^2}{2}\left(r_1^2 \sin^2 µ_1 + r_2^2 \sin^2 µ_2\right) \quad (5.53)$$

Since Â (1; 2) is a symmetric (triplet) spin states (S = 1 and M_s = 0; §1), we shall treat each case separately.

°.1.Results for the triplet ¡2^3S_0¢ ***state (***1s2s ***con…guration with*** M_l = 0***;*** S = 1 ***and*** M_S = 0***)*** In the triplet state only one of the electrons occupies the ground state, whereas the other one occupies already predominantly an excited state and thus gives rise to a lower correlation contribution than in the singlet ground state.

For this case, there is no linear Zeeman e¤ect, and only the quadratic term contributes to the variation of the energy.

Using Mathematica, we calculated all terms of the last Hamiltonian, and by varying the two variational parameters Z_i and Z_o, we obtained the binding energies of the triplet 2^3S_0 state with M_S = 0 of helium atom in strong magnetic …eld as shown in the Fig(5.5).

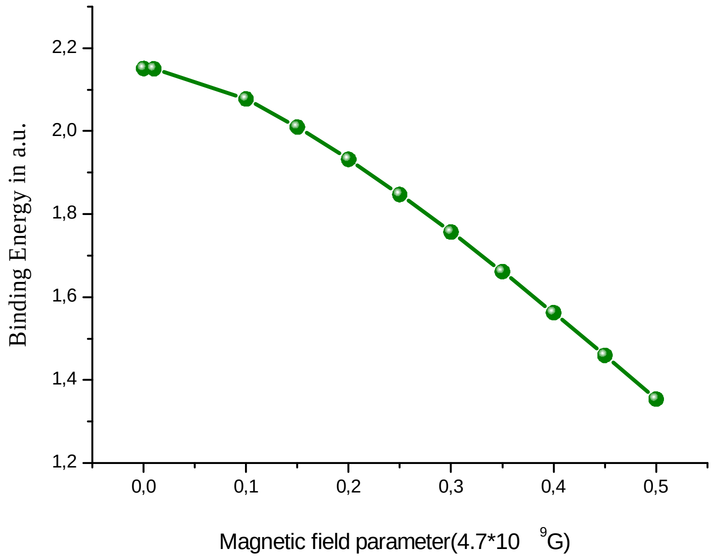

Figure 5-5: Variation of binding energies of the triplet1s2s state of helium atom in magnetic …eld with $S = 1$ and $M_S = 0$:

°.2. Results for the triplet **¡2^3S_0¢** ***state (*****1s2s** ***con…guration with*** **$M_l = 0$*;* $S = 1$** ***and*** **$M_S = +1$*)*** **We repeat the same steps of calculation showed above using Mathematica.**

Fig.(5:6) shows the variation of the corresponding binding energy.

°.3. Results for the triplet **¡2^3S_0¢** ***state (*****1s2s** ***con…guration with*** **$M_l = 0$*;* $S = 1$** ***and*** **M_S = ¡1*)*** **Among the three related triplet states with M_S = 0; §1 the one with M_S = ¡1 possesses the lowest energy due to the spin shift 2¯M_S (Fig. 5.7):**

The overall increase of the binding energies with increasing magnetic …eld strength has its origin in the strongly increasing kinetic energy in the presence of the external …eld.

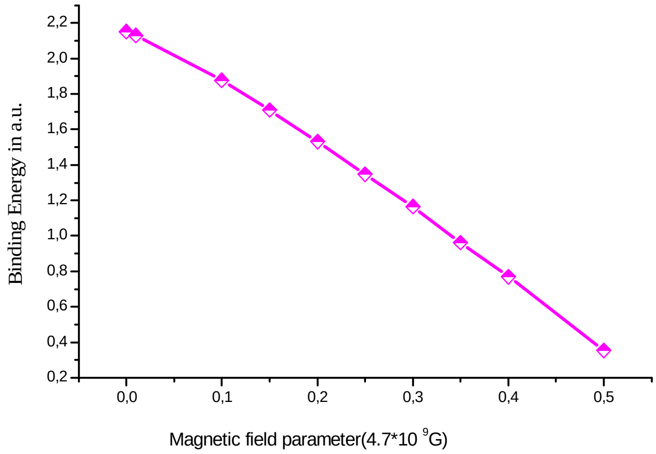

Figure 5-6: Variation of the binding energy of the triplet1s2s state of helium atom in magnetic field with S=1 and $M_S = +1$:

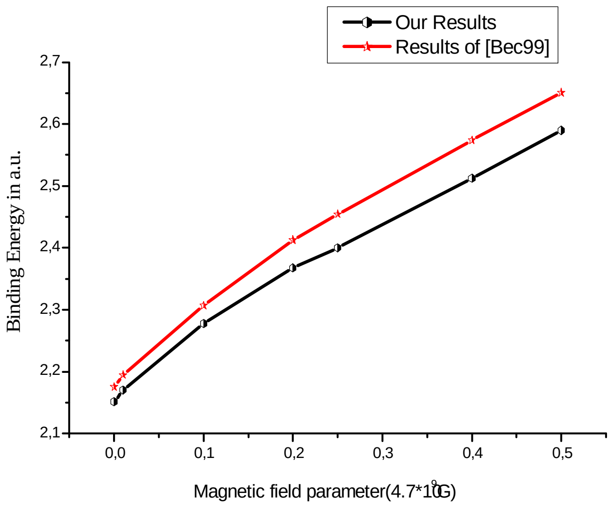

Figure 5-7: Comparison of binding energy for the triplet1s2s state of helium atom in strong magnetic field with S=1 and $M_S = -1$ with those of [Bec99] .

5.3 *Helium atom under an external strong static electric field*

Firstly, we can prove easily that, the Stark effect don't occur neither in the ground state nor in the $1s2p_0$ and in $1s2s$ configurations, which are studied above, due to our selected trial functions.

Considering an atom under a static electric field, thus, we have a large admixture of states which increases rapidly with increasing principle quantum number n. In order to show the effect of an external electric field on the helium atom, we must choose a trial function containing an admixture of states, thus, we may choose as a trial function with many variational parameter $(Z_i; Z_o; a_{l;m})$.

$$\Psi(q_1; q_2) = \psi_{1s}^{(Z_i)}(r_1) \times \sum_{n;l;m} a_{l;m} R_{n;l}^{(Z_o)}(r_2) Y_{l;m}(\theta_2; \varphi_2) \times \chi(1; 2) \tag{5.54}$$

However, if the admixture of different values of n is neglected, the trial function reduces to the form:

$$\Psi(q_1; q_2) = \psi_{1s}^{(Z_i)}(r_1) \times \sum_{l;m} a_{l;m} R_{2;l}^{(Z_o)}(r_2) Y_{l;m}(\theta_2; \varphi_2) \times \chi(1; 2) \tag{5.55}$$

The amount of calculations resulting from a large number of variational parameters is large. This work is in progress.

General Conclusion

Since the discovery of huge magnetic …elds in the surface of white dwarfs and neutron stars, much work has been done in calculating atomic energy values in the atmosphere of these compact objects. However, the study of binding energies and transition probabilities between levels of atoms in combined strong magnetic and electric …elds with arbitrary mutual orientations are almost missing.

In our work, we have studied the binding energies and the transition probabilities between the most bound states of hydrogen atom, …rstly, in strong magnetic …elds and static electric …elds separately, secondly, in magnetic plus a variable parallel static electric …elds and …nally, the e¤ect of magnetic and static electric …elds with arbitrary mutual orientations, on the structure of hydrogen atoms.

We have also tried to extend our work to helium atoms using the variational method. We have considered, as a …rst step, that the two electrons were in the ground state; after that we studied the 1s2p0 con…guration .

So, we obtained in our work these main results:

- The binding energies of the di¤erent states increase with increasing of magnetic …elds.
- The (magnetic) increasing of binding energies causes a great in‡uence on the transition probabilities. An even more dramatic e¤ect on the spectrum is obtained, if in addition, a strong electric …eld (either parallel or not to the magnetic …eld) is present.
- The wave functions of hydrogen atom in strong magnetic …eld are not strongly altered in comparison to the free case. Thus, we have used the spectroscopy labels for a free atom. However, in joint strong magnetic and electric …elds case, the wave functions are very di¤erent (basis-states mixing).
- The transition probabilities between the obtained states gives more information on the e¤ect of an intense magnetic and electric …elds.
- The linear Zeeman term in the interaction Hamiltonian of helium atom in the ground state with a magnetic …eld is zero, so there is no Zeeman splitting. Nevertheless, the quadratic term in the Hamiltonian produces a small shift in the energy, which depends on the magnetic …eld. However, we know that it is very di¢cult to produce high strengths of magnetic …eld in the laboratories; thus for small strengths which we can generated in laboratories, these shifts

in energy surely are far below the limits of spectroscopic observability.

² The study of the e¤ect of strong external …elds on hydrogen and helium atoms allows us to acquire a good knowledge on the white dwarfs, and we can go further to know other astrophysical compact object's structure where the magnetic …eld at their surface exceeds $10^{13 ¡ 15}$G(Magnetars).

² It is important to emphasize here that there exist no criterion for other observables to decide about which values of binding energies are more accurate. Thus, it is not clear so far which results for transition probabilities are better. Therefore, more investigations on the electromagnetic transitions in the hydrogen and helium atom in a strong magnetic and electric …elds, especially in the domain of strong magnetic and electric …elds with arbitrary mutual orientations, would be desirable in order to answer this question.

Bibliography

[1] [Ali06]: Alice Harding & D. Lai; arxiv: astro-ph/0606674v2/11 Jul 2006.

[2] [Ana06]:Anatoli Andreev; Atomic spectroscopy; Springer; 2006.

[3] [Ant04]:Anthony Mezzacappa & M. Fuller, Open Issues in Core Collapse Supernova Theory; University of Washington, Seattle 22-24 June 2004.

[4] [Ari02]:A.K.Aringazin; arxiv: physics/0202049v1[physics:chem ¡ ph]19 Feb 2002.

[5] [Arm06] :Armin Luhr & O-A Al-Hujaj & P.Schmelcher; arXiv:physics/0610238v1 [physics.atom-ph] 26 Oct 2006.

[6] [Bac00]:M.Bachmann &H.Kleinert & A.Pelster; arxiv: quant-ph/0005100v1/24May 2000.

[7] [Bec99]: W.Becken & P.Schmelcher & F.K. Diakonos; arXiv:physics/9902059v1 [physics.atom-ph] 22 Feb 1999.

[8] [Beth57]:A. Bethe &E. Salpeter; Quantum mechanics of one -and tow -electron; Springer-Verlag-Heidelberg;1957.

[9] [Blo04]: A.Blom; Arxiv:physics/0406141v1(phusics.atom-ph) 2004.

[10] [Bra83]:B.H Bransden & C.J.Joachain, Physics of atoms and molecules, Longman Scienti...c&Technical;1983.

[11] [Bur06]:E. Burkhardt &J.Leventhal; Topics in atomic physics; Springer; 2006.

[12] [Chan92]:G. Chanmugam; Rev. Astron. Astrophys.1992, 143-145.G.

[13] [Cla05]:Claude Aslangul; Applications de la mecanique quantique de l'atome au solide; 2005.

[14] [Dav83]:David Farrelly & P.Reinhardt; J. Phys. B: At. Mol. Phys. 16 (1983) 2103-2117.

[15] [Deh09] :DehuaWanga &K. Huanga & H. Zhoub & S. Linb; Journal of Electron Spectroscopy and Related Phenomena; 169 (2009) 8691.

[16] [Eng09] :D. Engel & M. Klewsb & G. Wunner; Computer Physics Communications 180 (2009) 302311.

[17] [Foo05]: J. Foot; Atomic physics; Oxford; 2005.

[18] [Gar76]: R.H.Garstang; Rep.prog.phy.1977 40 105-154.

[19] [Geo08]:Geo¤ Mcnamara;Clocks in the sky- the story of pulsars; Springer;2008.

[20] [Gor06]: Gordon W.F.Drake; Handbook of atomic, molecular and optical physics; Springer; 2006.

[21] [Hae07]:P. Haensel & A.Y. Potekhin & D.G. Yakovlev; Neutron Stars1- Equation of State and Structure; Springer; 2007.

[22] [Hey96]:J. S.Heyl & L. Hernquist, Phys.Rev.C,54, (1996), 5.

[23] [Hey98]:J.S.Heyl & L.Hernquist; arxiv:physics/9806040v1[physics:atom ¡ ph] 24 jun 1998.

[24] [Hoy06]:P.Hoyng ;Relativistic Astrophysics and Cosmolog;Springer; 2006.

[25] [Huj00] :O.-A. Al-Hujaj & P. Schmelcher; arXiv:physics/0003043v1 [physics.atom-ph] 20 Mar 2000.

[26] [Iva00]: V. Ivanov & P.Schmelcher; arXiv:physics/0006017v1 [physics.atom-ph] 7 Jun 2000.

[27] [Jor97] : Jorg Main & M.Schwacke & G.Wunner; Arxiv:quant-ph/9709011V2; 8 Sept 1997.

[28] [Kar04]:S.G. Karshenboim E. Peik; Astrophysics, Clocks And Fundamental Constants; Springer, Berlin Heidelberg 2004.

[29] [Ken95] : Ken-ichi Hiraizumi & Y. Ohshima & H.Suzuki; IU-MSTP/5; hep-th/9512197; December 1995

[30] [Khr03]:I.B.Khriplovich & G.Yu.Ruban; arxiv: quant-ph/0309014v2/ 3Dec2003.

[31] [Lai01]: D.Lai arxiv: astro-ph/0009333v2/ 24 Jan 2001.

[32] [Lop07] :J.C. Lopez Vieyra &H. O. Pilon; arxiv:0711.2553.v1[astro ¡ ph] 16 Nov 2007.

[33] [Lor03]: Lorenzo Curtis; Atomic Structure and Lifetimes; Cambridge; 2003.

[34] [Max07]:Max Camenzind ;Compact Objects in Astrophysics; Springer; 2007.

[35] [Med07]: Z.Medin & D.Lai &A.Y.Potekhin; arxiv: 0704.1598v1[astro ¡ ph] 12 Apr 2007.

[36] [Pot01]:A.Y.potkhin; arxiv: physics/ 0101050v4[physics:atom ¡ ph]18 April 2001.

[37] Ray03]:Raymond Brummelhuis; arxiv:math-ph/0308040v2.14Nov 2003.

[38] [Rau03]: A.R.P.Rau; Astronomy-inspired atomic and molecular physics; Kluwer Academic publishers 2003.

[39] [Sch02]:P. Schmelcher &W. Schweizer ;Atoms and Molecules in Strong External Fields; kluwer academic publishers; 2002.

[40] [Sho03]:S. N. Shore; The tapestry of modern astrophysics; Wiley interscience; 2003

[41] [Smi03]: B. M.Smirnov; Physics of atoms and ions; Springer; 2003.

[42] [Thi08]:A.Thirumalai & J. S. Heyl; arxiv: 0806.3113v1[astro ¡ ph] 19Jun 2008.

[43] [Vla 97]: Vladimir P.Krainov; Radiative processes in atomic physics: Wiley-Interscience Publication; 1997.

[44] [Wun85]:G.Wunner; 0022-3700/86/111623 ; 1985.

[45] [Wyn04]: Wynn C.G. Ho & D. Lai & A.Y. Potekhin b & G. Chabrier; Advances in Space Research 33 (2004) 537541.

[46] [Zac07]:Zach Medin & D. Lai ; arxiv: astro-ph/0607166v2; 5Jan 2007.

Appendix A

Appendix A

We begin with the non-relativistic Hamiltonian for the hydrogen atom in a strong magnetic field in spherical coordinates which is given by:

$$H = \underbrace{-\Delta - \frac{2}{|r|}}_{H_0} + \underbrace{\beta (L_z + 2S_z)}_{H_{LZ}} + \underbrace{\beta^2 r^2 \sin^2\theta}_{H_{QZ}} \tag{A.1}$$

We can write the expression of the Zeeman quadratic matrix elements term using the 3j symbols as:

$$\begin{aligned} \langle n l m_l m_s \,|\, H_{QZ} \,|\, n' l' m'_l m'_s \rangle &= \beta^2 \langle n l m_l m_s \,|\, r^2 \sin^2\theta \,|\, n' l' m'_l m'_s \rangle \\ &= \beta^2 \underbrace{\int_0^{\infty} R_{nl}(r) r^2 R_{n'l'}(r) r^2 dr}_{\mathrm{Radial-Part}} \times \underbrace{\int Y^*_{l,m_l}(\theta,\varphi) \sin^2\theta\, Y_{l',m'_l}(\theta,\varphi)\, d\Omega}_{\mathrm{Angular-part}} \end{aligned} \tag{A.2}$$

we have

$$Y_{20}(\theta) = \sqrt{\frac{5}{16\pi}} \left(3\cos^2\theta - 1\right) \tag{A.3}$$

so:

$$\sin^2\theta = \frac{2}{3} - \frac{1}{3}\sqrt{\frac{16\pi}{5}}\, Y_{20}(\theta) \tag{A.4}$$

By using the spherical harmonics property $Y^*_{lm_l}(\theta) = (-1)^m Y_{l,-m_l}(\theta)$ and

$$\int Y_{l_1,m_1}(\theta,\varphi)\,Y_{l_2,m_2}(\theta,\varphi)\,Y_{l_3,m_3}(\theta,\varphi)\,d\Omega = \sqrt{\frac{(2l_1+1)(2l_2+1)(2l_3+1)}{4\pi}} \times \begin{pmatrix} l_1 & l_2 & l_3 \\ 0 & 0 & 0 \end{pmatrix} \times \begin{pmatrix} l_1 & l_2 & l_3 \\ m_1 & m_2 & m_3 \end{pmatrix}. \tag{A.5}$$

where $\begin{pmatrix} l_1 & l_2 & l_3 \\ 0 & 0 & 0 \end{pmatrix} \neq 0$ if $(l_1+l_2+l_3)$ is even

and $|l_1 - l_2| \leq l_3 \leq (l_1+l_2)$.

While $\begin{pmatrix} l_1 & l_2 & l_3 \\ m_1 & m_2 & m_3 \end{pmatrix} \neq 0$ if $m_1+m_2+m_3 = 0$.

We get that :

$$\langle nlm_lm_s \,|\, H_{QZ} \,|\, n'l'm_l'm_s' \rangle = \beta^2 \delta_{m_l m_l'} \delta_{m_s m_s'} \times \left\{ \langle nl \,|\, r^2 \,|\, n'l' \rangle \times \left[\frac{2}{3}\delta_{ll'} - \frac{1}{3}\sqrt{\frac{16\pi}{5}}(-1)^m \sqrt{\frac{5(2l+1)(2l'+1)}{4\pi}} \times \begin{bmatrix} l & 2 & l' \\ 0 & 0 & 0 \end{bmatrix} \begin{bmatrix} l & 2 & l' \\ -m_l & 0 & m_l' \end{bmatrix} \right] \right\}, \tag{A.6}$$

We conclude that $l' = l, l \pm 2$; and $m_l = m_l'$; thus, H_{QZ} is diagonal in m_l and m_s but not in l.

Noting that $\begin{bmatrix} a & b & c \\ 0 & 0 & 0 \end{bmatrix} = (-1)^p \sqrt{\Delta(abc)} \dfrac{p!}{(p-a)!\,(p-b)!\,(p-c)!}$,

if $a+b+c = 2p$.

where $\Delta(abc) = \dfrac{(a+b-c)!\,(b+c-a)!\,(c+a-b)!}{(a+b+c+1)!}$.

Then, in our case we find:

$$\begin{pmatrix} l & 2 & l' \\ 0 & 0 & 0 \end{pmatrix} = \begin{cases} (-1)^l \sqrt{\dfrac{l(l+1)}{(2l+3)(2l+1)(2l-1)}} & \text{for} \quad l' = l; \\ (-1)^l \sqrt{\dfrac{3l(l+1)}{2(2l-3)(2l+1)(2l-1)}} & \text{for} \quad l' = l-2; \end{cases}$$

In addition:

$$\begin{pmatrix} a & b & c \\ \alpha & \beta & \gamma \end{pmatrix} = (-1)^{a-b-\gamma} \sqrt{\Delta(abc)} \sqrt{(a+\alpha)!\,(a-\alpha)!\,(b+\beta)!\,(b-\beta)!\,(c+\gamma)!\,(c-\gamma)!}$$

$$\times \sum_t (-1)^t \left[t!\,(c-b+t+\alpha)!\,(c-a+t-\beta)!\,(a+b-c-t)!\,(a-t-\alpha)!\,(b-t+\beta)!\right]^{-1}.$$

in which $\alpha+\beta+\gamma = 0$; and $|a-b| \le c \le a+b$.

Therefore,

$$\begin{pmatrix} l & 2 & l' \\ -m_l & 0 & m_l' \end{pmatrix} = \begin{cases} (-1)^{l-m} \dfrac{3m_l^2 - l(l+1)}{\sqrt{(2l-1)l(2l+1)(l+1)(2l+3)}} & \text{for} \quad l' = l; \\ (-1)^{l-2-m_l} \dfrac{\sqrt{3(l-m_l)(l-m_l-1)(l+m_l)(l+m_l-1)}}{\sqrt{(2l+1)l(2l-1)(2l-2)(2l-3)}} & \text{for} \quad l' = l-2; \end{cases}$$

We can write the matrix elements in the form:

$$\langle n l m_l m_s \,|\, H_{QZ} \,|\, n' l' m_l' m_s' \rangle = \beta^2 \delta_{m_l m_l'} \delta_{m_s m_s'} \times$$

$$\times \begin{cases} \langle nl \,|\, r^2 \,|\, nl \rangle \times \left(\dfrac{2\left(l^2+l-1+m_l^2\right)}{(2l+3)(2l-1)} \right) & \text{for} \quad l' = l; \\ -\langle nl \,|\, r^2 \,|\, n'l' \rangle \times \left(\dfrac{(l_<+m_l+2)(l_<+m_l+1)(l_<-m_l+2)(l_<-m_l+1)}{(2l_<+5)(2l_<+3)^2(2l_<+1)} \right)^{\frac{1}{2}} \sigma(nl;n'l') & \text{if} \quad l' = l \pm 2 \\ 0 & \text{Otherwise} \end{cases}$$

with $l_< = \min(l; l')$.

We turn now to caculation of the radial integral $\langle nl \mid r^2 \mid n'l' \rangle = \int_0^\infty R_{nl}(r) r^2 R_{n'l'}(r) r^2 dr$ where the radial wavefunction is giving by (with $\rho = \frac{2r}{n}$):

$$R_{n,l}(r) = -\left[\left(\frac{2}{n}\right)^3 \cdot \frac{(n-l-1)!}{2n[(n+l)!]^3}\right]^{\frac{1}{2}} e^{-\frac{\rho}{2}} \rho^l L_{n+l}^{2l+1}(\rho) \qquad \text{(A.7)}$$

Therefore, we obtain that:

$$\langle nl \mid r^2 \mid n'l' \rangle = \sqrt{\left(\frac{2}{n}\right)^3 \left(\frac{2}{n'}\right)^3 \frac{(n-l-1)!\,(n'-l'-1)!}{2n[(n+l)!]^3\, 2n'[(n'+l')!]^3}} \left(\frac{2}{n}\right)^l \left(\frac{2}{n'}\right)^{l'} \times \qquad \text{(A.8)}$$

$$\times \left(\sum_{k=0}^{n-l-1} (-1)^{k+1} \frac{[(n+l)!]^2}{(n-l-1-k)!\,(2l+1+k)!\,k!} \left(\frac{2}{n}\right)^k \right) \times$$

$$\times \int_0^\infty r^{4+l+l'+k+k'} \exp\left[-\left(\frac{1}{n} + \frac{1}{n'}\right) r\right] dr.$$

We remember that the last integral has a famous solution which is given using the integral by parts where

$$\int_0^\infty r^m \exp[-ar]\, dr = \frac{m!}{a^{m+1}}.$$

Appendix B

Appendix B

The details of our calculations corresponding to the discrete eigenstates of the hydrogen atom in strong external electric fields are given in this appencix, where the non-relativistic single particle Hamiltonian of a hydrogen atom in an electric field(parallel ti the z-axis) reads:

$$\Big[\underbrace{-\nabla^2 - \frac{2}{r}}_{H_0} + \underbrace{2f_q z}_{H_{St}}\Big]\psi = \varepsilon\psi \tag{B.1}$$

In spherical coordinates we have $z = r\cos\theta$; and we have also from the properties of the spherical harmonics that

$$\cos\theta = \sqrt{\frac{4\pi}{3}}\, Y_{10}(\theta) \tag{B.2}$$

so, we find that:

$$\langle n l m_l m_s \,|\, H_{St} \,|\, n' l' m_l' m_s' \rangle = 2f_q \langle n l \,|\, r \,|\, n' l' \rangle \delta_{m_s m_s'} \cdot \sqrt{\frac{4\pi}{3}} \times \int Y_{l m_l}(\theta;\varphi)\, Y_{10}(\theta)\, Y_{l' m_l'}(\theta;\varphi)\, d\Omega. \tag{B.3}$$

similarly to the previous appendix, we get that the matrix elements are written as:

$$\langle n l m_l m_s \,|\, H_{St} \,|\, n' l' m_l' m_s' \rangle = 2 f_q \langle nl \,|\, r \,|\, n' l' \rangle \delta_{m_s m_s'} \times \sqrt{\frac{4\pi}{3}} \times (-1)^{m_l} \sqrt{\frac{(2l+1)\,3\,(2l'+1)}{4\pi}} \begin{bmatrix} l & 1 & l' \\ 0 & 0 & 0 \end{bmatrix} \begin{bmatrix} l & 1 & l' \\ -m_l & 0 & m_l' \end{bmatrix}. \tag{B.4}$$

The 3j symbols vanishes unless : $(l + 1 + l')$ is even, this implies that $l + l'$ is an odd number , and we have also $|l - 1| \leq l' \leq l + 1$; but $l + l'$ must be odd number, thus we get $l' = l - 1$ or $l + 1$.

Moreover, $-m_l + 0 + m_l' = 0 \Rightarrow m_l' = m_l$.

After calculations of 3j symbols, we obtain for $l' = l + 1$:

$$\begin{bmatrix} l & 1 & l' \\ 0 & 0 & 0 \end{bmatrix} = (-1)^{l+1} \sqrt{\frac{(l+1)}{(2l+3)(2l+1)}} \tag{B.5}$$

$$\begin{bmatrix} l & 1 & l' \\ -m_l & 0 & m_l' \end{bmatrix} = (-1)^{l-1-m_l} \sqrt{\frac{2\,(l+m_l+1)(l-m_l+1)}{(2l+3)(2l+1)(2l+2)}}. \tag{B.6}$$

In the same way, we calculate the case of $l' = l - 1$;

Finally, after some simplifications we can write that:

$$\langle n l m_l m_s \,|\, H_{St} \,|\, n' l' m_l' m_s' \rangle = 2 f_q \times \langle nl \,|\, r \,|\, n' l' \rangle \delta_{m_l m_l'} \delta_{m_s m_s'} \times \begin{Bmatrix} \sqrt{\dfrac{(l+m_l+1)(l-m_l+1)}{(2l+3)(2l+1)}} & \text{if} \quad l' = l+1; \\ \sqrt{\dfrac{(l+m_l)(l-m_l)}{(2l+1)(2l-1)}} & \text{if} \quad l' = l-1 \end{Bmatrix}. \tag{B.7}$$

Appendix C

AppendixC

We recall that the trial wave function for $1s2p_0\ \left(2^1P_0\right)$ can be written as:

$$\Psi(q_1;q_2) = N_+\left[u_{1s}(r_1)\,v_{2p_0}(r_2) + v_{2p_0}(r_1)\,u_{1s}(r_2)\right] \times \chi(1;2) \qquad \text{(C.1)}$$

where

$$u_{1s}(r) = e^{-Z_e r}; \qquad v_{2p}(r) = r e^{-Z_e r/2} Y_{l;m_l}(\theta;\varphi) \qquad \text{with } m_l = 0;\pm 1: \qquad \text{(C.2)}$$

The Hamiltonian of the system consisting of two electrons and a nucleus in a homogeneous magnetic field B along the z-axis reads:

$$H = T_1 + T_2 - \frac{Z}{r_1} - \frac{Z}{r_2} + \frac{1}{r_{12}} + \gamma\left(l_z^{(1)} + l_z^{(2)} + 2\left(s_z^{(1)} + s_z^{(2)}\right)\right) + \frac{\gamma^2}{2}\left(r_1^2\sin^2\theta_1 + r_2^2\sin^2\theta_2\right)$$

Using the variational principle for the discrete eigenvalues of this Hamiltonian $E[\Psi] = \frac{\langle\Psi|H|\Psi\rangle}{\langle\Psi|\Psi\rangle}$, we get that :

$$E[\Psi] = \frac{\langle\Psi(q_1;q_2)|\,T_1 + T_2 - \frac{Z}{r_1} - \frac{Z}{r_2} + \frac{1}{r_{12}} + \gamma\left(l_z^1 + l_z^2 + 2\left(s_z^1 + s_z^2\right)\right) + \frac{\gamma^2}{2}\left(r_1^2\sin^2\theta_1 + r_2^2\sin^2\theta_2\right)|\,\Psi(}{\langle\Psi(q_1;q_2)|\Psi(q_1;q_2)\rangle} \qquad \text{(C.3)}$$

Where

•

$$\begin{aligned}
\langle\Psi(r_1;r_2)|\Psi(r_1;r_2)\rangle = & \int ([u_{1s}(r_1)\,v_{2p_0}(r_2)]^2 + [v_{2p_0}(r_1)\,u_{1s}(r_2)]^2 + \\
& [v_{2p_0}(r_2)\,u_{1s}(r_1) \times u_{1s}(r_2)\,v_{2p_0}(r_1)] + \\
& [u_{1s}(r_1)\,v_{2p_0}(r_2) \times v_{2p_0}(r_1)\,u_{1s}(r_2)])\,r_1^2 r_2^2\,dr_1 dr_2 d\Omega_1 d\Omega_2 \\
& \int_0^\infty\int_0^\infty e^{-2Z_e r_1} e^{-Z_e r_2} r_1^2 r_2^4\,dr_1 dr_2 \times \int Y^*_{1;0}(\theta_2;\varphi_2)\,Y_{1;0}(\theta_2;\varphi_2)\,d\Omega_1 d\Omega_2 \\
& + \int_0^\infty\int_0^\infty e^{-2Z_e r_2} e^{-Z_e r_1} r_1^4 r_2^2\,dr_1 dr_2 \times \int Y^*_{1;0}(\theta_2;\varphi_2)\,Y_{1;0}(\theta_2;\varphi_2)\,d\Omega_1 d\Omega_2 \\
& + \int_0^\infty e^{-Z_e r_1} e^{-Z_e r_1/2} r_1^3\,dr_1 \times \int Y^*_{1;0}(\theta_2;\varphi_2)\,d\Omega_1 \times \\
& \times \int_0^\infty e^{-Z_e r_2} e^{-Z_e r_2/2} r_2^3\,dr_2 \times \int Y^*_{1;0}(\theta_2;\varphi_2)\,d\Omega_2
\end{aligned} \tag{C.4}$$

Using Mathematica, we calculated these integrals and we found that:

$$\langle\Psi(r_1;r_2)|\Psi(r_1;r_2)\rangle = \frac{4\pi}{4Z_e^3}\frac{24}{Z_e^5} + \frac{4\pi}{4Z_e^3}\frac{24}{Z_e^5} + 2\frac{32}{27Z_e^4} \times 0 = \frac{48\pi}{Z_e^8} \tag{C.5}$$

• The kinetic energy is given by:

$$\begin{aligned}
\langle\Psi(r_1;r_2)|\,T_1\,|\Psi(r_1;r_2)\rangle &= -\frac{1}{2}\langle\Psi(r_1;r_2)|\,\nabla_1^2\,|\Psi(r_1;r_2)\rangle \\
&= -\frac{1}{2}\langle\Psi(r_1;r_2)|\left(\frac{1}{r_1^2}\frac{\partial}{\partial r_1}\left(r_1^2\frac{\partial}{\partial r_1}\right) - \frac{L^2}{r_1^2}\right)|\Psi(r_1;r_2)\rangle
\end{aligned} \tag{C.6}$$

Using the expression of ∇^2 and L^2 in spherical coordinates

$$\nabla^2 = \frac{1}{r^2}\frac{\partial}{\partial r}\left(r^2\frac{\partial}{\partial r}\right) - \frac{1}{r^2}L^2 \tag{C.7}$$

and

$$L^2 = -\left[\frac{1}{\sin\theta}\frac{\partial}{\partial\theta}\left(\sin\theta\frac{\partial}{\partial\theta}\right) + \frac{1}{\sin^2\theta}\frac{\partial^2}{\partial\varphi^2}\right] \tag{C.8}$$

we obtain:

$$\langle\Psi(r_1;r_2)|\,T_1\,|\Psi(r_1;r_2)\rangle = \frac{13\pi}{Z_e^6} + \frac{2\pi}{Z_e^6} \tag{C.9}$$

$$= \frac{15\pi}{Z_e^6} = \langle\Psi(r_1;r_2)|\,T_2\,|\Psi(r_1;r_2)\rangle$$

•

$$\langle\Psi(r_1;r_2)|\frac{1}{r_1}|\Psi(r_1;r_2)\rangle = \langle\Psi(r_1;r_2)|\frac{1}{r_2}|\Psi(r_1;r_2)\rangle \tag{C.10}$$
$$= \frac{30\pi}{Z_e^7}$$

• The interaction term has been calculated using an expansion over spherical harmonics:

$$\langle\Psi(r_1;r_2)|\frac{1}{r_{12}}|\Psi(r_1;r_2)\rangle = \sum_{l=0}^{\infty}\sum_{m_l=-l}^{l}\frac{4\pi}{2l+1}\int\Psi^*(r_1;r_2)\frac{r_<^l}{r_>^{l+1}}\Psi(r_1;r_2)\times \tag{C.11}$$
$$Y^*_{l,0}(\theta_1,\varphi_1)\,Y_{l,0}(\theta_2,\varphi_2)\,r_1^2r_2^2dr_1dr_2d\Omega_1d\Omega_2$$
$$= 4\pi\int_0^{\infty}e^{-2Z_er_1}r_1^2dr_1\left[\frac{1}{r_1}\int_0^{r_1}r_2^4e^{-Z_er_2}dr_2+\int_{r_1}^{\infty}r_2^3e^{-Z_er_2}dr_2\right]+$$
$$4\pi\int_0^{\infty}e^{-Z_er_1}r_1^4dr_1\left[\frac{1}{r_1}\int_0^{r_1}r_2^2e^{-2Z_er_2}dr_2+\int_{r_1}^{\infty}r_2e^{-2Z_er_2}dr_2\right]+$$
$$\frac{8\pi}{3}\int_0^{\infty}e^{-Z_er_1}e^{-Z_er_1/2}r_1^3dr_1\left[\frac{1}{r_1^2}\int_0^{r_1}r_2^4e^{-Z_er_2}e^{-Z_er_2/2}dr_2+r_1\int_{r_1}^{\infty}r_2e^{-Z_er_2}e^{-Z_er_2/2}dr_2\right]$$
$$= 4\pi\times\left[\frac{118}{81Z_e^7}+\frac{118}{81Z_e^7}+\frac{2}{3}\frac{224}{729Z_e^7}\right] = \frac{27280\pi}{2187Z_e^7}$$

Thus, Puting together the above results, we get:

$$E[\Psi] \approx E(Z_e) = \frac{2\times\frac{15\pi}{Z_e^6} - 2Z\times\frac{15\times2\pi}{Z_e^7} + \frac{27280\pi}{2187Z_e^7}}{\frac{48\pi}{Z_e^8}}$$
$$= \frac{5}{8}Z_e^2 - \frac{5}{4}ZZ_e + \frac{1705}{6561}Z_e \tag{C.12}$$

Now, we minimize $E(Z_e)$ using Mathematica language with respect to the variational parameter Z_e: Hence we write :

$$\frac{\partial E}{\partial Z_e} = \frac{10}{8}Z_e - \frac{5}{4}Z + \frac{1705}{6561} = 0$$

So, the effective charge parameter is:

$$Z_e = 1.7921048 \tag{C.13}$$

substituting this value in the equation of $E(Z_e)$, we get:

$$E[Z_e] = -2.00727 \text{ a.u.} \tag{C.14}$$

We note that we define our binding energies as positive values (energy of ionization).

• The linear Zeeman effect is depond on the spin state in which, since we select a symmetric spatial function, the spin state must be antisymmetric i.e.; $S = 0$ and $M_S = 0$, where $M_S = m_S^{(1)} + m_S^{(2)}$:

$$\Psi(q_1;q_2) = N_+ \left[u_{1s}(r_1)\, v_{2p_0}(r_2) + v_{2p_0}(r_1)\, u_{1s}(r_2)\right] \times \chi(1;2) \tag{C.15}$$

$$\begin{aligned}\left\langle \Psi(q_1;q_2) \right| \beta \left(l_z^{(1)} + l_z^{(2)} + 2\left(s_z^{(1)} + s_z^{(2)}\right)\right) \left| \Psi(q_1;q_2) \right\rangle &= \\ \beta \times \left(m_l^{(1)} + m_l^{(2)} + 2\left(m_s^{(1)} + m_s^{(2)}\right)\right)& \\ = 0&\end{aligned} \tag{C.16}$$

Therefore, there is no linear Zeeman effect.

• The quadratic Zeeman effect is given by:

$$\begin{aligned}\left\langle \Psi(q_1;q_2) \right| \frac{\beta^2}{2} \left(r_1^2 \sin^2\theta_1 + r_2^2 \sin^2\theta_2 \right) \left| \Psi(q_1;q_2) \right\rangle &= \\ \frac{\beta^2}{2} \left\langle \left[u_{1s}(r_1)\, v_{2p_0}(r_2) + v_{2p_0}(r_1)\, u_{1s}(r_2)\right] \right| \left(r_1^2 \sin^2\theta_1 \right) \left| \left[u_{1s}(r_1)\, v_{2p_0}(r_2) + v_{2p_0}(r_1)\, u_{1s}(r_2)\right] \right\rangle &+ \\ \frac{\beta^2}{2} \left\langle \left[u_{1s}(r_1)\, v_{2p_0}(r_2) + v_{2p_0}(r_1)\, u_{1s}(r_2)\right] \right| \left(r_2^2 \sin^2\theta_2 \right) \left| \left[u_{1s}(r_1)\, v_{2p_0}(r_2) + v_{2p_0}(r_1)\, u_{1s}(r_2)\right] \right\rangle &= \\ \frac{\beta^2}{2} \left[2 \times \frac{4\pi \times 84}{Z_e^2} \right]&\end{aligned} \tag{C.17}$$

We add this term to the last equation of $E[Z_e]$ we get:

$$E\left[Z_e\right] = \frac{5}{8}Z_e^2 - ZZ_e\frac{5}{4} + Z_e\frac{1705}{6561} + \frac{7\beta^2}{Z_e^2} \tag{C.18}$$

Now, we minimize $E(Z_e)$; using Mathematica, with respect to the variational parameter Z_e: Thus:

$$\frac{\partial E}{\partial Z_e} = \frac{10}{8}Z_e - \frac{10}{4} + \frac{1705}{6561} - \frac{14\beta^2}{Z_e^3} = 0$$

Mathematica used to calculate the effective charge Z_e corresponding to the magnetic field strength β, and therefore the energy $E(Z_e)$.

In the following table, we set our results ($E(Z_e)$) and (Z_e) corresponding to the magnetic field strength β:

β	Z_e	$E(Z_e)$ in a.u.
0	1.7921	2.00727
0.1	1.81096	1.98571
0.2	1.86155	1.92346
0.3	1.93190	1.82626
0.4	2.01209	1.70038
0.5	2.09613	1.55121

Table:17 : Variation of $1s2p_0$ (singlet state) binding energies for helium atom in strong magnetic field (1-electrons in 1s state and the other in $2p_0$).

We repeat these calculations for 1s2s with $S = 1$ and $M_S = 0, \pm 1$, where we obtain for $M_S = -1$ the results given in the following table.

¯	Our results $E(Z_e)$in a:u:	$E(Z_e)$ of [Bec99]in a:u:
0	2; 15138	2; 17522
0; 01	2; 17046	2; 19446
0; 1	2; 27761	2; 30672
0; 2	2; 36721	2; 41272
0; 25	2; 40016	2; 45435
0; 4	2; 51238	2; 57362
0; 5	2; 58972	2; 65066

Table:18 : Variation of 1s2s (triplet state) binding energies for helium atom in strong magnetic …eld with $S = 1$ and $M_S =$ ¡ 1.

Abstract

The motivation to study atoms in magnetic and electric …elds was in a large part due to its importance in various branches of fundamental physics: spectroscopy, plasma, astrophysicsbut the discovery of the strong magnetic and electric …elds in white dwarfs (B » 10^6 ¡ 10^9) G and neutron stars (B » 10^{11} ¡ 10^{13}) G as well as electric …eld (F » 10^6 ¡ 10^{11}) V/m were the reason for such interest.

The work described here presents an analytical and a numerical treatment of light atoms in stellar magnetic and static electric …elds, yielding accurate results on the binding energies of hydrogen and helium atoms in the whole range of magnetic …eld of strengths B » 2; 35 £ 10^9 G and electric …eld F < 10^{11}V=m, where we try to estimate its ground state and …rst few excited states energies focussing on such stellar magnetic and electric …elds as are believed to exist in the atmospheres of white dwarfs and neutron stars.

Moreover; the one of the main objectives of this thesis is presented the numerical values of the dipole strengths, oscillator strengths and transition probabilities which are giving much information about the structure and the spectrum of these light atoms which are existed in these strange compact objects.

Résumé

La raison principale de l'étude des atomes dans les champs magnétiques et électriques est due a son importance dans les di¤érentes branches de la physique tels que: la Spectroscopie, plasma et l'astrophysique ... mais la découverte de la présence d'un champ magnétique du rang de 10^6-10^9 G à la surface des naines blanches, et du rang de 10^{11}-10^{13} G dans les étoiles à neutrons , ainsi que la présence d'un champ électrique du rang de (10^6-10^{11}V /m) est la cause la plus importante de tel intérêt.

Cette étude qui décrit le traitement analytique et numérique des atomes légers en présence des champs magnétique et électrique forts dont les valeurs sont comparables à celles présentes dans les objets astrophysiques compacts, nous donne des résultats précis, pour l'hydrogène et l'hélium, dans l'intervalle des intensités des champs choisi, ou on a calculé les énergies de liaison de l'état fondamentales ainsi que celles (plus grandes) des premiers états excités.

La connaissance de quelques-unes des caractéristiques de l'énergie atomique et la perspective des probabilités de transitions d'un niveau à un autre dans les conditions posées dans ce travail, ce qui nous permet d'identi…er la structure et les spectres de ces atomes, et ainsi de détecter quels sont ces mystérieux objets astronomiques.